

BIOMECHANICS OF RHEOTAXIS IN HILL STREAM FISH

By

John Andrew Macdonnell

B.Sc. The University of British Columbia, 1988

A THESIS SUBMITTED IN PARTIAL FULFILLMENT OF  
THE REQUIREMENTS FOR THE DEGREE OF  
MASTER OF SCIENCE

in

THE FACULTY OF GRADUATE STUDIES

(Department of Zoology)

We accept this thesis as conforming  
to the required standard

THE UNIVERSITY OF BRITISH COLUMBIA

APRIL 1990

© John Andrew Macdonnell, 1990

In presenting this thesis in partial fulfilment of the requirements for an advanced degree at the University of British Columbia, I agree that the Library shall make it freely available for reference and study. I further agree that permission for extensive copying of this thesis for scholarly purposes may be granted by the head of my department or by his or her representatives. It is understood that copying or publication of this thesis for financial gain shall not be allowed without my written permission.

Department of Zoology.  
The University of British Columbia  
Vancouver, Canada

Date April 27, 1990.

## ABSTRACT

Behaviour to increased water velocity is examined in fast stream fish (*Otocinclus*, *Hypostomus*, *Pterygoplichthys*, *Chaetostoma* and *Gyrinocheilus*) and a slow water form (*Farlowella*). Behaviour can be divided into two stages; resting and adhesion (Chapter I). In *Otocinclus* a third fin extension stage is apparent. Based on the slipping velocity of live and dead fish it is determined that *Gyrinocheilus* has the greatest station holding ability on a smooth perspex surface. This is attributed to a complete seal produced by its oral sucker lips (closed sucker).

Station-holding ability is also examined on rougher surfaces. Slipping does not occur in any of the genera at water velocities up to  $90 \text{ cm s}^{-1}$ . Morphological adaptations (eg. oral sucker, pectoral fins, frictional pad and odontodes) that may contribute to increasing slipping velocity are examined. In *Otocinclus* these structures are analyzed using a Scanning Electron Microscope. *Otocinclus* is the only genera with the ventral dermal plates between the pelvic and pectoral fins organized laterally into a frictional pad.

Drag on fish is directly measured with strain gauges and used to calculate drag coefficients (0.10 - 0.94; Chapter II). Drag coefficients for low fineness ratio (length/height  $< 10$ ) forms at Reynold's numbers below  $10^4$  compare poorly with literature values for technical bodies. Drag coefficients determined for fish are high due to roughness and interference drag produced by the fins. Using morphological measurements, dead slipping velocities, drag coefficients, static frictional coefficients and submerged body weight, lift coefficients (-0.55 - 1.23)

are calculated.

Fast stream fish maximize slipping speed by having high frictional coefficients (0.67 - 0.95, on a smooth perspex surface), density (1.03 - 1.10 g cm<sup>-3</sup>), rheotactic suction pressure (13 - 173 N m<sup>-2</sup>) and negative lift. Although *Farlowella* has high density (1.129 g cm<sup>-3</sup>) and a low drag coefficient (0.23), its lift to drag ratio is high (6.71) and rheotactic suction pressures (2 - 27 N m<sup>-2</sup>) are low. In general *Farlowella* does not exhibit hydrodynamic, behavioural or morphological characteristics that enhance station-holding.

## TABLE OF CONTENTS

Abstract .....	ii
Table of Contents .....	iv
List of Tables .....	v
List of Figures .....	vi
List of Symbols .....	ix
Acknowledgements .....	xii
General Introduction .....	1
Chapter One:     Behaviour and Morphology	
Abstract .....	3
Introduction .....	5
Materials and Methods .....	7
Results .....	14
Discussion .....	29
Chapter Two:     Biomechanics and Energetics	
Abstract .....	36
Introduction .....	38
Materials and Methods .....	40
Results .....	57
Discussion .....	73
Concluding Remarks .....	87
Literature Cited .....	89

## LIST OF TABLES

Table 1.1	Ratio means ( $\overline{2b/h}$ , $\overline{l/h}$ , $\overline{x/l}$ , and $\overline{l/l_{sp}}$ ), best fit regression lines, multiple pair wise comparisons between means and slopes for <i>Otocinclus</i> , <i>Gyrinocheilus</i> , <i>Hypostomus</i> , <i>Pterygoplichthys</i> , <i>Chaetostoma</i> and <i>Farlowella</i> .	.....28
Table 2.1	Body density $\overline{\rho}$ , frictional coefficients $\overline{\mu}$ , projected frontal area of the anterior pectoral fin spine or ray $A_f$ and total area $A$ range for <i>Otocinclus</i> , <i>Gyrinocheilus</i> , <i>Hypostomus</i> , <i>Pterygoplichthys</i> , <i>Chaetostoma</i> , and <i>Farlowella</i> .	.....66
Table 2.2	The constants $a_1$ , $a_2$ and $a_3$ for the drag velocity curves in Fig. 2.10 ( $\text{Drag (Kg m s}^{-2}\text{)} = a_1 + a_2 (v) + a_3 (v^2)$ ).	.....67
Table 2.3	Hydrodynamic coefficients, ratios and rheotactic suction pressures for <i>Otocinclus</i> , <i>Gyrinocheilus</i> , <i>Chaetostoma</i> , <i>Pterygoplichthys</i> , fish 1, <i>Hypostomus</i> , and <i>Farlowella</i> .	.....68
Table 2.4	Comparison of measured and estimated drag coefficients.	.....83

## LIST OF FIGURES

- Figure 1.1: Pictures and tracings of side view, frontal cross .....8  
section, plan form view and morphological  
measurements made for *Otocinclus*, *Hypostomus*,  
*Pterygoplichthys*, *Farlowella*, *Chaetostoma*, and  
*Gyrinocheilus*.
- Figure 1.2: Recirculating perspex flow tank and shelf used for .....10  
behavioural observations.
- Figure 1.3: Bar plot of mean live slipping velocity  $\bar{V}_1$ , mean .....16  
dead slipping velocity  $\bar{V}_2$  and  $\bar{V}_1 - \bar{V}_2$  difference for  
*Otocinclus*, *Gyrinocheilus*, *Hypostomus*,  
*Pterygoplichthys*, *Chaetostoma*, and *Farlowella*.
- Figure 1.4: Scanning electron microscopy photographs of .....19  
*Otocinclus*'s oral sucker, pectoral fin, ventral  
frictional pad, and close up of the odontodes and  
dermal plates on the ventral frictional pad.
- Figure 1.5: Body width to height ratio (2b/h) plotted against .....24  
standard length for *Otocinclus*, *Gyrinocheilus*,  
*Hypostomus*, *Pterygoplichthys*, *Chaetostoma*, and  
*Farlowella*.
- Figure 1.6: Total length to height ratio (l/h) plotted against .....25  
total length for *Otocinclus*, *Gyrinocheilus*,  
*Hypostomus*, *Pterygoplichthys*, *Chaetostoma*, and  
*Farlowella*.

- Figure 1.7:** Distance from end of rostrum to maximal height to .....26  
total length ratio ( $x/l$ ) plotted against total  
length for *Otocinclus*, *Gyrinocheilus*, *Hypostomus*,  
*Pterygoplichthys*, *Chaetostoma*, and *Farlowella*.
- Figure 1.8:** Total length to spine length ratio ( $l/l_{sp}$ ) plotted .....27  
against total length for *Otocinclus*, *Gyrinocheilus*,  
*Hypostomus*, *Pterygoplichthys*, *Chaetostoma*, and  
*Farlowella*
- Figure 2.1:** Measurements required for estimating the total .....41  
projected frontal area of the fish.
- Figure 2.2:** Forces acting on the body of a hill stream fish .....42
- Figure 2.3:** Recirculating perspex flow tank and strain gauge .....48  
apparatus used for determining the drag acting on  
hillstream fish *Otocinclus*, *Hypostomus*,  
*Pterygoplichthys*, *Farlowella*, *Chaetostoma*, and  
*Gyrinocheilus*.
- Figure 2.4:** Typical boundary layer profile near the surface of .....50  
a force plate.
- Figure 2.5:** Calibration curve for the fine tip hot bead .....51  
anemometer used for boundary layer velocity  
measurement.
- Figure 2.6:** Relationship between the projected frontal area .....61  
determined from tracings and geometry for  
*Pterygoplichthys*.

- Figure 2.7: Linear regression lines of best fit for body .....62  
projected frontal area  $A_b$  plotted against standard  
length squared.
- Figure 2.8: Linear regression lines of best fit for submerged .....63  
body weight  $W_o$  plotted against total length cubed.
- Figure 2.9: Linear regression lines of best fit for density .....64  
plotted against total length  $l$ .
- Figure 2.10: Drag plotted against velocity for *Otocinclus*, .....65  
*Gyrinocheilus*, *Hypostomus*, *Pterygoplichthys*,  
*Chaetostoma* and *Farlowella*.
- Figure 2.11: Frontal drag coefficient plotted against Reynold's .....69  
number.
- Figure 2.12: Oxygen consumption and repositionings per minute .....71  
plotted against water velocity for  
*Pterygoplichthys*.

## LIST OF SYMBOLS

## LENGTH

$l$	total length
$l_s$	standard length
$x$	distance from $h$ to end of rostrum
$2b$	maximal body width
$l_{sp}$	length of the pectoral fin anterior spine or ray
$W$	pectoral fin anterior spine or ray width
$h$	maximal body height

## AREA

$A$	total projected frontal area ( $A_b + A_f$ )
$A_b$	projected frontal area of body, circle ( $\pi (h/2)^2$ ) or ellipse ( $\pi (b + h/2)$ )
$A_f$	projected frontal area of pectoral fin anterior spine

## ANGLES

$\emptyset$	angle between perspex plate and bottom
$\emptyset_s$	perpendicular angle relative to fin extension

## FORCES

$L$	lift
$D$	drag
$W_a$	weight of fish in air
$W_o$	weight of fish in water

## RHEOTACTIC SUCTION PRESSURE

- $S_1$  suction pressure referenced to total ventral surface area  
 $S_2$  suction pressure referenced to oral sucker surface area

## VELOCITY

- $V$  water velocity during drag measurement  
 $V_1$  slipping velocity of live fish  
 $V_2$  slipping velocity of dead fish

## COEFFICIENTS

- $\overline{C_D}$  mean drag coefficient  
 $\overline{C_L}$  lift coefficient calculated from  $\overline{C_D}$   
 $C_{L1}$  maximum lift coefficient calculated from the minimum  $C_D$   
 $C_{L2}$  minimum lift coefficient calculated from the maximum  $C_D$   
 $\mu$  static frictional coefficient

## DENSITY

- $\rho$  fish body density  
 $\rho_w$  water density (998.2 kg m<sup>-3</sup> at 26° C)

## REYNOLD'S NUMBERS

- $Re$  Reynold's number of flat plate normal to flow  
 $R_1$  Reynold's number of fish based on  $V_1$   
 $R_2$  Reynold's number of fish based on  $V_2$   
 $R_3$  Reynold's number of fish based on  $V$   
 $R_x$  critical Reynold's number

**VISCOSITY**

$\nu$  kinematic viscosity ( $8.97 \times 10^{-7} \text{ m}^2 \text{ s}^{-1}$  at  $26^\circ \text{ C}$ )

**BOUNDARY LAYER**

$\delta$  boundary layer thickness

$x$  critical transition point

## ACKNOWLEDGEMENTS

I would like to thank Dr. R. W. Blake, my research supervisor, for his continued support throughout this project and providing me with the opportunity to write my first scientific paper. Special thanks to Dr. J. M. Gosline and Dr. N. J. Wilimovsky for their valuable discussion and advice. I would also like to thank Mike Smith and Collin Brauner for their experimental assistance as well as the Vancouver Aquarium for providing me with a specimen of *Ptergoplichthys*. Thanks also to Mr. Robert Carveth whose discussion on taxonomy was of great value and whose wry perspective gave an added element to this thesis. This work could not have been completed without the assistance of members from the Biomechanic labs of Dr. R. W. Blake and Dr. J. M. Gosline (1988-1990).

## GENERAL INTRODUCTION

Organisms that live in fast flowing environments have developed a number of adaptations for preventing displacement (Nachtigall, 1974). These adaptations maximize slipping speed by opposing or reducing the forces of lift and drag. Arguably, adaptations for preventing displacement are selected.

Extensive work done by Hora between 1921 and 1930 on the hill stream fish (Cyprinoidea and Siluroidea) of India showed unique morphological adaptations that may be utilized to prevent displacement. These adaptations include skin folded into ridges, dorsal-ventral flattening, spines and oral suckers. Furthermore, a number of rheotactic behaviours have been documented suggesting that body and fin position improves station-holding (eg. Keenleyside, 1962; Arnold, 1969; Macdonnell and Blake, 1990). This thesis addresses the behavioural and morphological adaptations in five genera of fast stream fish (*Otocinclus*, *Gyrinocheilus*, *Hypostomus*, *Pterygoplichthys* and *Chaetostoma*) and a slower stream form (*Farlowella*). Although *Gyrinocheilus* is best known as a fast water form it also occurs in slower flow (Smith, 1945).

In the first chapter rheotactic behaviours and gross external morphology that may be used to maximize slipping speed are examined. Furthermore, geometric ratios are determined and compared to low drag forms of technical bodies (smooth blisters attached to a surface).

In the second chapter hydrodynamic characteristics are analyzed in fast and slow stream fish. The drag acting on these fish is directly measured and drag coefficients  $C_D$  determined. From drag coefficients,

dead slipping velocities  $V_1$  (Chapter I) morphological measurements and frictional coefficients  $\mu$ , lift coefficients  $C_L$  are calculated using a model developed by Arnold and Weihs (1978). In addition, the oxygen consumption rate at various water velocities is measured for a specimen of *Pterygoplichthys*.

Each chapter is written as a complete scientific paper with an Abstract, Introduction, Materials and Methods, Results and Discussion section. The last section of this thesis (Concluding Remarks) summarizes the main findings of each chapter and proposes further research suggested by this thesis.

## CHAPTER I

## BEHAVIOUR AND MORPHOLOGY

## ABSTRACT

Behaviour, morphology and geometry of five genera of fast stream fish (*Otocinclus*, *Gyrinocheilus*, *Hypostomus*, *Pterygoplichthys* and *Chaetostoma*) and one genus of slow stream fish (*Farlowella*) are studied to determine adaptations preventing displacement. All genera show rheotactic behaviour to increased water velocity. Fast and slow stream fish react actively and passively to increased water velocity respectively. Behaviour is divided into two stages, resting and adhesion. In *Otocinclus* a third fin extension stage occurs. In addition, the station-holding ability of *Gyrinocheilus*, (closed sucker) is compared to the loricariids (open sucker). To compare station-holding ability live and dead slipping velocities ( $\bar{V}_1$  and  $\bar{V}_2$  respectively) are measured on a smooth perspex surface. Based on  $\bar{V}_1$  (59.1 cm s<sup>-1</sup>) and  $\bar{V}_1 - \bar{V}_2$  (45.7 cm s<sup>-1</sup>) it is determined that *Gyrinocheilus* has the greatest station-holding ability. *Farlowella* has a relatively large  $\bar{V}_1$  (19.2 cm s<sup>-1</sup>) and  $\bar{V}_1 - \bar{V}_2$  (29.1 cm s<sup>-1</sup>), however, it has behavioural and morphological adaptations that do not enhance station-holding ability in fast flow (slow orientation to water flow and high fineness ratio; length/height = 21).

In addition, slipping velocity is measured on rough surfaces. Slipping did not occur in any of the genera because of effective frictional devices and oral suction. *Otocinclus*, *Hypostomus*, *Pterygoplichthys*,

*Chaetostoma* and *Farlowella* all have spines, odontodes and dermal plates that aid in station-holding. However, *Otocinclus* is the only form with the ventral dermal plates between the pectoral and pelvic fins organized laterally into a frictional pad. Gross morphological adaptations that could aid in station-holding besides the oral sucker are not apparent in *Gyrinocheilus*.

For fast stream fish fineness ratios (total length/maximal height,  $\overline{l/h}$ ) are between 6.7 and 9.0. Also, flattening (maximal body width/maximal height,  $\overline{2b/h} = 0.9 - 2.0$ ) and lengthening (distance from end of rostrum to maximal height/total length,  $\overline{x/l} = 0.17 - 0.22$ ) of the fore body is pronounced. Values of  $l/h$ ,  $2b/h$ , and  $x/l$  are similar to the optimal values corresponding to technical bodies of low drag (10, 2.0, and 0.3 for  $l/h$ ,  $2b/h$ , and  $x/l$  respectively for smooth blisters attached to surfaces). The form of fast stream fish is consistent with low drag.

## INTRODUCTION

Organisms face strong forces from water currents caused by tides, wave action or torrential streams (eg. Jones, 1968; Gibson, 1969; Vogel, 1981; Denny, 1988; Statzner and Holme, 1989). A number of studies have documented and analyzed rheotactic behaviours from a variety of perspectives (eg. Keenleyside, 1962; Arnold 1969; Nachtigall, 1974; Matthews, 1985; Taylor, 1988; Macdonnell and Blake 1990). Arnold and Weihs (1978) analyzed the rheotactic behaviour in the plaice (*Pleuronectes platessa*) and document adaptations that may diminish lifting forces. Blake (1985) analyzed the carapace design in crabs and argues that the design of *Cancer productus* maximizes slipping speed while *Lopholithodes mandtii* resists displacement by actively holding. Webb (1989) examined the rheotactic behaviour and station-holding ability in three species of benthic fish (*Pleuronectes platessa*, *Raja clavata* and *Myoxocephalus scorpius*), arguing that variation in body design results in different strategies of preventing displacement. Compressed forms (eg. *P. platessa* and *R. clavata*) are characterized by high lift and low drag, and exhibit behaviours which reduce lift. Fusiform fish (eg. *M. scorpius*) of high drag and low lift increase frictional forces to prevent displacement.

*Otocinclus*, *Hypostomus*, *Pterygoplichthys*, *Chaetostoma*, and *Farlowella* are armored catfish indigenous to the hill streams of Brazil (Sterba 1983). *Gyrinocheilus* is found in the hill streams of South Eastern Asia (Wheeler, 1975). All these fish are bottom dwellers and feed on algal mats using their oral sucker. *Otocinclus*, *Hypostomus*, *Pterygoplichthys*,

*Chaetostoma*, and *Gyrinocheilus* are found in fast flowing water and also use their oral sucker for preventing displacement (Burgess, 1989).

*Farlowella* occurs in slower water.

Annandale and Hora (1920, 1922, 1925), and Hora (1921, 1922, 1923a, 1923b, 1925a, 1925b, 1925c, 1927, 1930) examined the adhesive apparatus (spines and frictional pads) of torrential stream fauna in India and found a number of adaptations that could be used to prevent displacement.

Here, the behavioural and morphological adaptations for station-holding in rapidly moving water are investigated in six genera of hill stream fish.

## MATERIALS AND METHODS

### Fish

Specimens of *Otocinclus* (Cope, 1871), *Hypostomus* (Lacépède, 1803), *Pterygoplichthys* (Gill, 1858), *Farlowella* (Eigenmann and Eigenmann, 1889), *Chaetostoma* (von Tschudi, 1845), and *Gyrinocheilus* (Tirant, 1883) (Fig. 1.1) were obtained from a local, (Vancouver, B.C.), commercial dealer. Healthy animals were maintained in a fresh water aquarium, (75 cm X 40 cm X 50 cm), equipped with a recirculating charcoal filter and air stone. Temperature was maintained between 24° C and 28° C. Fish were fed food flakes and pellets.

Identification of the loricariids (*Otocinclus*, *Hypostomus*, *Pterygoplichthys*, *Chaetostoma* and *Farlowella*) and *Gyrinocheilus* was only possible to the genera level. Collection areas were unknown and unresolved taxonomy makes identification questionable using existing descriptions (eg. Fowler 1937; Smith 1945; Isbrücker, 1980; Roberts 1982). However, meristic characteristics were compared to eliminate obviously different species. Fish were deposited and catalogue in the Fish Museum at the University of British Columbia (No. B C 89-500).

Measurements were made using calipers (30 cm, Helios 0.005 ± 0.0025 cm). Total length  $l$ , standard length  $l_s$ , anterior spine or fin ray of the pectoral fin length  $l_{sp}$ , maximal body height  $h$ , maximal body width  $2b$ , and distance from  $h$  to rostrum  $x$  were measured (see Fig 1.1). In *Farlowella* the dorsal and ventral lobes of the tail are highly elongated and were not included in the  $l$  measurement.

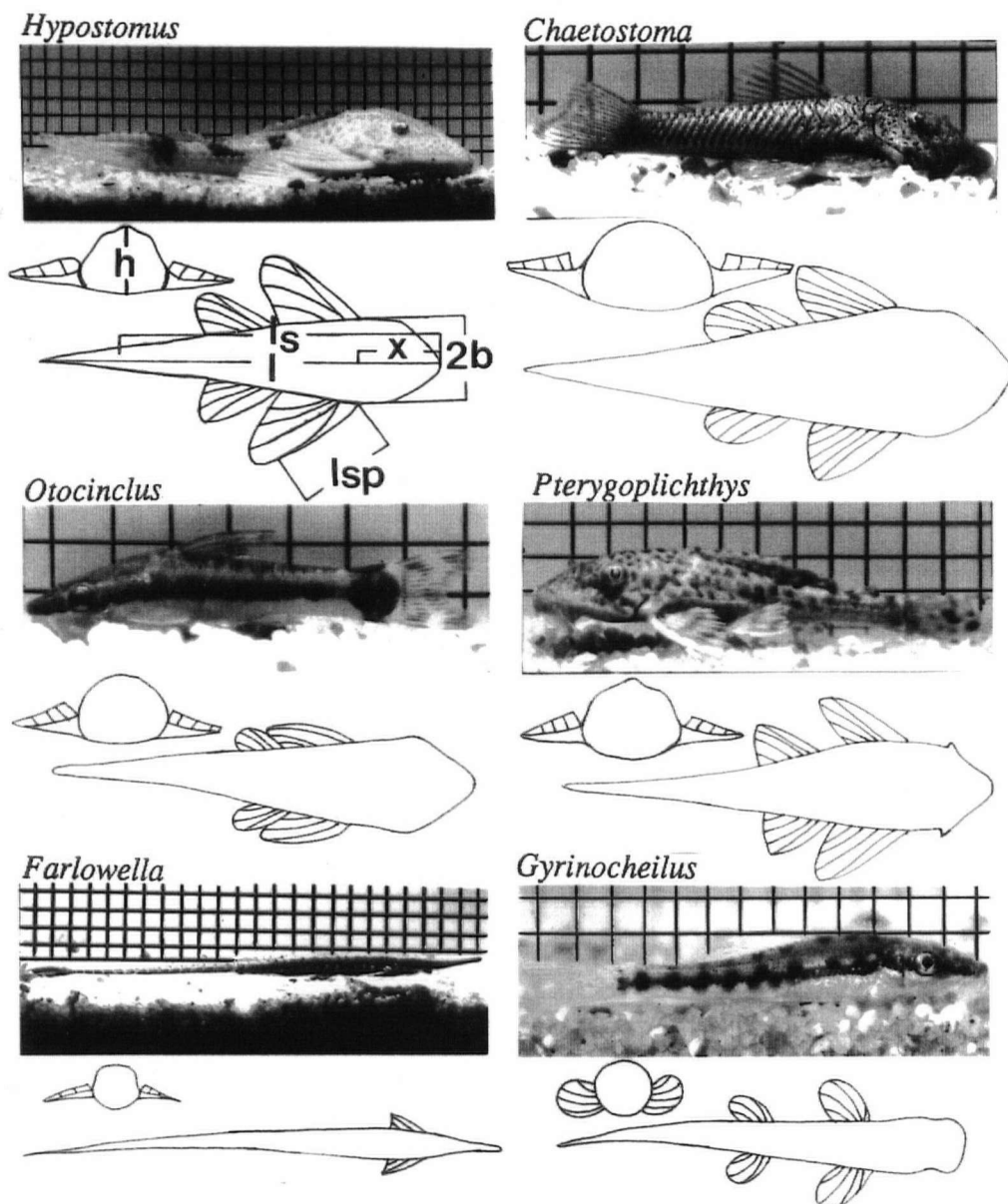


Fig. 1.1 Pictures and tracings of side view, frontal cross section and plan form view of *Otocinclus*, *Hypostomus*, *Pterygoplichthys*, *Farlowella*, *Chaetostoma*, and *Gyrinocheilus*. A 0.5 X 0.5 cm grid scale is used for the backdrop. The tracing of *Hypostomus* shows the morphological measurements made for all fish (total length  $l$ , standard length  $l_s$ , maximal body height  $h$ , distance from  $h$  to end of rostrum  $x$ , maximal body width  $2b$ , and spine length  $l_{sp}$ ).

### Flow tank

Behavioural observations were made in a perspex recirculating flow tank (250 cm X 25 cm X 60 cm). A 0.5 HP electric motor rotated a propeller (diameter 15 cm) to produce flow. A screen was placed at the end of the upper level to prevent fish, that opted to drift down stream, from being swept into the propeller. A flow rectifying grid (20 cm X 20 cm) made of straws (0.55 cm diameter) was located just in front of the propeller (Fig. 1.2). Temperature was maintained (24°-28° C) using a recirculating heater (Brinkmann instruments, Model IC-2, 1000 W).

Individual fish were placed into the upper level of the flow tank (Fig. 1.2). Water velocity was gradually increased by increments of 5.0 cm s<sup>-1</sup> starting at 0.0 cm s<sup>-1</sup> and maintained for 5 min at each velocity. The mean slipping velocity on a perspex surface for live fish  $\overline{V}_1$ , was recorded when the fish first began to slide backwards continuously (n = 10 trials per fish). Mean slipping velocity  $\overline{V}_2$  was also measured for dead fish (n = 10 trials per fish). Fish were killed with a strong solution of tricaine methanesulphonate (MS222) and preserved in a 37 % isopropyl alcohol solution. The freshly killed fish were placed 50 cm downstream of the flow rectifying grid facing head first upstream. Water velocity was increased by 2.0 cm s<sup>-1</sup> increments and left for 3 min at each velocity.  $\overline{V}_2$  was only recorded when the fish slipped directly backwards. If the fish turned side ways before slipping the measurement was not taken, but if rotation occurred after slipping these values were recorded following Arnold and Weihs (1978).

Behavioural observations on *Otocinclus* were more difficult due to

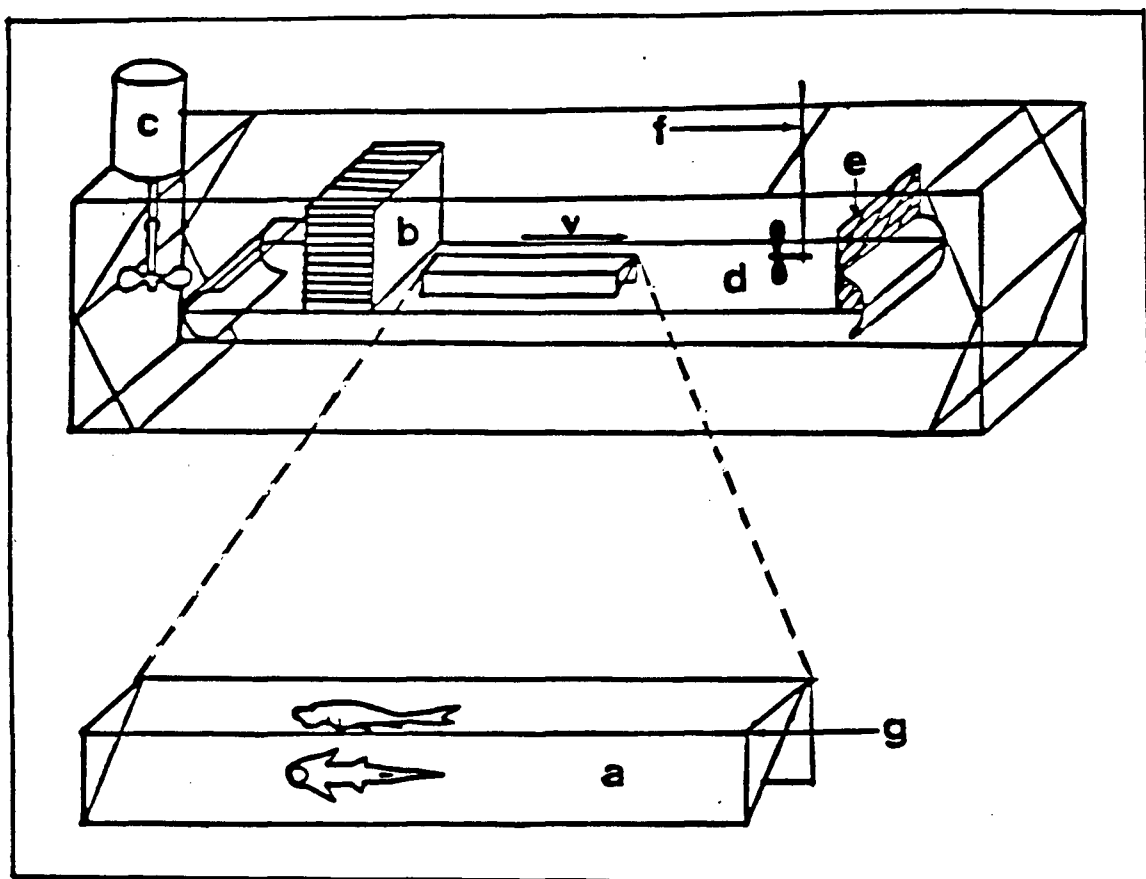


Fig. 1.2 Recirculating perspex flow tank and shelf used for behavioural observations (mirror a, flow rectifying grid b, 0.5 HP electric motor c, upper level d, screen for catching fish e, water velocity meter f, perspex shelf g, and water velocity direction v).

their small size. To see more clearly a mirror was angled at  $45^\circ$  and placed under a perspex shelf (50 cm X 10 cm X 10 cm). The shelf and mirror were then put into the flow tank and a specimen of *Otocinclus* was placed onto the shelf (Fig. 1.2). This gave a ventral and side view. *Otocinclus* was removed from the shelf and placed onto the upper level of the flow tank to record V<sub>2</sub>.

In addition, observations were also conducted on rougher surfaces for live specimens. Sand was sifted (Endecotts limited model E.V.F. 1 sifter) to produce three groups of sand grain diameters (0.695 mm - 0.355 mm, 0.355 mm - 0.180 mm, and 0.180 mm - 0.075 mm). The sand was placed into a tray and a piece of perspex, covered with contact cement, was placed face down onto it. This produced a uniform cover of sand on the perspex of a given grain size. Fish were placed onto the sand coated perspex plates and exposed to increasing water velocity.

Water velocities were determined using a battery operated current meter (A. OTT Kempton TYP. 12.400,  $\pm 0.50 \text{ cm s}^{-1}$ ). The current meter propeller was placed 75 cm down stream from the flow rectifying grid and 10 cm from the bottom (Fig. 1.2).

### Video and Still Photography

Rheotactic behaviour was recorded (Mitsubishi color monitor model CM-2501C, RCA closed-circuit video camera, Tamron 60-300 mm macro zoom lens,  $f$  3.8-32, Sony Beta Max VCR) at various water velocities. Photographs (Kodak TMAX-36, 100 ASA film at  $f$  8-11) were taken of side, top and front views of all six genera of fish using a Pentax Super

Program reflex camera with a Tamron macro zoom lens mounted on a tripod. Illumination was supplemented by two Crown 650 W SL tungsten lamps.

### Microscopy

Fish were examined using a dissecting microscope (Wild Leitz Heerbrugg, maximum magnification 15 X 40). *Otocinclus* was also observed under the scanning electron microscope (S. E. M., Stereoscan 250). S. E. M. preparations were dissected from freshly killed fish and placed into a primary fixative consisting of 2.5 % glutaraldehyde in 0.1 molar of sodium cacodylate and left three hours on ice. Preparations were then rinsed three times with 10 ml of 0.1 sodium cacodylate and placed into a secondary fixative (1 %  $O_3O_4$  in 0.1 molar of sodium cacodylate) for 1-2 hours. Dissections were washed three times with 10 ml of distilled water and dehydrated in consecutive washings of 30, 50, 70, 85, 95, 100, 100 percent alcohol, 10 minutes per step. Preparations were mounted on stubs and left for a day before they were critical-point dried (CPD 020 Balzers Union) and thinly gold coated (Nanoteck SEM Prep 2 Sputter Coater). S. E. M. was used to observe the mounts and photographs were taken (55 polaroid, 50 ASA) of the oral sucker, pectoral fin, ventral frictional pad and close up of the spines on the ventral frictional pad surface.

### Statistics

All regression lines for the four ratios  $2b/h$ ,  $l/h$ ,  $x/l$ , and  $l/sp$  were tested to see if the correlation coefficients were significantly

different from zero (t-test,  $H_0: \rho = 0$ ,  $p < 0.05$ ). Analysis of covariance was used to determine if there were significant differences among slopes ( $H_{0_1}: \beta_a = \beta_b = \beta_c = \beta_d = \beta_e = \beta_f$ ,  $p < 0.05$ ). Analysis of variance was used to test if a significant difference existed between means ( $H_{0_2}: \mu_a = \mu_b = \mu_c = \mu_d = \mu_e = \mu_f$ ,  $p < 0.05$ ). Multiple pair wise comparisons were done if  $H_{0_1}$  and  $H_{0_2}$  were rejected using the Tukey (HSD) test. All statistical operations were performed using the SYSTAT statistical package.

## RESULTS

### Behaviour

Rheotaxis towards increased water velocity, in *Gyrinocheilus*, *Hypostomus*, *Pterygoplichthys*, *Chaetostoma*, and *Farlowella* can be divided into two stages, resting and adhesion. In *Otocinclus* a third fin extension stage not seen in the other genera occurs (Macdonnell and Blake, 1990).

Resting occurs in still water. In *Otocinclus* the pectoral fins are folded along the sides of the body. However, in *Gyrinocheilus*, *Hypostomus*, *Pterygoplichthys*, *Chaetostoma* and *Farlowella* the pectoral fins are extended at all times when resting or adhered to the substrate. The only time the pectoral fins are folded against the body in these fish is when they are swimming against a current. Occasionally feeding activity is seen with the teeth rasping the bottom. The oral sucker is relaxed, and a large gap exists between the anterior and posterior lips of the sucker for all genera. When resting, the body of *Otocinclus* and *Gyrinocheilus* is suspended between the pelvic fins and oral sucker, leaving a space between the ventral surface and the bottom. In *Hypostomus*, *Pterygoplichthys*, *Chaetostoma*, and *Farlowella* the ventral surface is in contact with the bottom.

Adhesion occurs in all genera when water velocity is increased ( $10.0 \text{ cm s}^{-1}$  -  $20.0 \text{ cm s}^{-1}$ ). Initially fish respond to increased water velocity by passively or actively orientating themselves head first into the flow, if they are not already in this position. In *Otocinclus*, *Gyrinocheilus*,

*Hypostomus*, *Pterygoplichthys*, and *Chaetostoma* an increase in water velocity results in a release of suction and active swimming facilitating upstream orientation. *Farlowella* remains attached to the substrate, allowing the current to push the tail down stream, using the oral sucker as a pivot until the fish is facing into flow direction. This passive mode of orientation is much slower than the active process observed in the other genera.

Once orientated upstream the fish move about the perspex surface seeking regions for adhesion. When a place is found the sucker tightly clamps to the surface. In the loricariids this greatly decreases the respiratory gap posterior to the maxillary barbel and stops displacement. In *Gyrinocheilus* the gap between the anterior and posterior lips completely disappears. The dorsal fin in all genera is depressed and the tail is folded. This occurs during up stream orientation. The dorsal fin is erected when water velocity is stopped or the fish begin swimming.

At water velocities  $V_1$  fish begin to slip backwards on a smooth perspex surface. The mean for  $V_1$ ,  $V_2$  and their difference is given for all genera in Fig. 1.3.  $V_1$  in *Otocinclus*, *Gyrinocheilus*, *Hypostomus*, *Pterygoplichthys*, *Chaetostoma*, and *Farlowella* ranges from 19-35  $\text{cm s}^{-1}$ , 50-67  $\text{cm s}^{-1}$ , 22-40  $\text{cm s}^{-1}$ , 32-48  $\text{cm s}^{-1}$ , 42-56  $\text{cm s}^{-1}$  and 42-56  $\text{cm s}^{-1}$  respectively. Fish adhere to the bottom and are pushed down stream while maintaining suction during slipping.

At  $V_1$  the pectoral fin extension stage occurs in *Otocinclus*. During this stage the pectoral fins are unfolded to clamp the anterior spine to the substrate, and the ventral surface is pressed down. This stage does not occur in the other genera where the pectoral fins are extended

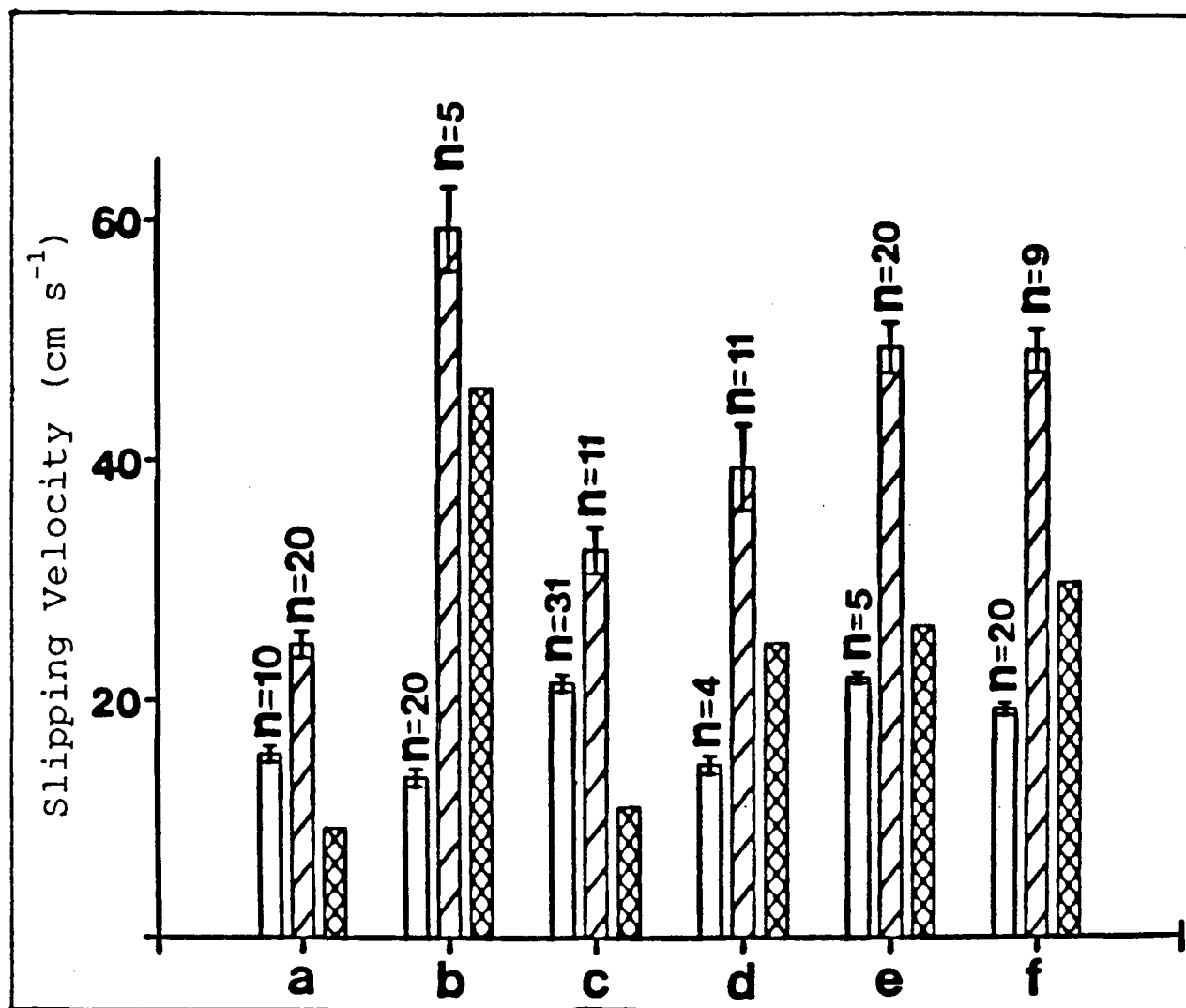


Fig. 1.3 Mean live slipping velocity  $V_1$  (hatched bar), mean dead slipping velocity  $V_2$  (solid bar),  $V_1 - V_2$  difference (cross-hatched bar) and number of fish  $n$  for *Otocinclus* a, *Gyrinocheilus* b, *Hypostomus* c, *Pterygoplichthys* d, *Chaetostoma* e, and *Farlowella* f with standard error bars on  $V_1$  and  $V_2$ .

already, however, the pectoral fins are applied to the substrate. In all genera the pectoral fin rays angled upward from the anterior spine (loricariids) or anterior fin ray (*Gyrinocheilus*) so that they are orientated at a negative angle to the oncoming flow. In addition, the pelvic fins become more erect and spread out in all genera. This behaviour causes the dorso-ventrally flattened head of the loricariids to be pushed down and brings the anterior spines of the pectoral fins in closer contact with the bottom. This is greatly exaggerated in *Otocinclus*, and *Gyrinocheilus* relative to *Farlowella*. While slipping the pectoral fins and oral sucker remain firmly pressed against the bottom. In *Otocinclus* the space between the ventral surface and bottom is also reduced.

If the current is stopped the pectoral fins of *Otocinclus* fold in and a resting posture is resumed. The pectoral fins of the other genera remain extended. All fish move forward and reposition themselves when water velocity is decreased. At times slipping is compensated for by rapid tail beating to reclaim lost ground. When suction is released, the pectoral fins are folded, and swimming occurs in the free stream. All genera are able to move forward using their oral sucker in currents of the order of  $V_1$ .

In the loricariids the gap in the oral sucker posterior to the maxillary barbel decreases its size at higher water velocities. Flaring of this gap is out of phase with contractions of the buccopharynx. Even at higher water velocities, when slipping becomes more pronounced, the respiratory gap does not disappear in the loricariids and movements of the buccopharynx continue for all fish.

At water velocities greater than  $V_1$  the tail and caudal peduncle of *Farlowella* begins to move erratically, destabilizing the fish. This is also observed in *Gyrinocheilus* when water velocity is increased rapidly not allowing the fish a chance to gain proper position with the pelvic fins. *Gyrinocheilus* is able to maintain position with the oral sucker, however, the pelvic fins are not firmly stationed and the caudal peduncle and tail are lifted away from the bottom.

There is a difference between slipping and foraging. Foraging occurs in any direction along the surface with noticeable abduction of the oral sucker lips. During slipping abduction of the lips does not occur and the fish moves directly backwards.

Similar rheotactic behaviour is observed on the rougher surfaces. However, steady slipping is not seen on any of the three rough surfaces at water velocities up to  $90.0 \text{ cm s}^{-1}$ . *Chaetostoma*, and *Gyrinocheilus* show a jerky downstream movement that is too irregular to consider slipping. In addition, *Gyrinocheilus* is the only fish that shows a preference for the perspex surface. *Gyrinocheilus* often drifts downstream from the roughness element and adheres to the perspex. This occurs most frequently on the coarser sanded perspex plate (0.695-0.355 mm).

### Morphology

Morphological features that might contribute to maintaining position in fast flowing water are examined (definitions of the terms used to describe S.E.M. photographs are given in Fig. 1.4). All genera studied have an external oral sucker. Fig. 1.4A, shows a ventral view of the oral

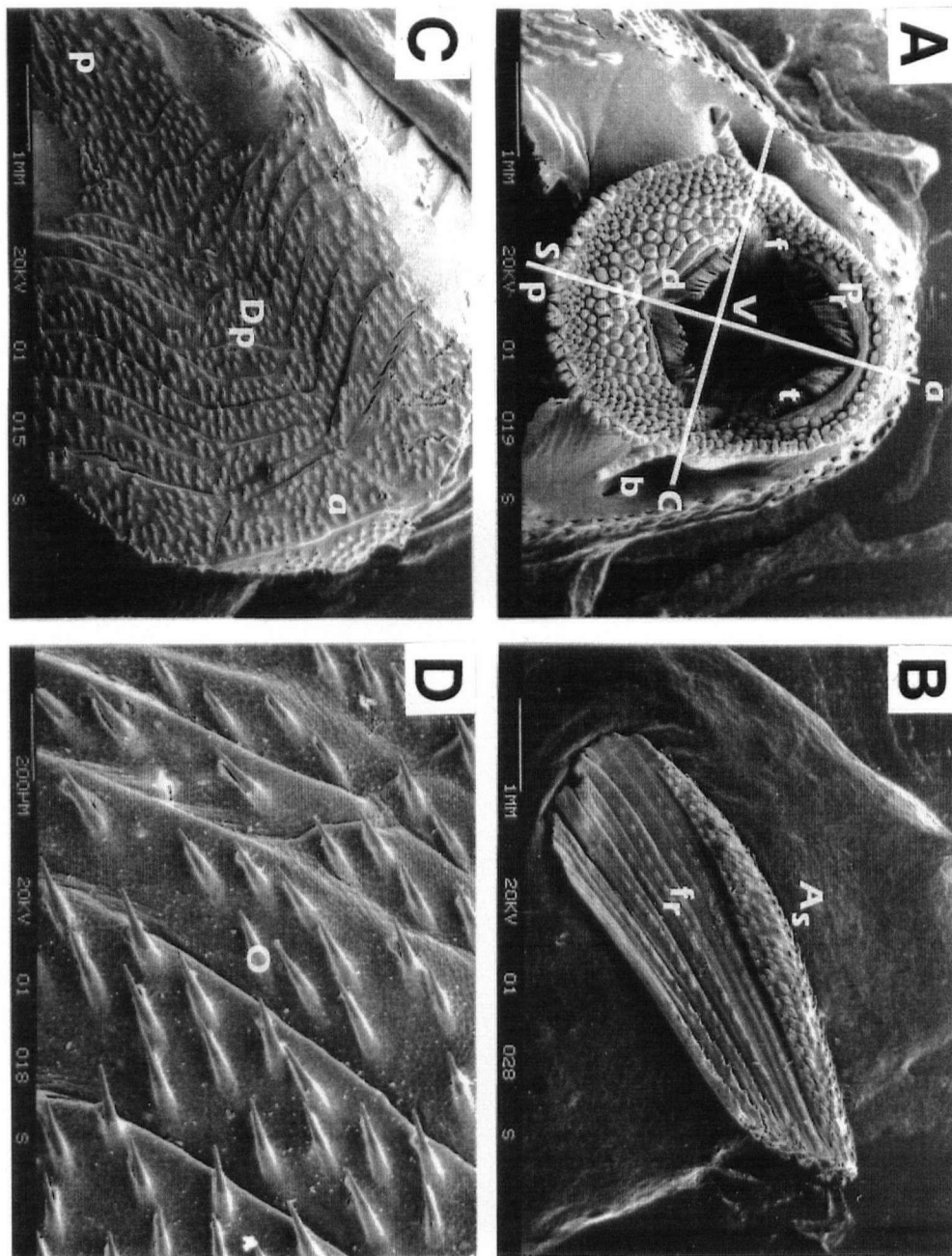


Fig. 1.4 S. E. M. photographs of *Otocinclus*'s oral sucker A (Outside diameter  $\approx 3.3$  mm) pectoral fin B (Anterior spine length  $\approx 5.4$  mm), ventral frictional pad C (length from anterior to posterior end  $\approx 7.1$  mm), and close up of the odontodes and dermal plates ( $\approx 200$   $\mu$ m in length) on the ventral frictional pad D. Scale is located in the bottom left hand corner of each picture. a anterior, p posterior, c cross-sectional axis, s sagittal axis, t teeth, v oral valve, f respiratory fissure, b maxillary barbel, As anterior pectoral fin spine, fr fine rays, Dp dermal plates, O odontodes, d dentary, Pr premaxillae.

sucker of *Otocinclus* which is covered in papillae. The teeth are spatulate and bifurcated distally. The posterior and anterior teeth are attached to the dentary and premaxillae respectively (Eaton, 1935). Teeth of the posterior and anterior oral sucker lips point towards the cross sectional axis running through the respiratory fissure. The teeth are separated into posterior and anterior, left and right by a septum lying in the saggital axis on each lip. Posterior to the maxillary barbels, between the posterior and anterior lips, is the respiratory fissure water passes through to enter the buccopharynx when the lips are applied to the substrate. The posterior lips are approximately 3.5 times thicker (thickness, measured from the inside to outside margin along the saggital axis) than the anterior lips (1.13 mm and 0.32 mm respectively). The oral valve lies in the center of the oral sucker and isolates the sucker from the buccopharynx.

*Hypostomus*, *Pterygoplichthys*, and *Farlowella* have oral sucker morphology that most closely resembles that of *Otocinclus*. In *Chaetostoma* the oral sucker lips are broader and the anterior and posterior lips are of equal size. For *Gyrinocheilus* the posterior and anterior oral sucker lips are fleshier than in the loricariids (see Benjamin, 1986 for a detailed description of the oral sucker in *Gyrinocheilus aymonieri*).

All the loricariid's have curved spines (odontodes) distributed in sockets of the dermal plates along their surface (Ørvig, 1977). Fig. 1.4D shows a magnified view of the ventral frictional pad in *Otocinclus*. The spiny odontodes that sit in sockets are scattered across the dermal plates surface. The arrangement of the odontodes along the body in *Pterygoplichthys* is different from the other species of loricariids

examined. In *Pterygoplichthys* dermal plates with odontodes are located in discrete lines running parallel with the body from the pectoral fins to the caudal peduncle. The odontode pattern in *Otocinclus*, *Hypostomus*, *Chaetostoma* and *Farlowella* covers the body more densely and is not isolated in lines along the body. Fig. 1.4B shows the pectoral fin of *Otocinclus*. The five loricariids examined all have odontodes covering their ventral and dorsal surface, pectoral and pelvic fin spines, pectoral and pelvic fin rays and dorsal fin rays and spines as seen in *Otocinclus*. *Pterygoplichthys* and *Chaetostoma* are the only genera that have no odontodes or dermal plates on the ventral surface in the area between the pelvic and pectoral fins.

*Otocinclus* is the only genus examined that has dermal plates on the ventral surface between the pelvic and pectoral fins organized laterally into a frictional pad (Fig. 1.4C). The spines are pointed and dermal plates overlapped in the downstream direction (Fig. 1.4D). In all genera the odontodes covering the body are curved in the direction of water flow and tend to lie parallel with the length of the body (Fig. 1.4A and 1.4B). However, in *Chaetostoma* the dorsal surface of the anterior pectoral fin spine has large odontodes projecting vertically from it. The five loricariids examined all have large anterior pectoral fin spines relative to their fin rays (Fig. 1.4B).

*Gyrinocheilus* has no obvious gross morphological features on the paired fins, dorsal and ventral surfaces that might act as frictional pads or anchoring devices other than its oral sucker.

## Geometry

Four ratios are determined,  $2b/h$ ,  $l/h$ ,  $x/l$ , and  $l/sp$  to allow for a comparison of overall form. Correlation coefficients significantly different from zero are found in all ratio plots against standard and total length (Fig. 1.5 - 1.8).

Fig. 1.5 shows the plot body width to height ratio ( $2b/h$ ) versus standard length. Only *Pterygoplichthys* shows a correlation coefficient significantly different from zero. Multiple pair wise comparisons between  $\overline{2b/h}$  values show significant differences between all of the means for *Otocinclus*, *Gyrinocheilus*, *Hypostomus*, *Chaetostoma*, and *Farlowella* (Table 1.1). For all genera examined  $\overline{2b/h}$  is significantly different from a ratio of one (two-tailed t-test, reject  $H_0: \mu=1$ ,  $p<0.05$ ) except *Gyrinocheilus* ( $p<0.05$ ,  $t = 0.886$ ,  $n = 25$ ). *Chaetostoma* has the flattest frontal profile (Table 1.1 and Fig 1.1).

Fineness ratio ( $l/h$ ) is plotted against total length in Fig. 1.6. *Chaetostoma* and *Farlowella* have correlation coefficients significantly different from zero (Table 1.1). Multiple pair wise comparisons between  $\overline{l/h}$  for *Otocinclus*, *Gyrinocheilus*, *Hypostomus*, and *Pterygoplichthys* show no significant difference between three of the loricariids (*Otocinclus*, *Hypostomus*, and *Pterygoplichthys*). It is not possible to determine which population *Pterygoplichthys* belongs to (Table 1.1). *Farlowella* has the highest fineness ratio (Table 1.1 and Fig. 1.1).

In Fig. 1.7  $x/l$  is plotted against total length. *Otocinclus*, *Chaetostoma*, and *Farlowella* have correlation coefficients not statistically different from zero. Multiple pair wise comparisons

between  $\overline{x/T}$  in these fish are significantly different from one another in all cases (Table 1.1). *Gyrinocheilus*, *Hypostomus*, and *Pterygoplichthys* have similar slopes (Table 1.1). *Otocinclus* and *Farlowella* have the point of maximal thickness displaced down the body the furthest and least respectively.

The total length to spine length ratio ( $l/l_{sp}$ ) is plotted against total length in Fig. 1.8. For *Gyrinocheilus*, *Pterygoplichthys*, *Hypostomus*, and *Chaetostoma* correlation coefficients are not statistically different from zero. Multiple pair wise comparisons between  $\overline{l/l_{sp}}$  indicate that there is a significant difference between means except for *Hypostomus* and *Pterygoplichthys* (Table 1.1). The slopes of *Otocinclus* and *Farlowella* are not significantly different from one another. The greatest  $\overline{l/l_{sp}}$  ratio is seen in *Farlowella* (Table 1.1 and Fig. 1.1).

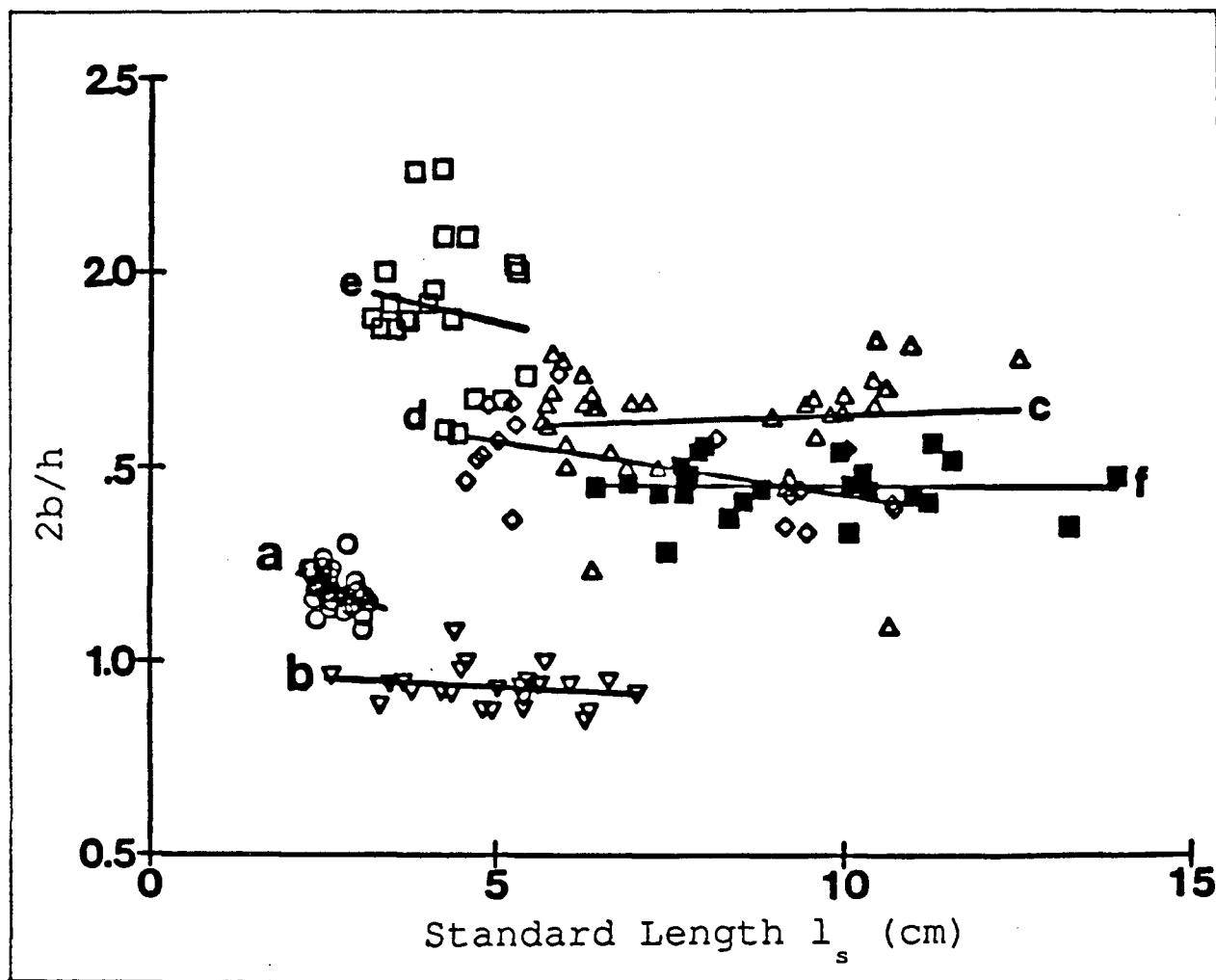


Fig. 1.5 Lines of best fit for body width to height ratio  $2b/h$  versus standard length for *Otocinclus* a (○), *Gyrinocheilus* b (▽), *Hypostomus* c (△), *Pterygoplichthys* d (◇), *Chaetostoma* e (□), and *Farlowella* f (■). The only line with a correlation coefficient ( $r^2 = 0.30$ ) significantly different from zero (t-test, reject  $H_0: \rho = 0$ ,  $p < 0.05$ ) is *Pterygoplichthys* (Table 1.1).

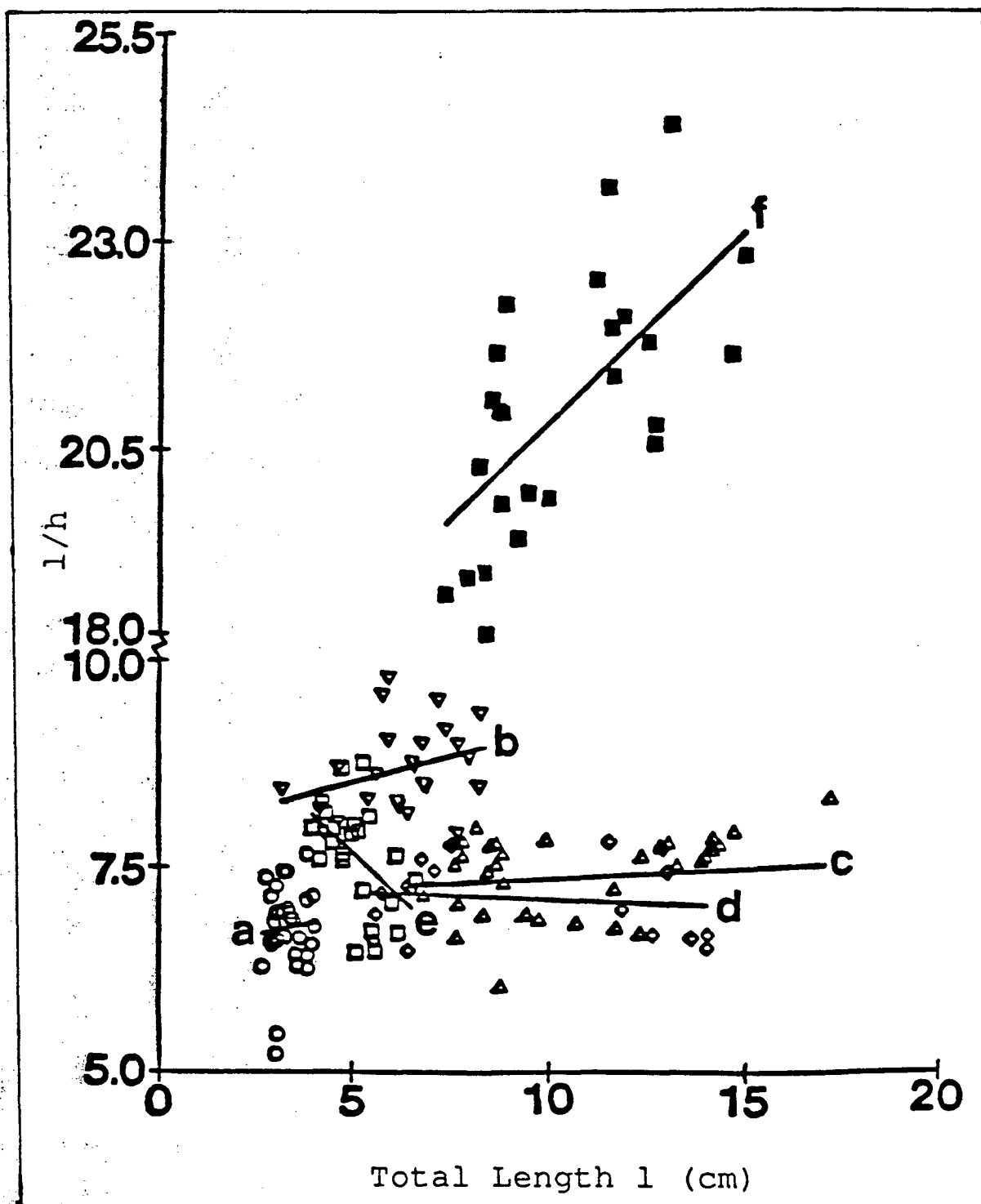


Fig. 1.6 Lines of best fit for fineness ratio versus total length for *Otocinclus* a (○), *Gyrinocheilus* b (▽), *Hypostomus* c (△), *Pterygoplichthys* d (◇), *Chaetostoma* e (□), and *Farlowella* f (■). *Chaetostoma* and *Farlowella* have correlation coefficients ( $r^2 = 0.24$  and  $0.43$ , respectively) significantly different from zero (t-test, reject  $H_0: \rho=0$ ,  $p < 0.05$ ; Table 1.1).

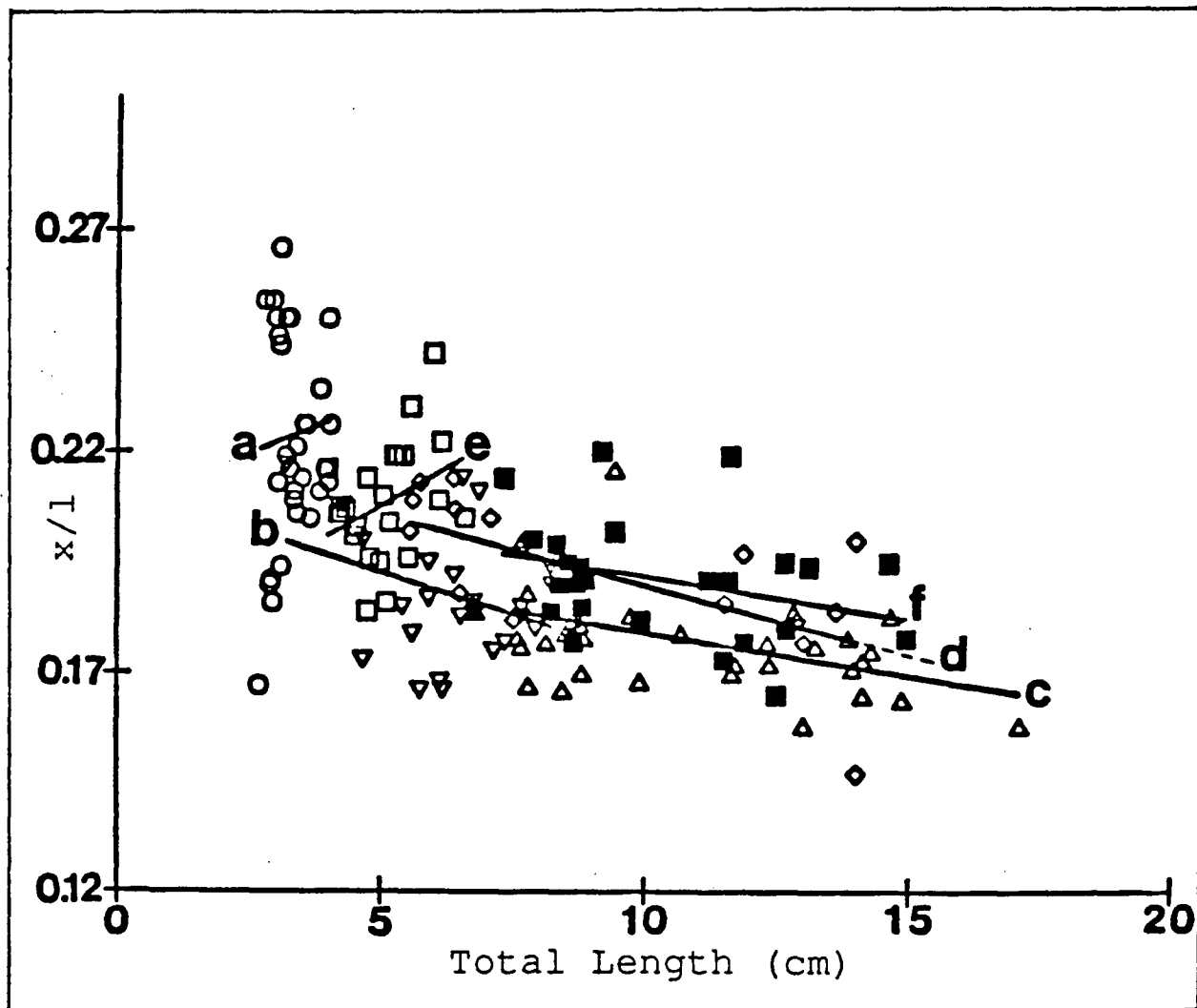


Fig. 1.7 Lines of best fit for  $x/l$  versus total length for *Otocinclus* a (o), *Gyrinocheilus* b ( $\nabla$ ), *Hypostomus* c ( $\Delta$ ), *Pterygoplichthys* d ( $\diamond$ ), *Chaetostoma* e ( $\square$ ), and *Farlowella* f ( $\blacksquare$ ). *Gyrinocheilus*, *Hypostomus* and *Pterygoplichthys* have correlation coefficients ( $r^2 = 0.11, 0.22$  and  $0.42$  respectively) significantly different from zero (t-test, reject  $H_0: \rho=0$ ,  $p < 0.05$ ) and common slope ( $b_c = -0.003$ ,  $p < 0.05$ ; Table 1.1).

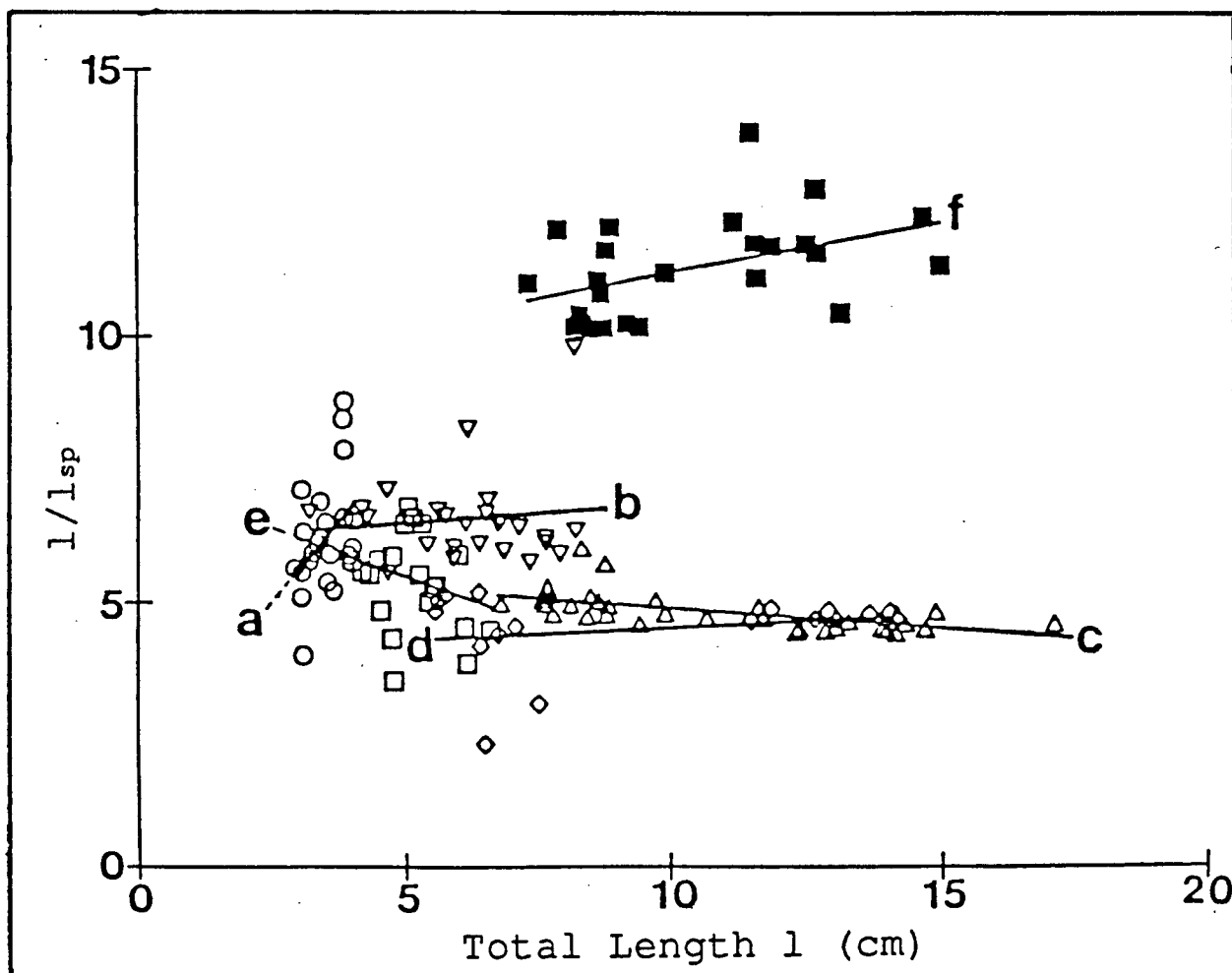


Fig. 1.8 Lines of best fit for  $l/l_{sp}$  versus total length for *Otocinclus* a (○), *Gyrinocheilus* b (▽), *Hypostomus* c (△), *Pterygoplichthys* d (◇), *Chaetostoma* e (□), and *Farlowella* f (■). *Otocinclus* and *Farlowella* have correlation coefficients ( $r^2 = 0.17$  and  $0.21$  respectively) significantly different from zero (t-test, reject  $H_0: \rho=0$ ,  $p<0.05$ ; Table 1.1).

	n	2b/h =	r <sup>2</sup>	2b/h	S.E.	1/h =	r <sup>2</sup>	1/h	S.E.	x/1 =	r <sup>2</sup>	$\bar{x}/T$	S.E.	1/I <sub>sp</sub> =	r <sup>2</sup>	T/I <sub>sp</sub>	S.E.
a) <i>Otocinclus</i>	35	-0.075(1 <sub>S</sub> )+1.384	0.18	1.183	0.008	0.102(1)+6.416	0.01	6.756	0.085	0.005(1)+0.208	0.01	0.224	0.004	1.203(1)+2.012	0.17 <sup>*</sup>	6.223	0.222
b) <i>Gyrinocheilus</i>	25	-0.009(1 <sub>S</sub> )+0.979	0.05	0.969	0.035	0.127(1)+7.881	0.10	8.670	0.104	-0.004(1)+0.212	0.11 <sup>*</sup>	0.188	0.003	0.065(1)+6.139	0.01	6.542	0.172
c) <i>Hypostomus</i>	36	0.006(1 <sub>S</sub> )+1.570	0.01	1.622	0.025	0.024(1)+7.110	0.01	7.370	0.104	-0.002(1)+0.199	0.22 <sup>*</sup>	0.178	0.002	-0.075(1)+5.632	0.04	4.822	0.057
d) <i>Pterygoplichthys</i>	17	-0.027(1 <sub>S</sub> )+1.701	0.30 <sup>*</sup>	1.465	0.056	-0.019(1)+7.287	0.02	6.916	0.253	-0.003(1)+0.222	0.42 <sup>*</sup>	0.192	0.004	0.047(1)+4.052	0.05	4.494	0.176
e) <i>Chaetostoma</i>	22	-0.041(1 <sub>S</sub> )+2.072	0.02	1.918	0.048	-0.450(1)+9.929	0.24 <sup>*</sup>	7.620	0.138	0.007(1)+0.174	0.12	0.209	0.003	-0.359(1)+7.259	0.07	5.416	0.201
f) <i>Farlowella</i>	25	-0.0002(1 <sub>S</sub> )+1.454	0.01	1.452	0.014	0.459(1)+16.76	0.43 <sup>*</sup>	21.51	0.308	-0.002(1)+0.211	0.10	0.191	0.003	0.193(1)+9.223	0.21 <sup>*</sup>	11.22	0.187
Multiple Comparisons																	
Among Slopes. H <sub>0</sub> :p=0		d	<u>c</u> <u>f</u>		<u>b c d</u> , b <sub>c</sub> =-0.003		<u>a f</u> b <sub>c</sub> =0.218										
rejected (p < 0.05)			q=3.98, d.f.=110		q=3.92, d.f.=148		q=3.92, d.f.=135										
Multiple Comparisons																	
Among Means. H <sub>0</sub> :p=0		<u>a b c e f</u>	<u>a d c b</u>		<u>a c f</u>		<u>e c d b</u>										
accepted (p < 0.05)		q=3.66, d.f.=138	q=3.74, d.f.=109		q=3.40, d.f.=79		q=3.74, d.f.=95										

Table 1.1 Sample size n, ratio means ( $2b/h$ ,  $1/h$ ,  $\bar{x}/T$ , and  $1/I_{sp}$ ) coefficient of determination  $r^2$ , multiple pair wise comparisons among slopes and means, common slope  $b_c$  and best fit regression equations for Fig. 1.5 to 1.8 in *Otocinclus*, *Gyrinocheilus*, *Hypostomus*, *Pterygoplichthys*, *Chaetostoma*, and *Farlowella*. Correlation coefficients significantly different from zero (\*) Tukey statistic q and degrees of freedom df.

## DISCUSSION

Fast stream fish face the continuous task of preventing displacement. Fish may accomplish this by seeking cover behind large stones and back eddies or burrowing into the substrate (Daniels, 1989; Burgess, 1989). However, the need to find food (algal mats, Colgan and Cross 1982) exposes them to fast currents. Morphology and behaviour that reduces displacement is, therefore, advantageous.

The main adaptations of fish in this study to station-holding are oral suction, spines, overlapping dermal plates and odontodes pointing in the downstream direction (Fig. 1.4C and D). Odontodes, spines and dermal plates provide a method of increasing frictional coefficients by acting as anchors on substrates. In particular, the ventral location of *Otocinclus*'s frictional pad (Fig. 1.4C and D) provides a weight bearing surface which enhances its effect. In addition, the long anterior spines of the loricariids (Fig. 1.4B) provide anchors which resist displacement. *Hypostomus*, *Pterygoplichthys*, and *Chaetostoma* have the lowest  $l/l_{sp}$  ratios (Table 1.1). These fish are also found in the fastest waters (Burgess, 1989). Longer anterior spines projecting from the body may increase drag, however, this is countered by providing a greater surface for anchorage and increasing frictional coefficients.

*Gyrinocheilus*'s pectoral and pelvic fins are flexible compared to those of the loricariids. This flexibility allows bending and greater contact between the fin rays and substrate helping to maximize slipping speed (Fig. 1.3). In the loricariids the lack of flexibility in the pectoral and pelvic fins is compensated for by odontodes covering the fin

spines. From roughness element results it is apparent that frictional pads (*Otocinclus*), fin spines and odontodes are advantageous to increasing frictional coefficients and acting as anchors on coarse surfaces in all loricariids (Fig. 1.4). These spines may anchor the fish to algal mats on which they feed. There is no obvious gross external morphology in *Gyrinocheilus* in the form of frictional pads or spines that may be used to prevent displacement. However, Lundberg and Marsh (1976) found that the anterior fin ray segments of the pectoral fins have been shortened to possibly resist pressure due to fin appression. In addition, thickened skin and spines along the fins surface of *Gyrinocheilus* and loricariids respectively can act to prevent mechanical abrasion similar to the keratinized skin of the cat fish *Bagarius bagarius* (Mittal and Whitear, 1979). In a natural habitat, fish may have the option of choosing a particular substrate where morphology is best adapted to maximize friction and slipping speed.

The loricariids erect the pelvic fins, pushing the head against the substrate to form a wedged posture that may increase their station-holding ability in a similar manner as that observed in the crayfish (Maude and William, 1983). In *Otocinclus* this brings the frictional pad (Fig. 1.4C) into contact with the substrate allowing the bony scutes to act as frictional devices. Furthermore, the negative angle of the pectoral fins in all genera (Fig. 1.1) may produce forces pushing the fins against the substrate (negative lift). Matthews (1985) argues that the pectoral fins do not act as negative lift hydrofoils (based on the results of amputation experiments) in darters (*Percina roanoka* and *Etheostoma flabellare*). Negative lift may not produce detectable changes

in slipping velocity on smooth surfaces, however, on rougher surfaces negative lift may maintain stability and keep the fins stationed for anchorage.

There are a number of descriptions of the environments occupied by fish in this study (eg. Boseman, 1968; Sterba, 1983; Burgess, 1989). Species of the genus *Chaetostoma* (*C. fischeri*) are found in high altitude mountain streams or large rivers where water velocities exceed  $40 \text{ cm s}^{-1}$  (Gee, 1976). Even on a smooth perspex surface these fish are able to prevent displacement nearly  $10 \text{ cm s}^{-1}$  above this value (Fig 1.3). The lack of ventral dermal plates provides increased contact between the smooth perspex surface and body. This may result in increased frictional forces and the high  $V_1$  and  $V_2$  observed. Members of *Hypostomus* and *Pterygoplichthys* are often found in riffles or cataracts (water velocity  $\gg 40.0 \text{ cm s}^{-1}$ ) and are unable to exploit slower flow habitats (Burgess, 1989). Boseman (1968) records that during dam construction, where back flooding produced stagnant pools, large numbers of *Hypostomus* died because adults were unable to traverse slower moving waters of lower oxygen content. For *Hypostomus*  $V_1 - V_2$  is lower than *Pterygoplichthys*. Under similar flow conditions *Hypostomus* may place a greater reliance on friction rather than suction relative to *Pterygoplichthys*. The loriciid's odontodes and spines may be less effective than suction for gripping the smooth perspex surface. Therefore, fish that rely on friction for preventing displacement have reduced station-holding ability. The movement of *Pterygoplichthys* on the roughness element may be attributed to low friction (lack of dermal plates and odontodes between the pelvic and pectoral fins) and suction (inadequate seal). Arguably,

fish of similar morphology with relatively high  $\overline{V_2}$  and low  $\overline{V_1 - V_2}$  place a greater reliance on frictional devices rather than suction.

The pectoral fin extension stage of *Otocinclus* is not seen in the other genera of fish. A possible reason is that the ventral frictional pad is sufficient to hold station up to  $V_1$ . For *Otocinclus*, fin extension may only become necessary for additional anchorage when slipping occurs.

Whenever water velocity is increased adhesion occurs. The suction force and other rheotactic behaviour preventing displacement are reflected by the  $\overline{V_1 - V_2}$  difference shown in Fig. 1.3. The ability to maximize  $\overline{V_1 - V_2}$  will vary between genera depending on the effectiveness of rheotactic behaviours. In the loricariids the respiratory gap remains open under all flow conditions. Water is drawn through the fissure (Fig 1.4A), posterior to the maxillary barbel and pushed past the gills by contractions of the buccopharynx. During contraction of the buccopharynx an oral valve (Fig. 1.4A) closes isolating the oral sucker (Gradwell, 1971). The fissure posterior to the maxillary barbel must remain open to allow water flow. This prevents the formation of a complete seal by the oral sucker lips (Alexander, 1965). Although this is the case it is apparent that loricariids produce suction (Alexander, 1965). Loricariids have several options for producing suction. Water can be drawn rapidly through spaces between the papillae and respiratory fissure which will form a partial vacuum (open sucker), or the respiratory current may be stopped and the oral sucker cavity isolated (closed sucker) by sealing the lips to the substrate similar to *Gyrinocheilus*. Benjamin (1986) suggests that due to oral sucker structure, vacuum suction using a complete seal is not possible for loricariids (eg. *Plecostomus punctatus*

and *Otocinclus mariae*). Observations support these conclusions and indicate that during fast flow the size of the fissure becomes smaller but, does not close. Vandewalle et al. (1986) also noticed that narrowing of the fissure occurred during adhesion in *Plecostomus punctatus*. A reduction in oxygenated water passing by the gills can be compensated for by water pumped into the intestine by contractions of the cloaca (Sawaya and Petrini, 1960). In addition, movement of the operculum can produce water circulation that aids in providing oxygen.

*Gyrinocheilus*'s high slipping velocity may be attributed to its ability to form a complete seal with its oral sucker. In *Gyrinocheilus* during adhesion water flows into the buccopharynx through oral valves (modifications of the brachial chambers) above the operculum. Sealing the oral sucker lips onto a surface and isolating the oral cavity allows the formation of a closed vacuum sucker. This is reflected in the high  $V_1 - V_2$  for *Gyrinocheilus* (Fig. 1.3). The tendency for *Gyrinocheilus* to drift off of the roughness element and adhere to the perspex indicates it may find a seal easier to attain on a smoother surface. This behaviour is supported by Benjamin (1986), where it was found that *Gyrinocheilus* had difficulty attaching to surfaces in which holes or grooves had been made.

Arguably, *Farlowella*'s oral sucker functions to a greater extent for feeding rather than preventing displacement. It has been suggested that *Farlowella* uses its long slender profile (high  $l/h$ , Fig. 1.1 and Table 1.1) and elongated rostrum for camouflage. *Farlowella* resembles twigs or branches when hiding in rotting leaves along the banks of rivers (Wheeler, 1975). *Farlowella*'s passive orientation to water flow suggests that it would have difficulty coping with swiftly moving water even

though  $\sqrt{V_1 - V_2}$  is large (Fig. 1.3). Having no way of attaching the extended caudal peduncle (past the pelvic fins) to the substrate can produce the destabilizing effect observed at higher water velocities due to lift over this portion of the body. Camouflage from predators (birds and fish) may have higher priority in determining body design (Power, 1984). *Gyrinocheilus* may also experience lifting forces similar to *Farlowella* over the latter half of the body. *Gyrinocheilus* is another high fineness ratio form (Table 1.1 and Fig. 1.6) and has difficulty keeping its tail on the bottom when caught with the pelvic fins off the substrate by a rapid increase in water velocity. However, unlike *Farlowella*, its rheotactic adaptations are able to effectively counter lift and bring the body back against the substrate.

Geometry (ratios  $2b/h$ ,  $l/h$  and  $x/l$ ) effects the lift, drag and flow conditions experienced. These ratios are plotted against length (Fig. 1.5 - 1.7) to determine if they are near values for low drag and if there is consistency in geometry with length in genera. For technical bodies attached to a surface the ratios of  $l/h$ ,  $2b/h$ , and  $x/l$  for low drag and lift are approximately 10, 2.0 and 0.3 respectively (Hoerner, 1965). The fast stream fish *Chaetostoma* has similar values for these ratios (Table 1.1). In general the frontal profile and fore body ( $x$ ) of the fast stream loricariids is flattened and extended respectively (Table 1.1). Extending and flattening the fore body delays separation of the boundary layer reducing pressure drag (Hoerner, 1965). In addition, folding of the tail and dorsal fin against the body would reduce drag in all genera. *Farlowella*, a slower stream fish, has a  $l/h$  above and  $x/l$  below low drag values (Fig. 1.6, 1.7 and Table 1.1). Trade offs between lift and drag

are influenced by body morphology. Unlike *Farlowella*, rheotactic behaviour in the plaice, *Pleuronectes platessa*, compensates for high lift forces caused by its flattened profile and high fineness ratio (Arnold and Weihs, 1978; Webb, 1989).

Geometry is consistent over the range of lengths measured within genera with correlations being low (Fig. 1.5 - 1.7 and Table 1.1). Burgess (1989) records that generally, smaller loricariids are found near the edges of fast flowing rivers where water velocity is diminished. Matthews (1985) suggests that differences in morphology between species of darters allows for the exploitation of different benthic, riffle, micro habitats. Statzner and Holme (1989) analyzed the water flow around several lotic macro invertebrates and concluded that to accommodate Reynold's number effects body geometry must change as the organism grows (lotic invertebrates). Based on the above hydrodynamic considerations changes in geometry with size may also effect the distribution of fast stream fish within rivers.

In general, *Otocinclus*, *Gyrinocheilus*, *Hypostomus*, *Pterygoplichthys*, and *Chaetostoma* face fast currents and maximize slipping speed by using frictional devices (spines, odontodes and frictional pad) and rheotactic behaviour (suction and fin extension). Although *Farlowella* is able to maintain station at higher water velocities, morphological and behavioural characteristics suggest that other constraints besides fast flow are more important for governing adaptation to its habitat. This leads to considerations, addressed in Chapter II, about the hydrodynamic forces acting on these fish.

## CHAPTER II

## MECHANICS AND ENERGETICS

## ABSTRACT

The behavioural and morphological adaptations of hill stream fish found in fast flow (*Otocinclus*, *Gyrinocheilus*, *Hypostomus*, *Pterygoplichthys*, and *Chaetostoma*) and slow flow (*Farlowella*) are analyzed using a hydrodynamic model developed by Arnold and Weihs (1978). Drag coefficients are directly measured using strain gauges and force platforms. Lift coefficients are determined from the model (based on the slipping velocities of dead fish and morphological measurements from Chapter I).

Mean drag coefficients (referenced to projected frontal area) in fast stream fish range between 0.2 and 0.9. Drag coefficients are elevated due to roughness and interference drag produced by the pectoral fins. Fast stream fish compensate for higher drag coefficients and maximize slipping speed through high density ( $1.06 \text{ g cm}^{-3}$  -  $1.10 \text{ g cm}^{-3}$ ), frictional coefficients (0.63 - 0.95, on a perspex surface) and rheotactic suction pressure ( $2.0 \text{ N m}^{-2}$  -  $173 \text{ N m}^{-2}$ ). In addition, negative lift coefficients are calculated for *Pterygoplichthys* (-0.03) and *Chaetostoma* (-0.29 to -0.55). These values are attributed to forces produced by the pectoral fins that are orientated at a negative angle to the flow.

*Farlowella*, a slower water form, is characterized by relatively low drag coefficients (0.23), high fineness ratio (total length/height  $\approx 21$ )

and density ( $1.129 \text{ g cm}^{-3}$ ). However, orientation to water flow is slow, the lift to drag ratio and lift coefficient are high (6.7 and 1.52 respectively) and rheotactic suction pressure ( $2.0 \text{ N m}^{-2}$  -  $27 \text{ N m}^{-2}$ ) is low.

In addition, estimated drag coefficients are compared to measured values. The closest agreement is for high fineness ratio forms (eg. *Farlowella*). It is shown that force coefficients for forms of low fineness ratio ( $l/h < 10$ ) at low Reynold's number ( $< 10^4$ ) attached to a surface can not be accurately predicted from data on technical bodies.

Oxygen consumption is measured in a specimen of *Pterygoplichthys* (mass = 318.5 g) at various water velocities ( $20 \text{ cm s}^{-1}$  -  $160 \text{ cm s}^{-1}$ ). The mean  $\text{O}_2$  consumption rate increases from  $52 \text{ mg O}_2 \text{ kg}^{-1} \text{ hr}^{-1}$  to  $97 \text{ mg O}_2 \text{ kg}^{-1} \text{ hr}^{-1}$  when slipping occurs and repositionings per minute increase (slipping velocity =  $110 \text{ cm s}^{-2}$ ). Oxygen consumption rates at higher water velocities ( $110 \text{ cm s}^{-1}$  -  $160 \text{ cm s}^{-1}$ ) are lower than those for fish of similar size swimming in the free stream. Station holding on a substrate reduces the energy required to maintain position against rapidly moving water.

## INTRODUCTION

Arnold and Weihs (1978) developed a mathematical model for analyzing the hydrodynamic forces acting on the plaice (*Pleuronectes platessa*). Webb (1989) applied this model to *Pleuronectes platessa*, *Raja clavata* and *Myoxocephalus scorpius*. These fish experience forces from ocean currents and show behaviour that may be advantageous to maintaining position by reducing or opposing lift and drag acting on the body. The difficulty faced in both these studies in assessing forces on the body is that either the lift coefficient  $C_L$  or drag coefficient  $C_D$  must be known.  $C_D$  and  $C_L$  are not easily attained. Both Arnold and Weihs (1978) and Webb (1989) resort to estimates of  $C_D$  based on technical data for blisters attached to smooth surfaces. Blake (1985) was able to measure the lift and drag force acting on the carapaces of three crab species (*Callinectes sapidus*, *Cancer productus*, and *Lopholithodes mandtii*). Fish found in rivers may experience higher and more consistent water flow than ocean currents. Body morphology and behaviour that aids in station-holding reduces the energy required to prevent displacement expended through swimming or actively holding to the substrate. Arguably, preventing displacement and adaptations for station-holding are important. Fish may maximize slipping speed by increasing friction and submerged weight (density), decreasing drag, reducing positive lift or producing negative lift.

In this study the drag coefficients  $C_D$  in members of the South American and East Asian hill stream fish belonging to the genera *Otocinclus*, *Hypostomus*, *Pterygoplichthys*, *Chaetostoma*, *Farlowella* and

*Gyrinocheilus* are determined. From drag, morphological and slipping velocity measurements (Chapter I and II) the effectiveness of body design and rheotactic behaviour in hill stream fish is assessed. In addition, the oxygen consumption rate of a specimen of *Pterygoplichthys* is measured.

## MATERIALS AND METHODS

To estimate the projected frontal area of fish, measurements of maximal body width  $2b$ , maximal body height  $h$ , and spine length  $l_{sp}$  were taken from Chapter I. Additional morphological measurements (perpendicular angle relative to fin extension,  $\phi$ , and anterior pectoral fin spine width  $W$ ) were made using calipers (30 cm, Helios  $0.005 \pm 0.0025$ ). Spine width was measured from the center of the anterior pectoral fin spine or ray (see Fig. 2.1).

### Model

Hill stream fish face two main forces that act to displace them down stream; drag and lift. For the fish to slip the drag  $D$  required must be equal to the product of the frictional forces generated by their weight  $W_o$  and the static frictional coefficient  $\mu$  between the substrate and the ventral surface of the fish (see Fig 2.2; Arnold and Weihs, 1978).

$$D = \mu W_o \quad (2.1)$$

However, as water flows over the fish lift  $L$  acts on  $W_o$ .

$$D = \mu (W_o - L). \quad (2.2)$$

Fig. 2.2 illustrates the forces acting on a hill stream fish. Lift may act in a positive (away from the substrate) or negative (towards the

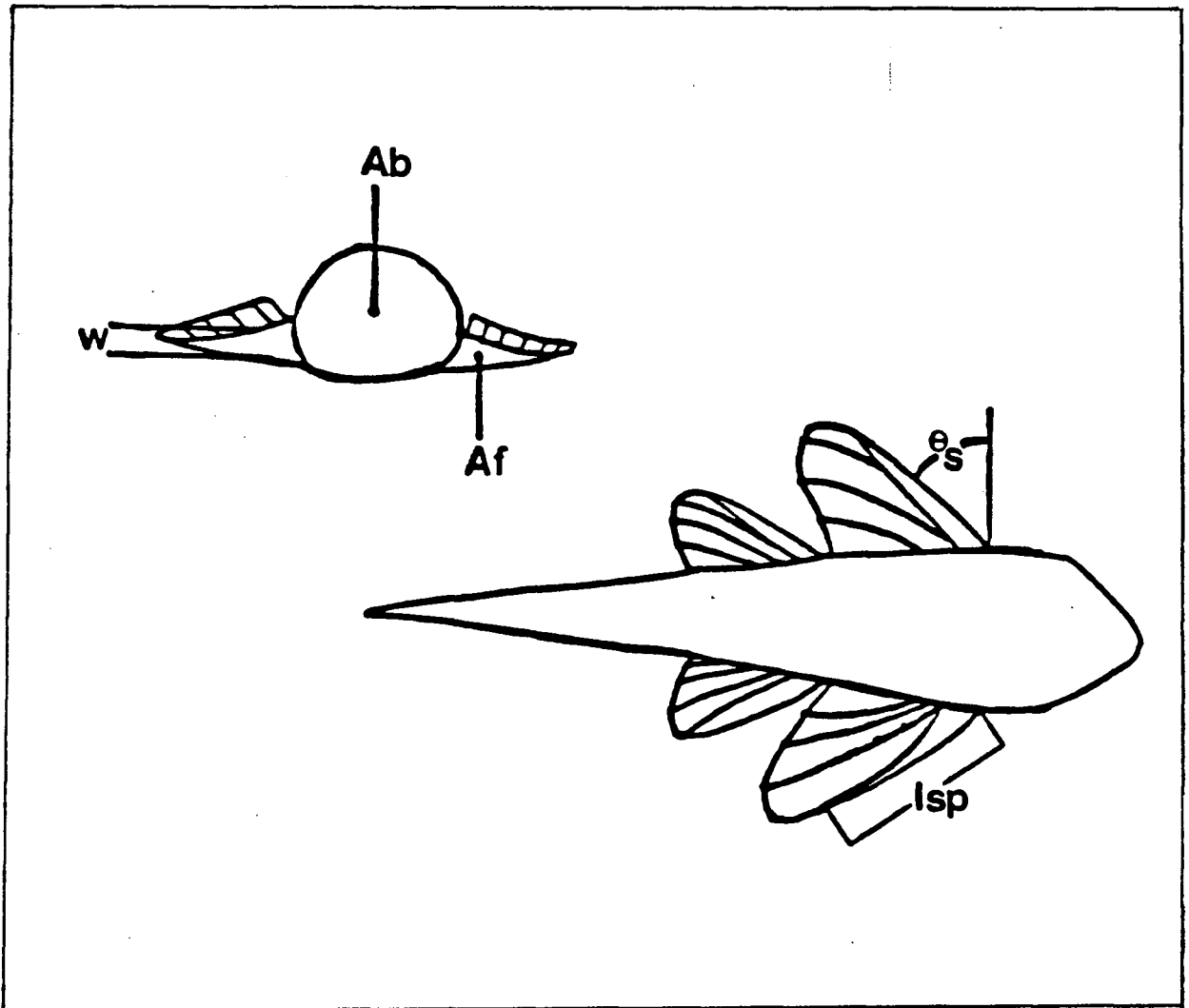


Fig. 2.1 Measurements required for estimating the projected frontal area of the body  $Ab$ , and projected frontal area of pectoral fin anterior spine or fin ray  $Af$ . Pectoral spine width  $W$ , perpendicular insertion angle of the pectoral fin spine  $\theta_s$ , and spine length  $l_{sp}$ .

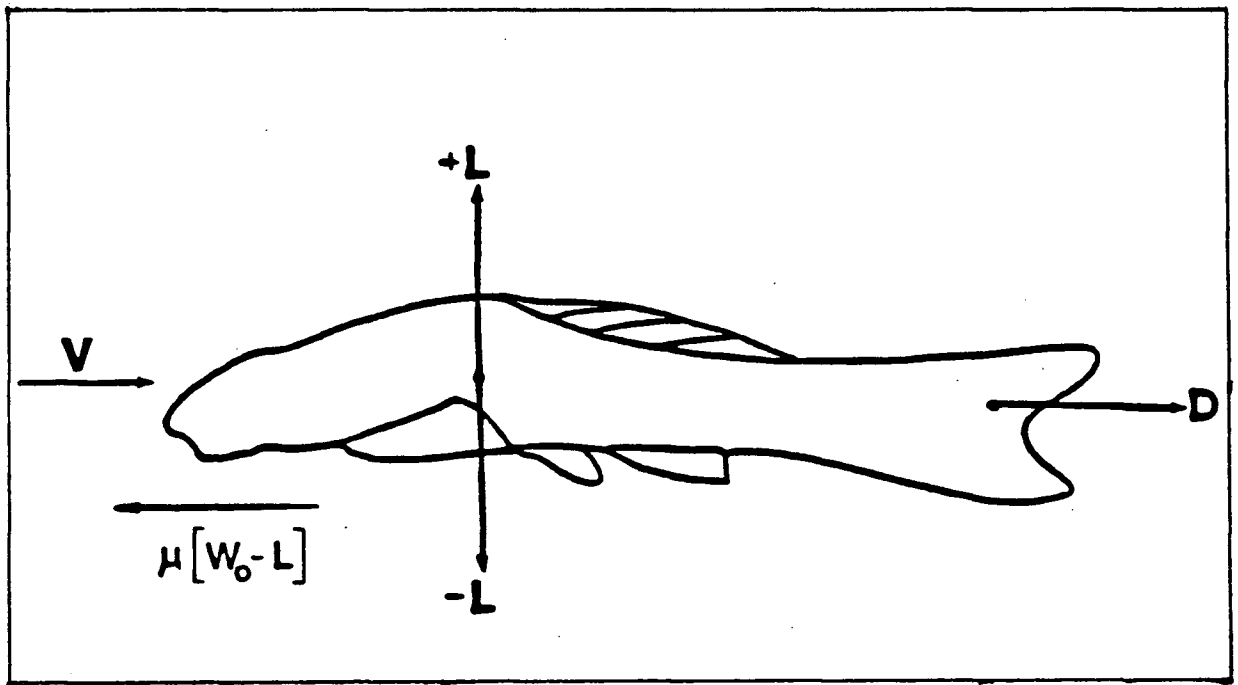


Fig. 2.2 Forces acting on the body of a hill stream fish. Lift  $L$  (negative and positive), drag  $D$ , submerged body weight  $W_0$ , static frictional coefficient  $\mu$  and velocity  $V$ . Slipping speed is maximized by increasing  $-L$ ,  $\mu$ , and  $W_0$  and reducing  $D$ .

substrate) direction. Positive lift acts to reduce the submerged weight of the fish and, therefore, the frictional forces opposing drag. Negative lift acts in the opposite manner. When the frictional force becomes less than the drag force slipping occurs. Drag at slipping can be expressed as

$$D = \frac{1}{2} A C_D V_2^2 \rho_w, \quad (2.3)$$

where  $A$  is the total projected frontal area,  $C_D$  is the frontal drag coefficient,  $V_2$  is the dead slipping velocity (determined in Chapter I) and  $\rho_w$  is the density of the water (998.2 kg m<sup>-3</sup> at 26° C). Lift at slipping is given by

$$L = \frac{1}{2} A C_L V_2^2 \rho_w, \quad (2.4)$$

where  $C_L$  is the lift coefficient referenced to  $A$ . By inserting equations 2.3 and 2.4 into 2.2 we have (Arnold and Weihs, 1978)

$$\frac{A C_L V_2^2 \rho_w}{2 \mu} = W_o - \frac{1}{2} A C_D V_2^2 \rho_w \quad (2.5)$$

and

$$\frac{2 W_o}{\rho_w A V_2^2} = C_L + \frac{C_D}{\mu}, \quad (2.6)$$

$W_o$ ,  $A$ ,  $V_2$ ,  $\mu$  and  $C_D$  of this equation are measured here, leaving  $C_L$  as an unknown, which can be solved for

$$C_L = \frac{2 W_o}{\rho_w A V_2^2} - \frac{C_D}{\mu}. \quad (2.7)$$

### Rheotactic Pressure

The suction pressure produced for station-holding by rheotactic behaviour was not directly measured. Suction pressure was estimated based on morphological measurements, slipping velocities, and drag coefficients. Using equation 2.3 the drag on live and dead fish at  $V_1$  and  $V_2$  (live and dead slipping velocities respectively on a smooth perspex surface; Chapter I) was determined. The difference between the drag on a live and dead fish is an estimate of the lateral force applied by suction and other rheotactic behaviour that opposes displacement. Dividing the force by a surface area (total ventral area or sucker area) yields a pressure ( $S_1$  or  $S_2$  respectively,  $\text{N m}^{-2}$ ).

### Model Variables

Total projected frontal area  $A$  is the sum of the frontal area of the body  $A_b$  and anterior pectoral fin spine or ray  $A_f$  ( $A = A_b + A_f$ ). For the loricariids (*Otocinclus*, *Hypostomus*, *Pterygoplichthys*, *Farlowella*, and *Chaetostoma*)  $A_b$  was estimated using the equation for the area of an ellipse  $\pi (b (h/2))$  and for *Gyrinocheilus* the area of a circle  $\pi (h/2)^2$ . To ensure that this was an accurate representation of  $A_b$  a different method of estimation was also used. Head on photographs of fish were taken (see Chapter I for method). Outlines were then traced using a Houston Instruments Hipad digitizer and mouse to estimate the area. For convenience the geometric method was employed to determine  $A_b$ . Tracings were also taken and digitized to determine the ventral surface area of

the body and sucker for calculating  $S_1$  and  $S_2$  respectively.

$A_f$  was estimated by considering the angle which the anterior pectoral fin spines made relative to a perpendicular line drawn from the insertion point in the body  $\emptyset_s$ , its length  $l_{sp}$  and width  $W$  (Fig. 2.1).

$$A_f = W (l_{sp} \cos \emptyset_s) \quad (2.8)$$

This estimate is based on the assumption that  $W$  is constant from the point of insertion to the distal end. In reality this is not the case. The spines are slightly tapered towards the distal end. Measurement of the spine was made from the center giving an estimate of  $W$ . Only the anterior spine was considered for determining projected frontal area of pectoral fins in the loricariids because it was the only portion of the fin that appeared to have a stable projected area during drag measurements. However, *Gyrinocheilus*'s fin rays were relatively stable and made up a significant proportion of  $A$  (40 % - 50 %). Estimates of fin ray area in *Gyrinocheilus* were made using frontal photographs and were included in  $A$ . In addition,  $\emptyset_s$  was determined based on the observed angle of the fins for fish in a rheotactic posture ( $\emptyset_s \approx 10^\circ$  for *Otocinclus*, *Hypostomus*, *Pterygoplichthys*, *Chaetostoma* and *Farlowella*;  $\emptyset_s \approx 5^\circ$  for *Gyrinocheilus*). For fish with the dorsal fin extended during drag measurements similar methods were applied to estimate the projected frontal area of the dorsal spine.

### Coefficient of Friction

A freshly killed fish was placed, facing uphill in the center and parallel with the length of a submerged perspex plate (20 cm X 20 cm). The plate was secured at one end by a hinge and gently raised by a string attached to the other end. As soon as the fish began slipping backwards raising of the plate was stopped and the string secured. The angle between the bottom and perspex plate  $\emptyset$  was then measured with a protractor and calculated using  $\mu = \tan \emptyset$ .

### Density

Dry and submerged mass was measured with a Mettler PK 300 ( $\pm 0.0005$  g) weighing scale and suspension apparatus. Fish were killed with a strong solution of MS222 shortly before being placed on the scale. Submerged mass included gas trapped in their bone-encased swim bladder and accessory respiratory organ (Gee, 1976). Air bubbles trapped in their oral sucker during transfer to the scale were tapped out with a dissecting needle. Submerged mass was multiplied by the gravitational acceleration constant ( $9.78 \text{ m s}^{-2}$ ) to determine the weight of the fish. The density of a fish  $\rho$  was determined from

$$\rho = \frac{W_a}{(W_a - W_o)} \rho_w, \quad (2.9)$$

where  $W_a$  and  $W_o$  is the dry and wet weight of the fish respectively.

## Flow tank

For these experiments the flow tank described in Chapter I was modified. A perspex plate (0.6 cm X 20 cm X 10 cm) was fitted in front of the flow straightener to prevent over flow. In addition, a forward (0.6 cm X 40 cm X 20 cm), center (0.6 cm X 20 cm X 20 cm) and end (0.6 cm X 16 cm X 20 cm) perspex plate, was fitted on the top of the flow tank level with the flow rectifying grid and secured using rubber stoppers. A hole was cut into the center plate for the insertion of a force plate. Four different center plates were made to accommodate four different shaped force plates. The water level was kept at 1.0 cm above the plates (Fig. 2.3).

Four sizes of perspex force plates, 0.6 cm thick (4.5 cm X 4.0 cm; 4.8 cm X 2.3 cm; 7.2 cm X 2.5 cm; and 9.0 cm by 6.0 cm) were machined for the differently sized and shaped fish (Fig. 2.3). The force plates were shaped as blunt elongated diamonds to form to the fish body and reduce frictional drag. To each force plate two extension struts (0.3 cm diameter by 3.0 cm long) were attached which in turn were attached to a another perspex plate (0.2 cm X 1.5 cm X 7.5 cm). On either end of the plate threaded blocks (1.5 cm X 1.5 cm X 1.5 cm) were glued that joined the force plate to the strain gauges via the shim stock with screws. The two struts were used to extend the shim stock above the water line which reduced the drag acting on the system.

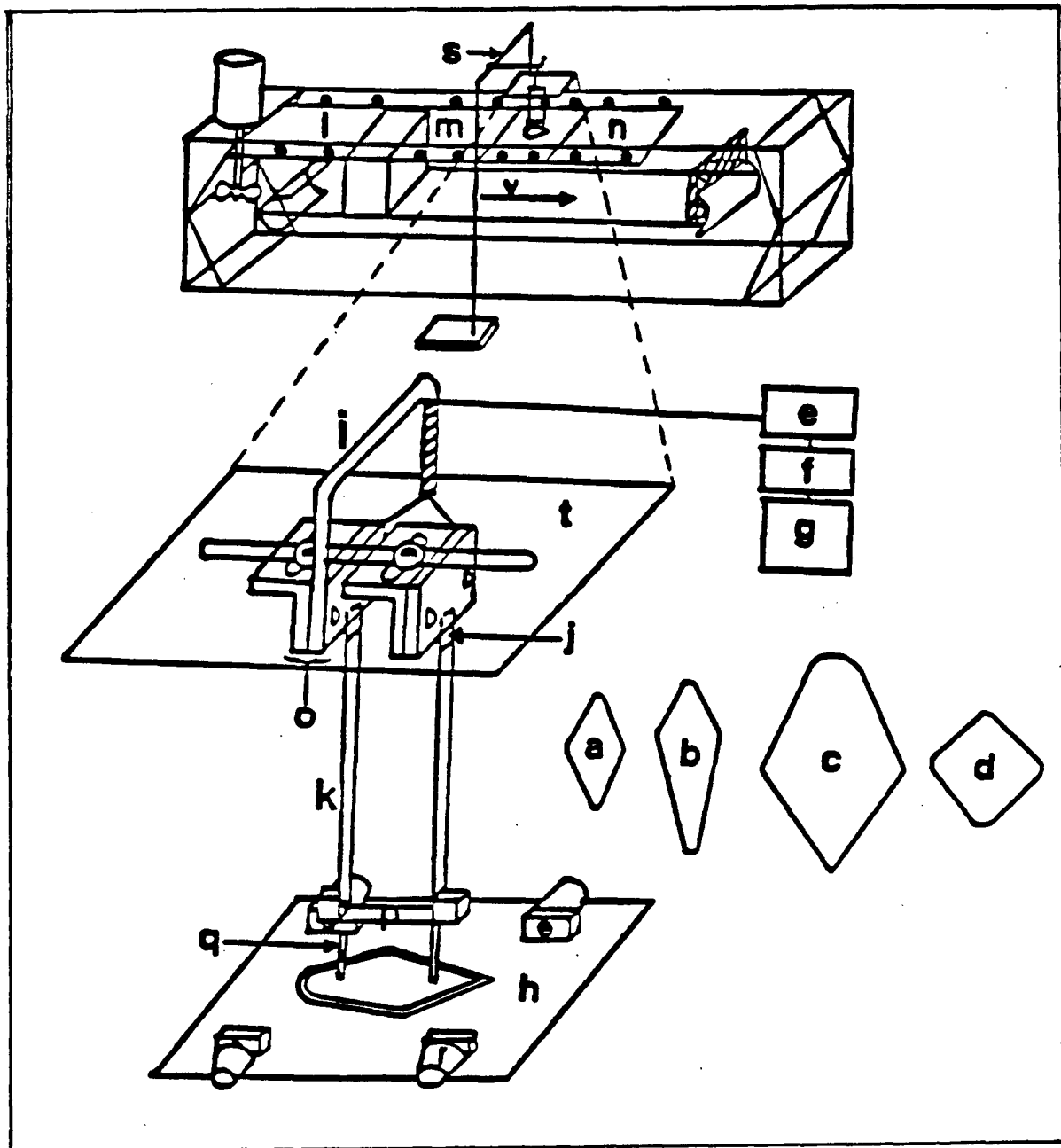


Fig. 2.3 Recirculating perspex flow tank used for determining the drag acting on hillstream fish (*Otocinclus*, *Hypostomus*, *Pterygoplichthys*, *Farlowella*, *Chaetostoma*, and *Gyrinocheilus*). Force plates for *Otocinclus* a, *Gyrinocheilus* and *Farlowella* b, *Hypostomus* and *Pterygoplichthys* c, *Chaetostoma* d, amplifier e, low pass filter f, digital oscilloscope g, center plate h, U-shaped aluminum bar i, strain gauge j, shim stock k, perspex over flow plate l, forward perspex plate m, end perspex plate n, clamps o, perspex plate p, extension strut q, rubber stopper r, scaffolding s, support plate t, water velocity direction v.

### Boundary Layer Effects

Drag measurements were taken 50 cm downstream from the flow rectifying grid. Two boundary layer characteristics are considered here. First, boundary layer thickness defined as the, distance from the bottom to the start of free stream velocity  $\delta$ . Second, boundary layer type (turbulent or laminar) and particularly the critical point (distance transition occurs from the leading edge of the plate; Streeter and Wylie, 1979).

$\delta$  for laminar flow is calculated from

$$\delta = \frac{4.65 x}{\sqrt{R_x}} \quad (2.10)$$

where  $x$  is the distance from the leading edge of the plate (50 cm), and  $R_x$  is the Reynold's number based on  $x$ , water velocity  $V$ , and kinematic viscosity of the water  $\nu$ .

$$R_x = \frac{x V}{\nu} \quad (2.11)$$

$\delta$  calculated from these equations for five free stream water velocities, (14.0, 17.0, 21.9, 25.8, and 28.6 cm s<sup>-1</sup>) are 0.83 cm, 0.75 cm, 0.67 cm, 0.61 cm, and 0.58 cm respectively. Water velocities in the boundary layer were measured using a fine point hot bead anemometer at free stream water velocities between 14.0 cm s<sup>-1</sup> and 30.0 cm s<sup>-1</sup>. The anemometer tip was placed into the space between the force plate and center plate. Fig. 2.4 is a typical boundary layer profile obtained during measurement.

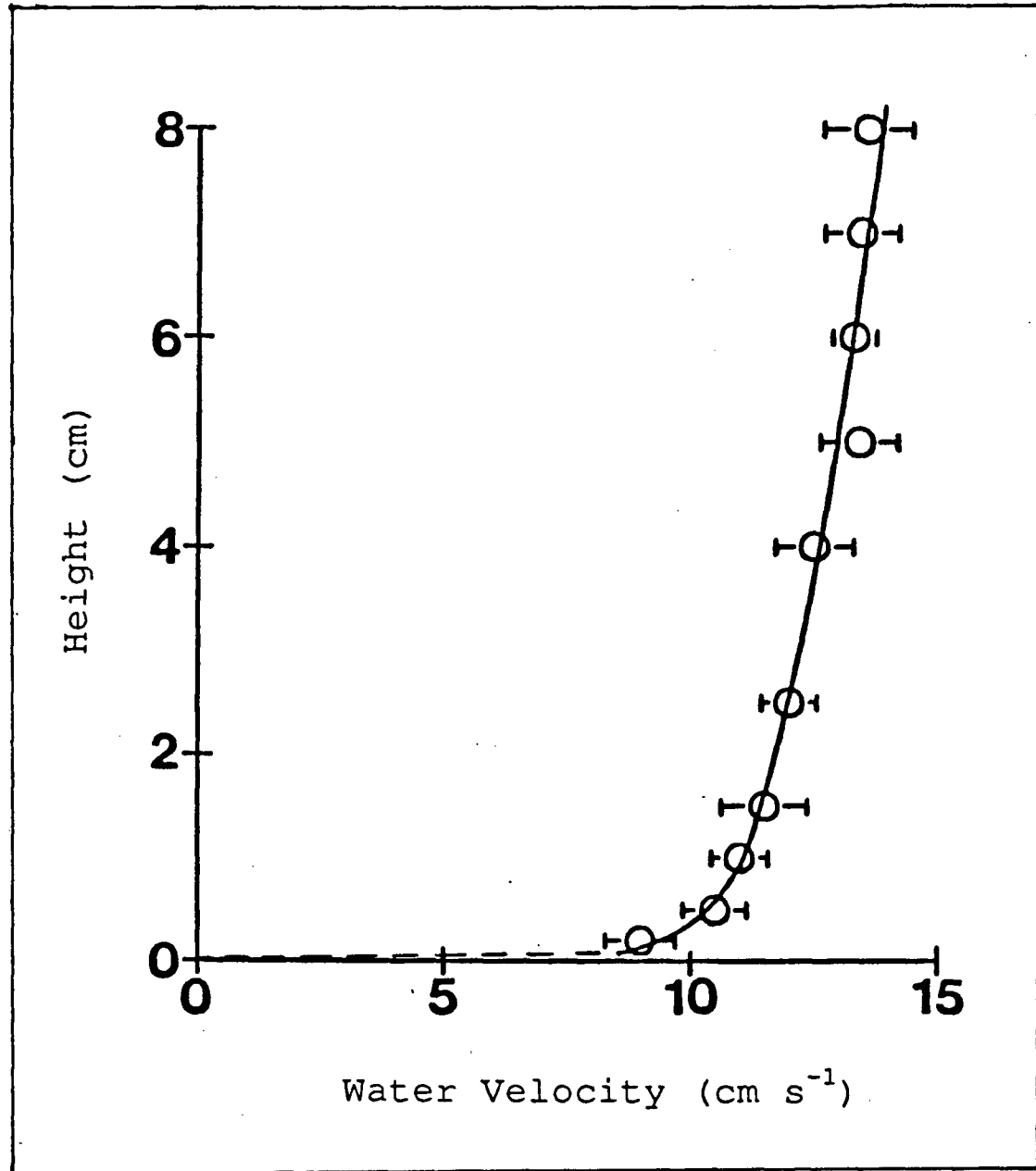


Fig. 2.4 Typical boundary layer profile near the surface of a force plate at a freestream velocity of  $14.0 \text{ cm s}^{-1}$ , 50 cm downstream of the flow rectifying grid. Standard error bars are for water velocity,  $n = 5$ .

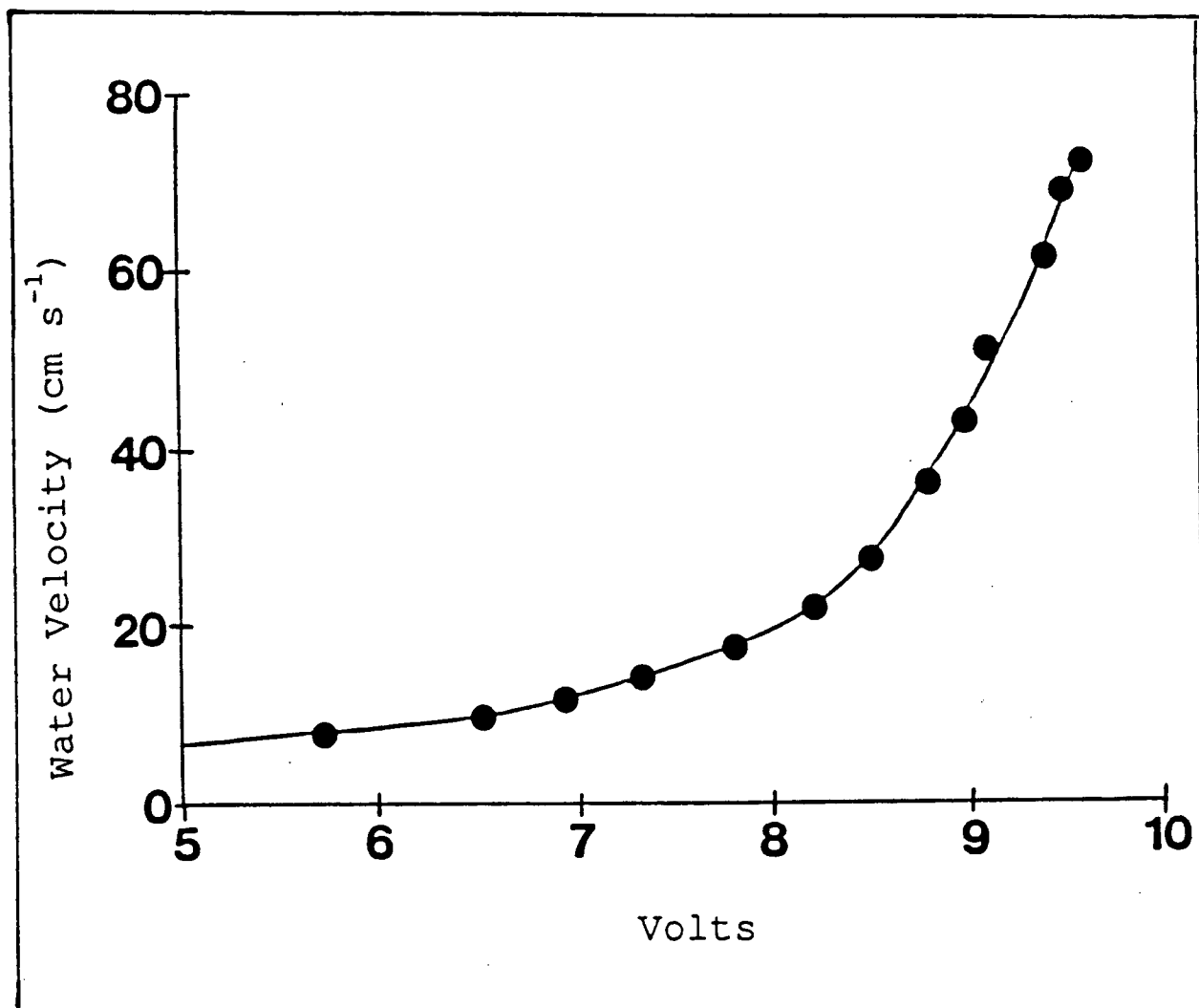


Fig. 2.5 Calibration curve for the fine tip hot bead anemometer used for boundary layer velocity measurement. Water velocity was determined in the free stream using a A. OTT Kempton TYP. 12.400 velocity meter.

Estimates of boundary layer thickness based on equation 2.10 are within 85 % of measured values. Calibration of the anemometer was in the free stream using the current meter previously described (Chapter I). Fig. 2.5 is the calibration curve obtained.

Laminar tends to turbulent flow at critical Reynold's numbers ranging from  $5 \times 10^5$  to  $1 \times 10^6$  (Blake, 1983). Using equation 2.11 we can find the critical point for water flowing over a smooth perspex surface. Using a conservative critical Reynold's number of  $5 \times 10^5$  and water velocity range between  $14.0 \text{ cm s}^{-1}$  and  $28.6 \text{ cm s}^{-1}$  the transition point  $x$  is calculated to be between 319 cm and 156 cm downstream respectively. Drag measurements were made well upstream of the lowest theoretical transition point (156 cm).

### Strain Gauges

Strain gauges (BLH Electronics, SR-4, resistance =  $350.0 \pm 0.5$  ohms) were mounted on shim stock (1000 gauge, 1.0 cm X 17.5 cm) using EPY-500 two part epoxy. They were then sandwiched between a clamp (3.0 cm X 3.0 cm) made of 0.2 cm aluminum angle-bar and a piece of aluminum (3.0 cm X 3.0 cm) using two screws for each clamp. The clamps and strain gauges were coated (Sr-4 Barrier 4 Protective Coating 2 component epoxy resin system) to protect them from water. At the end and center of the shim stock, furthest from the clamps, holes were drilled for attachment to the force plates. Each clamp was slotted (0.7 cm) at right angles to a slot in a support plate. The support plate (0.6 cm 20 cm X 20 cm) was attached to a U-shaped aluminum bar (1.3 cm diameter) with screws. The whole

apparatus was suspended by a scaffolding separate from the flow tank and rested on rubber pads in order to minimize vibrations produced by the electric motor (Fig. 2.3). Furthermore, the space between the force plate and center plate ( $\approx 2.0$  mm) was minimized to reduce the spaces effect on water flowing over it.

Four strain gauges mounted on either side of two pieces of parallel shim stock were wired into a full bridge. The deflection of the shim stock was measured as a voltage change on a digital oscilloscope (Nicolet XF-44). The oscilloscope was set to take an average of consecutive sweeps. Fish were mounted upside down to the underside of the force plate, using perspex glue and the force plate was attached to the shim stock. Fish were only attached to the force plate in areas that were naturally in contact with the substrate (ventral side of the oral sucker, anterior pectoral and pelvic fin spines, anal fin, frictional pad and tail). Furthermore, fish were positioned in a rheotactic posture (dorsal fin folded, pectoral fin extension angle  $5^\circ - 10^\circ$ ). The apparatus was then attached to the scaffolding and the force plate centered and leveled in the central plate. This left approximately a 2.0 mm gap between the force plate and the center plate which allowed for free deflection of the shim stock. Before each measurement an average voltage was taken at zero water velocity. Water velocity was then increased to the correct value and the voltage was allowed to stabilize before a reading was taken. The voltage change (measured in millivolts, mv) was determined by taking the difference between the voltage at zero water velocity and final water velocity. Drag measurements were made at five water velocities  $V$ , (14.0, 17.4, 21.9, 25.8 and 28.6  $\text{cm s}^{-1}$ ) for five fish of each species (except

*Chaetostoma*,  $n = 2$  fish). 10 drag measurements were taken per velocity and averaged. Strain gauges were wired through a amplifier and a 1 Hz low pass filter (Fig. 2.3). The oscilloscope was set to a sampling rate of 100  $\mu$ s per point, 1 volt scale and measured to  $\pm 0.1$  mv.

The drag acting on the fish alone was determined by subtracting the drag on the force plate and extension struts, from the drag of the system (force plate, extension struts and fish) at equivalent water velocities. From the drag forces  $D$  measured with the strain gauges a drag coefficient  $C_D$  was determined

$$C_D = \frac{2 D}{\rho_w A V^2} \quad (2.12)$$

Drag coefficients for fish of the same genera and similar Reynold's number range were averaged to give a mean drag coefficient  $\overline{C_D}$ . Drag coefficients  $C_D^*$  for fish with the dorsal fin extended during drag measurement were calculated and averaged separately. Furthermore, the mean drag coefficient for fish number 1 of *Pterygoplichthys*, was calculated separately.

The Reynold's number  $R_{1,2,3}$  for fish was calculated from

$$R_{1, 2, 3} = \frac{l V}{\nu}, \quad (2.13)$$

where  $l$  is the total length of the fish,  $\nu$  is the kinematic viscosity ( $8.97 \times 10^{-7} \text{ m}^2 \text{ s}^{-1}$  at  $26^\circ \text{ C}$ ) and  $V$  is live slipping, dead slipping (Chapter I) and drag velocity corresponding to  $R_1$ ,  $R_2$ , and  $R_3$  respectively.

## Calibration

Sto-A-Weigh calibration weights (1 g - 1 kg) lead shot (0.04 g / shot) and tin foil were used to calibrate the strain gauges. The apparatus was removed from the scaffolding and attached in the same position to a stand with a vertical metal rod. A thread was then attached to the base of the posterior extension strut of the force plate and brought over a pulley (friction = 0.001 g) level with the plate. To the end of the thread various weights could be hung to correlate force with voltage. At the beginning and end of each series of measurements the system was calibrated.

The system was then checked for accuracy by determining the known drag coefficient of a three dimensional flat plate orientated normal to flow ( $C_D \approx 1.2$ , Reynold's numbers =  $10^3$ - $10^4$ ; Hoerner, 1965). The plate (0.1 cm X 2.5 cm X 2.5 cm) was suspended by a spar (0.3 cm diameter, 2.0 cm long) from the center of the force plate. The drag was measured with the flat plate and spar and then with just the spar. The two drags were then subtracted to determine the drag acting on the plate alone. Drag measurements on the plate correspond to drag coefficients ( $\pm$  S.E.,  $n = 5$ ) of  $1.20 \pm 0.12$ ,  $1.19 \pm 0.15$ ,  $1.21 \pm 0.23$  and  $1.15 \pm 0.21$  at Reynold's numbers of  $3.9 \times 10^3$ ,  $4.7 \times 10^3$ ,  $6.1 \times 10^3$  and  $7.9 \times 10^3$  respectively.

## Respirometry

Respirometry experiments were conducted on a specimen of *Pterygoplichthys* (Weight = 318.5 g,  $l = 34.5$  cm and  $l_s = 27$  cm). The fish

was placed into the respirometer (modified Brett-type) and allowed to acclimatize for 24 hours before experiments were started and remained here until the experiment was over. The respirometer had a standard water volume of 37.5 l. Temperature was maintained by a controller (model FTS TC-400) and recirculating cooler (model FTS RC-100). The partial pressure of oxygen  $pO_2$  was set with a artificial lung (Sci-Med Membrane Blood Oxygenator 2500). Oxygen consumption could be measured at maximal water velocities of  $2.5 \text{ m s}^{-1}$  with fish up to 2 kg in weight. Data acquisition was performed by computer and initial analysis done using a number of macro commands in a LOTUS 1-2-3 spread sheet (Gehrke et al. 1990).

Temperature and pH were maintained at  $26^\circ \text{ C}$  and 7 respectively. The system was pressurized to 30 KPa and  $pO_2$  stabilized at 156 mm Hg inside the respirometer. The water was allowed to mix for approximately 5 minutes before measurements were taken to ensure a uniform distribution of oxygen. Oxygen consumption rates were measured (continuous automated samples) for a 20 min to 40 min period at fourteen different water velocities. Between each measurement a 30 min to 45 min recovery period was allowed. Background measurements (without fish) were conducted three times and the mean was subtracted from the oxygen consumption rates determined.

In addition, the number of times the fish repositioned itself over the measurement interval was recorded at eight water velocities using a video system (see Chapter I for details). Repositioning was defined as a release of suction from the bottom and a shift in position.

## RESULTS

### Calibration Equations

The calibration equations relating drag force to voltage output from the strain gauges for *Otocinclus*, *Gyrinocheilus*, *Hypostomus*, *Pterygoplichthys*, *Chaetostoma*, *Farlowella* and the flat plate are; Drag ( $\text{Kg m s}^{-2}$ ) =  $9.98 \times 10^{-5}(\text{mv})$ ,  $7.58 \times 10^{-5}(\text{mv})$ ,  $2.39 \times 10^{-4}(\text{mv})$ ,  $9.98 \times 10^{-5}(\text{mv})$ ,  $3.03 \times 10^{-4}(\text{mv})$ ,  $5.32 \times 10^{-5}(\text{mv})$  and  $9.17 \times 10^{-5}(\text{mv})$  respectively. The calibration remained linear over the forces measured ( $r^2 = 0.99$ ). Between Reynold's numbers  $10^3$  and  $10^4$  the mean drag coefficient for the flat plate normal to flow is 1.19 (see Materials and Methods, Chapter II).

### Geometry and Density

In Fig. 2.6 the projected frontal area of the body determined from tracings versus the geometric method (area of a equivalar ellipse,  $\pi 1/2h$  b) is plotted for *Pterygoplichthys*. The best fit regression line is Geometric area = Trace area (0.96) + 0.013,  $r^2 = 0.86$ . A 6.8 % difference is found between estimates based on geometry and traces. The dotted line in Fig. 2.6 represents the trace equals geometric axis.

In Fig. 2.7  $A_b$  is plotted against  $l_s^2$ . The insert is taken from the cluster of data points between 0 - 1.2  $\text{cm}^2$  and 0 - 30  $\text{cm}^2$  for  $A_b$  and  $l_s^2$  respectively. A two tailed t-test ( $p < 0.05$ ) shoes no significant difference in the mean  $2b/h$  ratio from one in *Gyrinocheilus* (Chapter I).

Therefore, the area of a circle rather than an ellipse is used to determine  $A_b$  for this fish. The coefficients of determination range between 0.89 and 0.94. The greatest and least slope is obtained in *Hypostomus* and *Farlowella* respectively.  $A_f$  and  $A_b$  range between 0.01 - 1.6  $\text{cm}^2$  and 0.10 - 7.50  $\text{cm}^2$  respectively for all genera (Table 2.1).

In Fig. 2.8  $W_o$  is plotted against  $l^3$ . The coefficient of determination ranges between 0.86 and 0.97. The greatest and least slope is obtained in *Chaetostoma* and *Farlowella* respectively. The insert in Fig. 2.8 is taken from the cluster of data points between 0-400  $\text{g cm s}^{-2}$  and 0-600  $\text{cm}^3$  for  $W_o$  and  $l^3$  respectively.

The maximum and minimum mean body density  $\bar{\rho}$ , 1.035  $\text{g cm}^{-3}$  and 1.129  $\text{g cm}^{-3}$  occurs in *Pterygoplichthys* and *Farlowella* respectively. For *Otocinclus*, *Gyrinocheilus*, *Hypostomus* and *Chaetostoma*  $\bar{\rho}$  ranges from 1.062  $\text{g cm}^{-3}$  to 1.097  $\text{g cm}^{-3}$  ( $\pm$  S.E. = 0.003 - 0.004, Table 2.1). In Fig. 2.9 *Otocinclus* and *Gyrinocheilus* have correlation coefficients significantly different from zero (t-test,  $H_o: \rho = 0$ ,  $p < 0.05$ ).

### Hydrodynamic and Frictional Coefficients

Drag forces measured (water velocity range 14.0 - 28.6  $\text{cm s}^{-1}$ ) are between  $5.43 \times 10^{-5}$  and  $8.07 \times 10^{-3}$  Newtons ( $\text{Kg m s}^{-2}$ ) in all genera (Fig. 2.10). Fish number 1, 2, 2 and 2 of *Otocinclus*, *Hypostomus*, *Farlowella* and *Chaetostoma* respectively have their dorsal fin extended during measurement, resulting in the steeper slopes of the drag velocity curves (Fig. 2.10). The best fit second degree regression constants, coefficients of determination, standard and total length for each fish of

the drag versus velocity plots (Fig. 2.10) are given in Table 2.2. The maximum and minimum mean drag coefficients  $\overline{C}_D$  determined using the force platform are 0.23 and 0.87 for *Farlowella* and *Chaetostoma* respectively. *Otocinclus*, *Gyrinocheilus*, *Hypostomus*, and *Pterygoplichthys* have  $\overline{C}_D$  between 0.29 and 0.50 ( $\pm$  S.E. = 0.015 - 0.035).  $\overline{C}_D^*$  is generally higher than the  $\overline{C}_D$  for fish with the dorsal fin folded (Table 2.3).

Lift coefficients  $C_{L1}$ ,  $C_{L2}$ , and  $\overline{C}_L$  are determined using maximum, minimum and mean drag coefficients respectively in Table 2.3. *Otocinclus*, *Pterygoplichthys*, and *Chaetostoma* have negative lift coefficients. For *Otocinclus* and *Pterygoplichthys* negative lift coefficients are only obtained when calculated with maximal drag coefficients. *Chaetostoma* has a negative lift coefficient for all  $C_D$  values. The minimum (-0.55) and maximum (1.70) lift coefficients are found in *Chaetostoma* and *Farlowella* respectively.

In Fig. 2.11 frontal drag coefficient is plotted against Reynold's number. The best fit second degree regression line for all genera is  $C_D = 6.81 \times 10^{-1} - 2.23 \times 10^{-5}R_3 + 2.96 \times 10^{-10}R_3^2$ ,  $r^2 = 0.32$ . Fish number 1 of *Pterygoplichthys* has generally lower drag coefficients than the other specimens of the same genera (Table 2.3 and Fig. 2.11;  $R_3 = 1.80 \times 10^4 - 3.67 \times 10^4$ ).

The minimum (0.71) and maximum (1.85) value for the ratio  $2W_0/\rho_w A V_2^2$  occurs in *Chaetostoma* and *Farlowella* respectively. The standard error for this ratio is between 0.03 and 0.21. This ratio is used to calculate the lift coefficients ( $\overline{C}_L$ ,  $C_{L1}$ ,  $C_{L2}$ ) in Table 2.3 using equation 2.7.

The minimum and maximum  $\overline{\mu}$  is 0.63 and 0.95 for *Pterygoplichthys* and

*Gyrinocheilus* respectively. *Otocinclus*, *Hypostomus*, *Chaetostoma*, and *Farlowella* have  $\overline{\mu}$  between 0.67 and 0.74 ( $\pm$  S.E. = 0.015 - 0.021, Table 2.1).

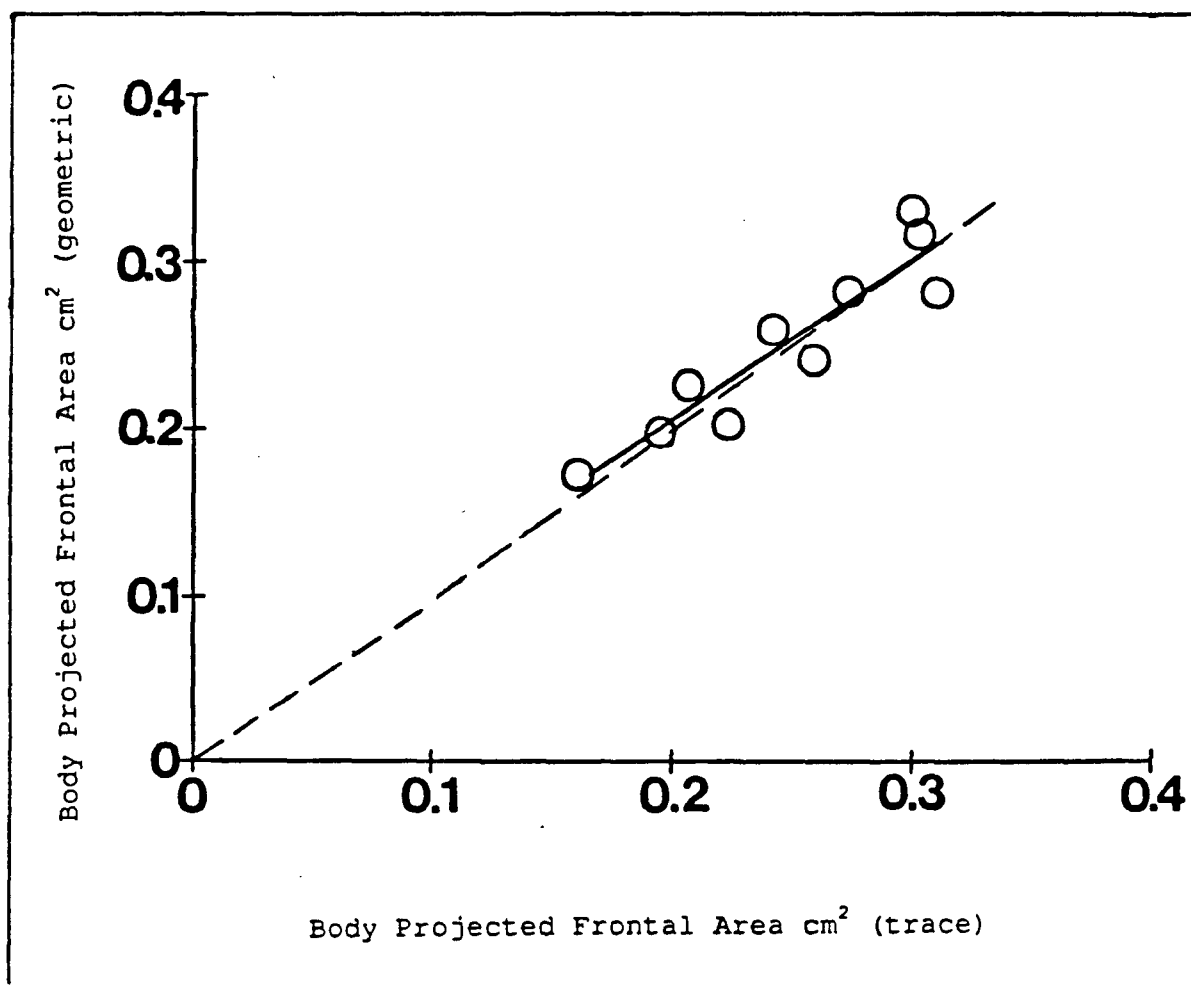


Fig. 2.6 Relationship between the projected frontal area of the body determined by tracings and geometry for *Pterygoplichthys* (Geometric =  $0.962 \text{ Trace} + 0.01$ ,  $r^2 = 0.86$ ). There is a 6.8 % difference between the two methods of estimating body frontal area. The dotted line is the X equals Y axis.

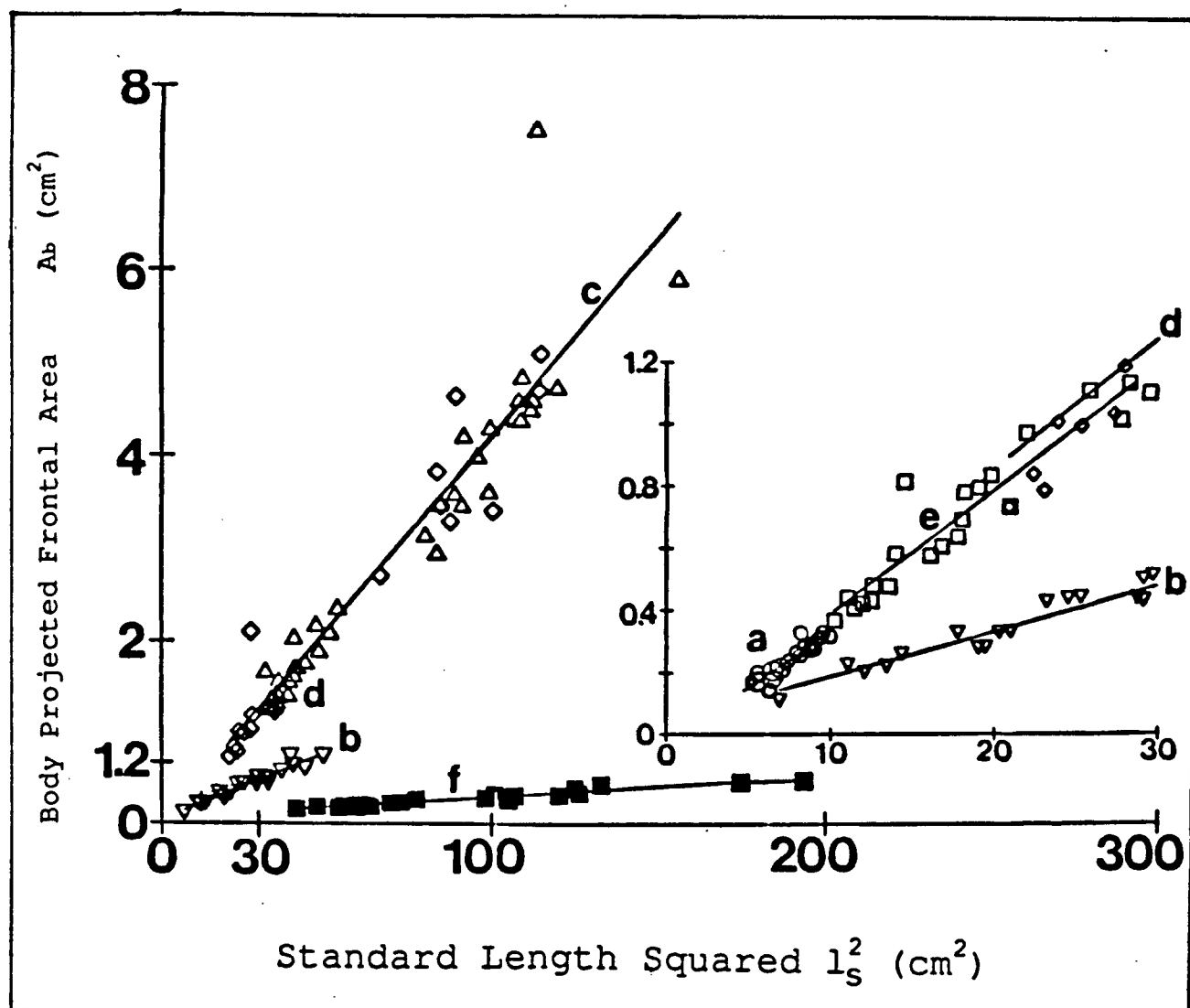


Fig. 2.7 Linear regression lines of best fit for body projected frontal area  $A_b$  versus standard length squared  $l_s^2$  for *Otocinclus* a, o ( $n = 35$ ,  $A_b = l_s^2(0.039) - 0.050$ ,  $r^2 = 0.90$ ), *Gyrinocheilus* b,  $\nabla$  ( $n = 25$ ,  $A_b = l_s^2(0.015) + 0.043$ ,  $r^2 = 0.93$ ), *Hypostomus* c,  $\Delta$  ( $n = 36$ ,  $A_b = l_s^2(0.042) - 0.031$ ,  $r^2 = 0.89$ ), *Pterygoplichthys* d,  $\diamond$  ( $n = 17$ ,  $A_b = l_s^2(0.041) + 0.034$ ,  $r^2 = 0.93$ ), *Chaetostoma* e,  $\square$  ( $n = 22$ ,  $A_b = l_s^2(0.040) + 0.066$ ,  $r^2 = 0.94$ ) and *Farlowella* f,  $\blacksquare$  ( $n = 25$ ,  $A_b = l_s^2(0.002) - 0.010$ ,  $r^2 = 0.90$ ). Insert is expanded from the large plot for the ranges 0 - 1.2  $\text{cm}^2$  and 0 - 30  $\text{cm}^2$  for  $A_b$  and  $l_s^2$  respectively.

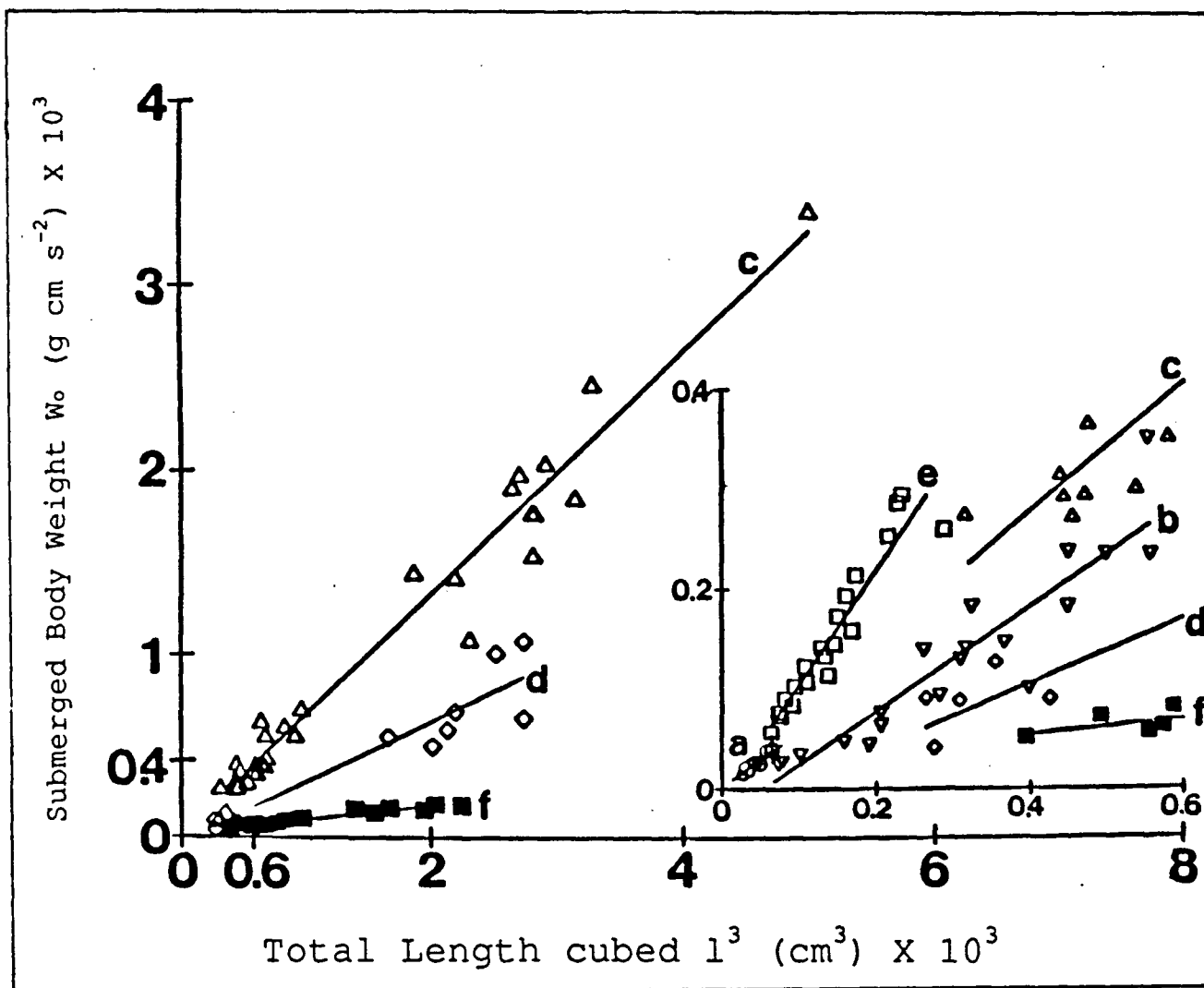


Fig. 2.8 Linear regression lines of best fit for submerged body weight  $W_0$  versus total length cubed  $l^3$  for *Otocinclus* a, o ( $n = 21$ ,  $W_0 = l^3(0.699) - 4.999$ ,  $r^2 = 0.89$ ), *Gyrinocheilus* b,  $\nabla$  ( $n = 20$ ,  $W_0 = l^3(0.529) - 27.48$ ,  $r^2 = 0.86$ ), *Hypostomus* c,  $\Delta$  ( $n = 31$ ,  $W_0 = l^3(0.651) + 20.28$ ,  $r^2 = 0.97$ ), *Pterygoplichthys* d,  $\diamond$  ( $n = 12$ ,  $W_0 = l^3(0.327) - 24.47$ ,  $r^2 = 0.89$ ), *Chaetostoma* e,  $\square$  ( $n = 20$ ,  $W_0 = l^3(1.149) - 9.138$ ,  $r^2 = 0.91$ ) and *Farlowella* f,  $\blacksquare$  ( $n = 20$ ,  $W_0 = l^3(0.075) + 24.99$ ,  $r^2 = 0.93$ ). The insert is expanded from the large plot for the ranges  $0 - 0.4 \times 10^3$  and  $0 - 0.6 \times 10^3$  for  $W_0$  and  $l^3$  respectively.

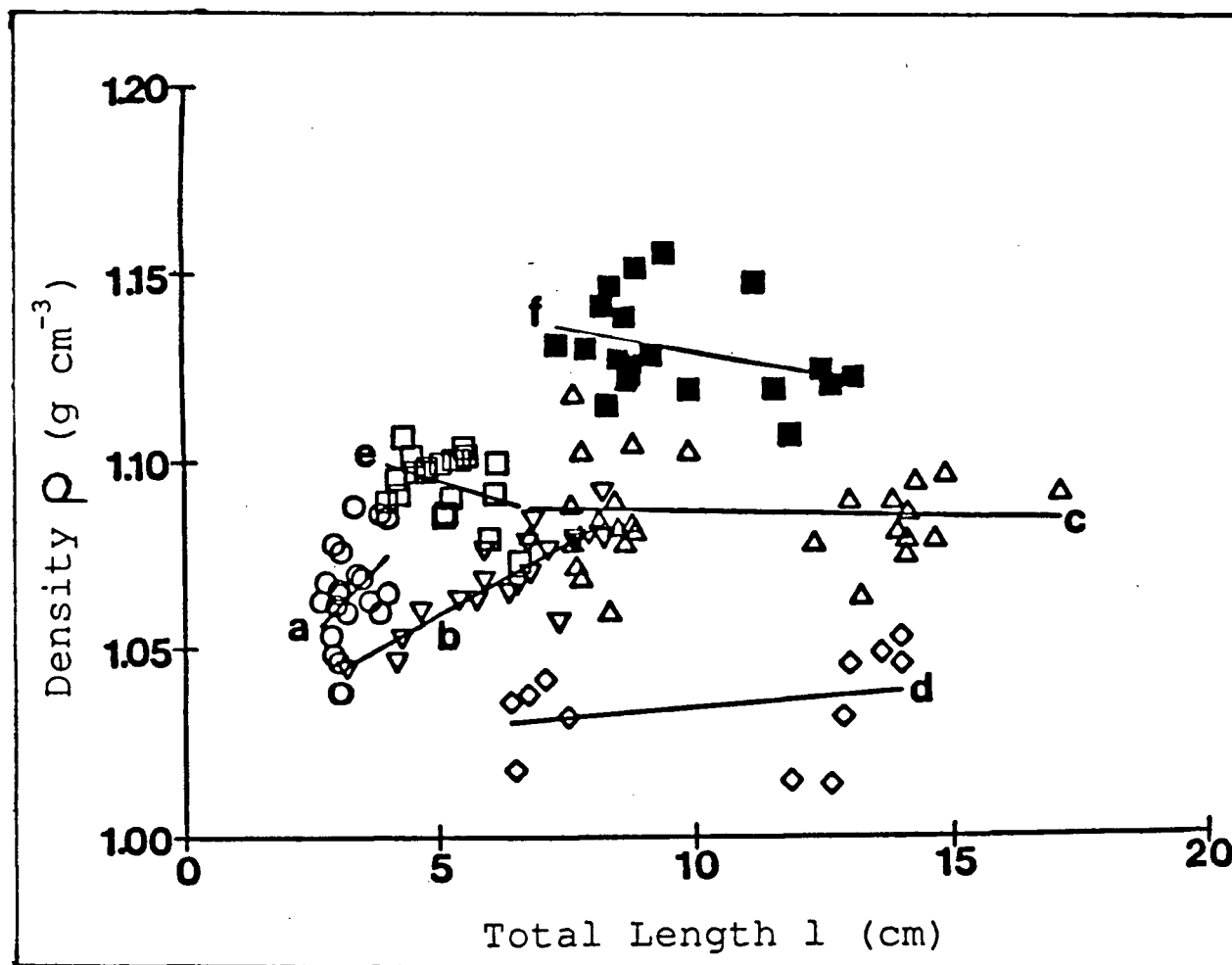


Fig. 2.9 Linear regression lines of best fit for density versus total length  $l$  for *Otocinclus* a,  $\circ$  ( $n = 21$ ,  $\rho = l(0.023) + 0.987$ ,  $r^2 = 0.26$ ), *Gyrinocheilus* b,  $\nabla$  ( $n = 20$ ,  $\rho = l(0.007) + 1.022$ ,  $r^2 = 0.73$ ), *Hypostomus* c,  $\Delta$  ( $n = 29$ ,  $\rho = l(-0.001) + 1.089$ ,  $r^2 = 0.01$ ), *Pterygoplichthys* d,  $\diamond$  ( $n = 12$ ,  $\rho = l(0.001) + 1.023$ ,  $r^2 = 0.08$ ), *Chaetostoma* e,  $\square$  ( $n = 20$ ,  $\rho = l(-0.003) + 1.109$ ,  $r^2 = 0.01$ ) and *Farlowella* f,  $\blacksquare$  ( $n = 20$ ,  $\rho = l(-0.003) + 1.153$ ,  $r^2 = 0.12$ ). *Otocinclus* and *Gyrinocheilus* have correlation coefficients significantly different from zero (t-test, reject  $H_0: \rho=0$ ,  $p<0.05$ ).

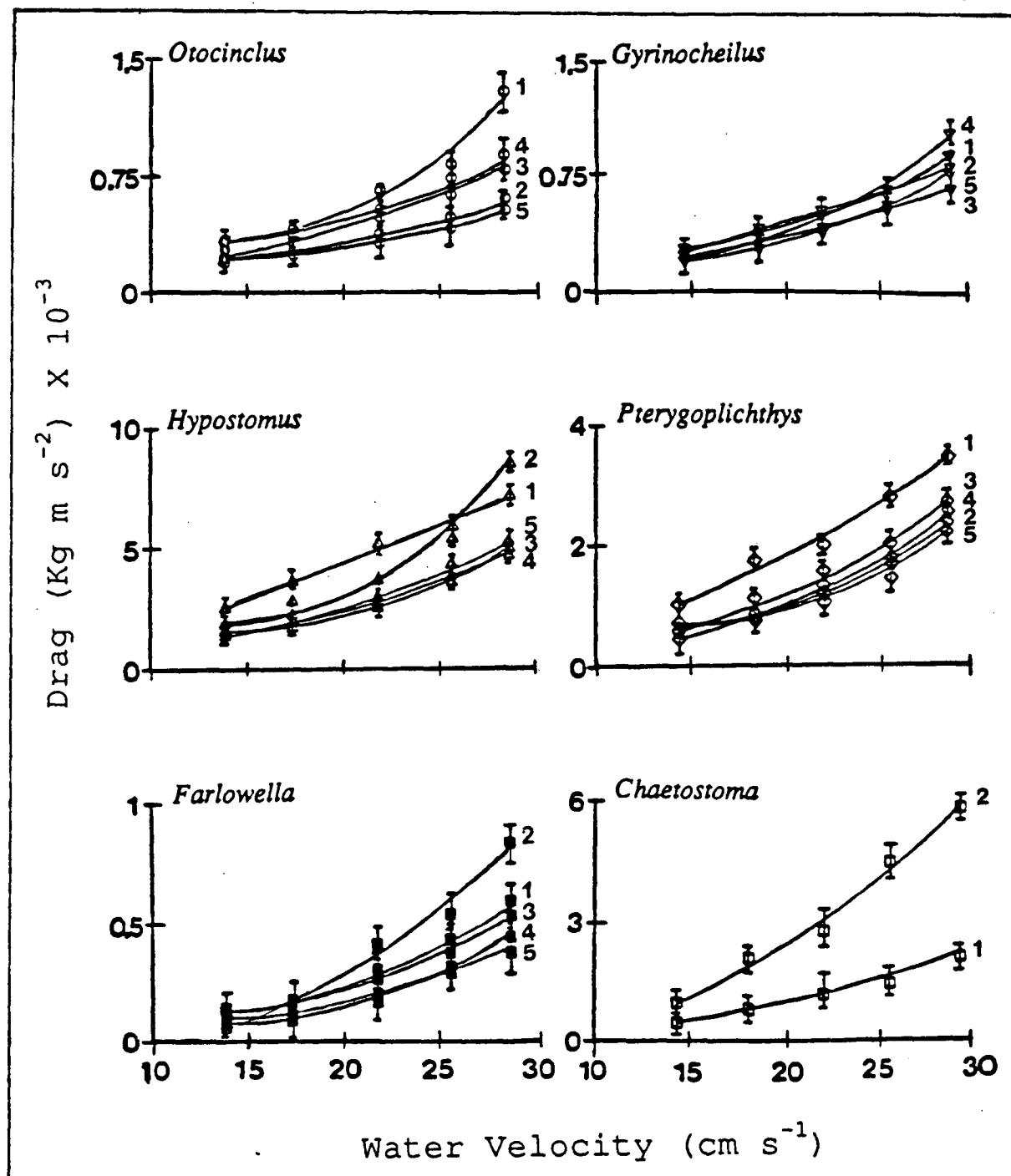


Fig. 2.10 Drag (Newtons =  $\text{kg m s}^{-2}$ ) versus velocity ( $\text{cm s}^{-1}$ ) plots for *Otocinclus* (o), *Gyrinocheilus* (V), *Hypostomus* ( $\Delta$ ), *Pterygoplichthys* ( $\diamond$ ), *Chaetostoma* ( $\square$ ) and *Farlowella* ( $\blacksquare$ ) with standard error bars ( $n = 10/\text{symbol}$ ). Constants and coefficients of determination for the regression lines are in Table 2.2. Fish number 1, 2, 2, and 2 have their dorsal fins extended for *Otocinclus*, *Hypostomus*, *Farlowella* and *Chaetostoma* respectively.

	n	$\bar{\mu}$	S.E.	n	$\bar{\rho}$ (g cm <sup>-3</sup> )	S.E.	A <sub>r</sub> range (cm <sup>2</sup> )	A range (cm <sup>2</sup> )
<i>Otocinclus</i>	17	0.67	0.02	21	1.062	0.004	0.02-0.06	0.10-0.40
<i>Gyrinocheilus</i>	20	0.95	0.02	20	1.069	0.003	0.18-0.80	0.40-1.60
<i>Hypostomus</i>	26	0.70	0.02	29	1.086	0.003	0.22-1.58	1.40-7.50
<i>Pterygoplichthys</i>	12	0.63	0.02	12	1.035	0.004	0.10-1.10	0.80-6.00
<i>Chaetostoma</i>	19	0.74	0.02	20	1.097	0.004	0.07-0.30	0.40-1.30
<i>Farlowella</i>	20	0.70	0.02	20	1.129	0.003	0.02-0.10	0.10-0.60

Table 2.1 Sample size n, standard error S.E., mean body density  $\bar{\rho}$ , mean frictional coefficient on a smooth perspex surface  $\bar{\mu}$ , projected frontal area of the anterior pectoral fin or ray range A<sub>r</sub> and total frontal area range A for *Otocinclus*, *Gyrinocheilus*, *Hypostomus*, *Pterygoplichthys*, *Chaetostoma*, and *Farlowella*.

Fish	a1	a2	a3	r <sup>2</sup>	l (cm)	l <sub>s</sub> (cm)
<i>Otocinclus</i>						
1	9.24 x 10 <sup>-4</sup>	-1.02 x 10 <sup>-2</sup>	3.76 x 10 <sup>-2</sup>	0.97	4.03	3.15
2	7.55 x 10 <sup>-5</sup>	-1.17 x 10 <sup>-3</sup>	1.16 x 10 <sup>-2</sup>	0.99	3.94	3.09
3	-3.09 x 10 <sup>-4</sup>	2.63 x 10 <sup>-3</sup>	3.33 x 10 <sup>-3</sup>	0.99	3.59	2.89
4	6.82 x 10 <sup>-5</sup>	-2.53 x 10 <sup>-5</sup>	7.96 x 10 <sup>-3</sup>	0.99	3.09	2.97
5	-2.10 x 10 <sup>-5</sup>	6.07 x 10 <sup>-4</sup>	3.16 x 10 <sup>-3</sup>	0.99	3.54	2.80
<i>Gyrinocheilus</i>						
1	-1.76 x 10 <sup>-4</sup>	1.80 x 10 <sup>-3</sup>	4.97 x 10 <sup>-3</sup>	0.99	4.66	3.88
2	4.80 x 10 <sup>-5</sup>	-2.82 x 10 <sup>-4</sup>	9.40 x 10 <sup>-3</sup>	0.99	6.52	5.40
3	-7.98 x 10 <sup>-5</sup>	6.87 x 10 <sup>-4</sup>	6.01 x 10 <sup>-3</sup>	0.99	6.13	4.82
4	4.54 x 10 <sup>-4</sup>	-6.06 x 10 <sup>-3</sup>	2.70 x 10 <sup>-2</sup>	0.99	6.18	4.96
<i>Hypostomus</i>						
1	-4.74 x 10 <sup>-4</sup>	1.01 x 10 <sup>-2</sup>	5.20 x 10 <sup>-2</sup>	0.99	12.35	9.54
2	8.56 x 10 <sup>-3</sup>	-9.68 x 10 <sup>-2</sup>	3.28 x 10 <sup>-1</sup>	0.97	12.82	9.43
3	9.72 x 10 <sup>-4</sup>	-1.31 x 10 <sup>-2</sup>	8.46 x 10 <sup>-2</sup>	0.99	11.64	9.14
4	7.29 x 10 <sup>-4</sup>	-1.01 x 10 <sup>-2</sup>	7.78 x 10 <sup>-2</sup>	0.99	10.68	8.95
5	-9.32 x 10 <sup>-4</sup>	5.00 x 10 <sup>-3</sup>	4.77 x 10 <sup>-2</sup>	0.99	11.70	9.19
<i>Pterygoplichthys</i>						
1	-3.09 x 10 <sup>-4</sup>	3.73 x 10 <sup>-3</sup>	2.92 x 10 <sup>-2</sup>	0.99	11.50	8.15
2	2.20 x 10 <sup>-3</sup>	-2.50 x 10 <sup>-2</sup>	8.94 x 10 <sup>-2</sup>	0.97	6.38	4.89
3	1.25 x 10 <sup>-3</sup>	-1.50 x 10 <sup>-2</sup>	6.22 x 10 <sup>-2</sup>	0.99	5.61	4.80
4	7.79 x 10 <sup>-5</sup>	-4.33 x 10 <sup>-3</sup>	4.01 x 10 <sup>-2</sup>	0.99	5.75	4.57
5	1.07 x 10 <sup>-3</sup>	-1.37 x 10 <sup>-2</sup>	6.52 x 10 <sup>-2</sup>	0.99	5.55	4.73
<i>Chaetostoma</i>						
1	-4.84 x 10 <sup>-4</sup>	4.49 x 10 <sup>-3</sup>	1.23 x 10 <sup>-2</sup>	0.99	4.74	3.53
2	-1.59 x 10 <sup>-4</sup>	-4.83 x 10 <sup>-3</sup>	8.57 x 10 <sup>-2</sup>	0.99	4.97	3.81
<i>Farlowella</i>						
1	-4.22 x 10 <sup>-5</sup>	-1.45 x 10 <sup>-3</sup>	1.51 x 10 <sup>-2</sup>	0.98	14.94	13.91
2	-1.22 x 10 <sup>-5</sup>	-6.34 x 10 <sup>-4</sup>	8.97 x 10 <sup>-2</sup>	0.99	11.60	10.97
3	3.27 x 10 <sup>-4</sup>	-3.92 x 10 <sup>-3</sup>	1.49 x 10 <sup>-2</sup>	0.99	11.49	10.25
4	4.34 x 10 <sup>-5</sup>	-4.48 x 10 <sup>-3</sup>	1.67 x 10 <sup>-2</sup>	0.98	12.65	11.52
5	8.80 x 10 <sup>-5</sup>	-9.06 x 10 <sup>-4</sup>	6.58 x 10 <sup>-3</sup>	0.97	14.62	13.21

Table 2.2 The coefficient of determination  $r^2$ , standard length  $l_s$ , total length  $l$  and constants  $a_1$ ,  $a_2$  and  $a_3$  for the drag velocity curves in Fig. 2.10 (Drag (kg m s<sup>-2</sup>) =  $a_1 + a_2 (v) + a_3 (v^2)$ ).

	n	$\overline{C_D}$	S.E.	$\overline{C_D}^*$	S.E.	$\overline{C_D}$ range	$\frac{2}{\rho_w A} \frac{W_o}{V_2^2}$	S.E.	$C_{L1}$	$C_{L2}$	$\overline{C_L}$	$\frac{\overline{C_L}}{\overline{C_D}}$	$R_1$ ( $\times 10^4$ )	$R_2$ ( $\times 10^4$ )	$R_3$ ( $\times 10^4$ )	n	$S_1$ ( $N\ m^{-2}$ )	S.E.	$S_2$ ( $N\ m^{-2}$ )	S.E.
<i>Otocinclus</i>	20	0.46	0.02	0.63	0.04	0.32-0.77	0.78	0.05	-0.37	0.30	0.09	0.20	0.52-1.55	0.45-0.88	0.55-1.28	10	2.65	0.53	52.6	13.4
<i>Gyrinocheilus</i>	25	0.42	0.03	—	—	0.23-0.69	1.68	0.21	0.95	1.44	1.23	2.93	3.22-4.40	0.36-1.67	0.59-2.08	5	9.75	0.13	94.7	14.4
<i>Hypostomus</i>	20	0.29	0.02	0.32	0.04	0.17-0.45	1.14	0.06	0.50	0.90	0.73	2.60	2.24-6.21	1.27-4.31	1.93-4.10	5	2.35	0.12	13.4	6.70
<i>Pterygoplichthys</i>	20	0.47	0.02	—	—	0.31-0.65	1.00	0.13	-0.03	0.64	0.26	0.57	5.09-7.01	0.98-3.15	0.87-2.03	4	9.90	0.17	140	21.3
Fish 1	5	0.24	0.01	—	—	0.23-0.26	—	—	—	—	0.62	2.62	—	—	1.80-3.67	—	—	—	—	
<i>Chaetostoma</i>	5	0.87	0.04	0.82	0.05	0.74-0.94	0.71	0.03	-0.55	-0.29	-0.47	-0.52	2.72-3.38	0.93-1.70	0.74-1.58	5	23.6	5.26	173	54.2
<i>Farlowella</i>	20	0.23	0.02	0.29	0.03	0.10-0.36	1.85	0.12	1.34	1.70	1.52	6.71	3.47-7.69	1.34-3.16	1.79-4.76	9	2.04	0.20	26.2	3.54

Table 2.3 Hydrodynamic coefficients for *Otocinclus*, *Gyrinocheilus*, *Chaetostoma*, *Pterygoplichthys*, *Hypostomus*, and *Farlowella*. Sample size n, standard error S.E., mean drag coefficients with dorsal fin folded  $\overline{C_D}$  and extended  $\overline{C_D}^*$  (n=5), drag coefficient range, Reynold's number range for live slipping, dead slipping and drag velocities  $R_1$ ,  $R_2$  and  $R_3$  respectively; maximum, minimum, and mean lift coefficients  $C_{L1}$ ,  $C_{L2}$ , and  $\overline{C_L}$  respectively; mean lift to drag ratio  $\overline{C_L}/\overline{C_D}$ , rheotactic suction pressure  $S_1$  and  $S_2$  determined from total ventral area and sucker area respectively and  $2W_o/\rho_w AV_2^2$  ratio.

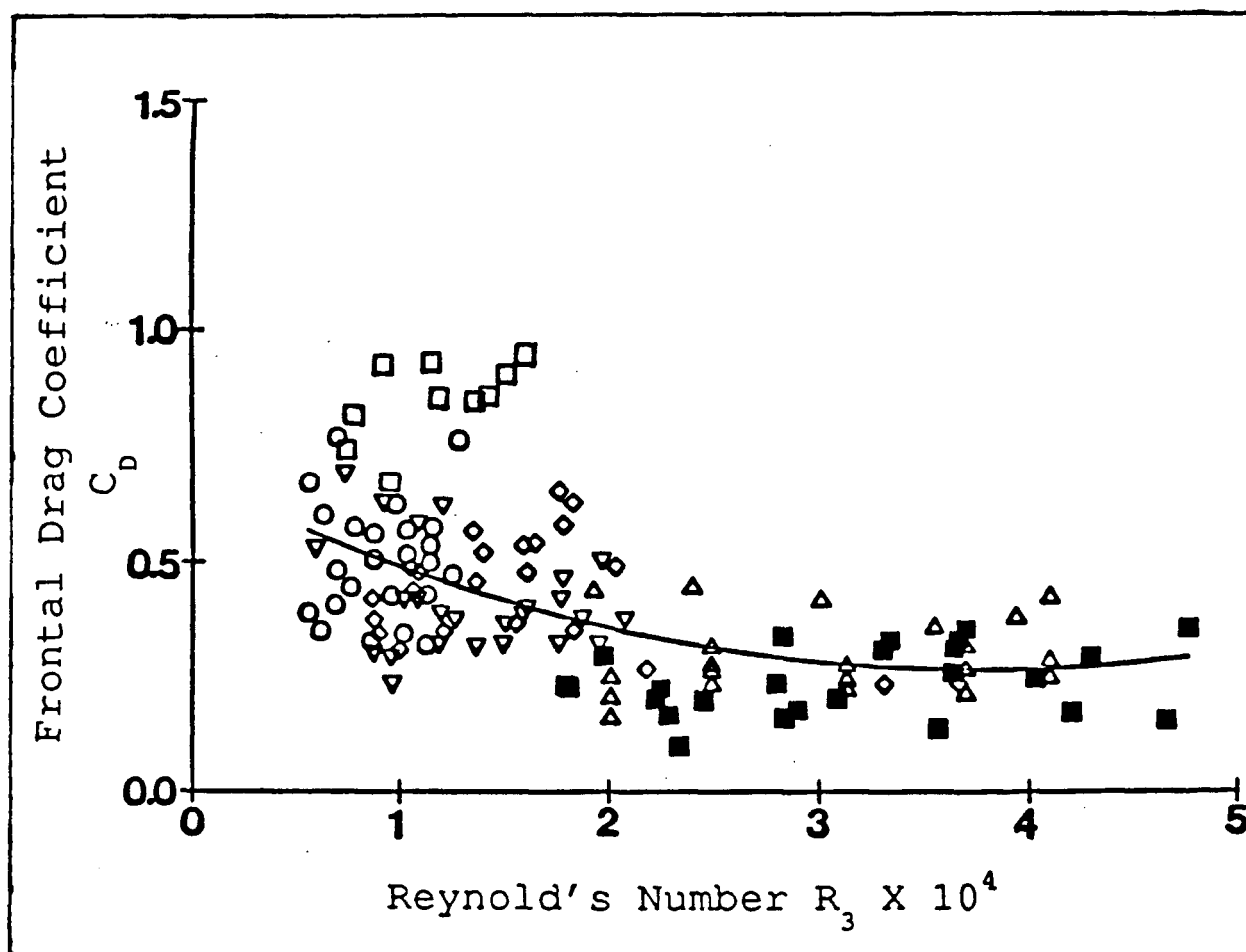


Fig. 2.11 Frontal drag coefficient versus Reynold's number for *Otocinclus* (o), *Gyrinocheilus* (▽), *Hypostomus* (Δ), *Pterygoplichthys* (◇), *Chaetostoma* (□) and *Farlowella* (■). The solid line is the best fit second degree regression curve for all genera ( $C_D = 6.81 \times 10^{-1} - 2.23 \times 10^{-5}R_3 + 2.96 \times 10^{-10}R_3^2$ ,  $r^2 = 0.32$ ,  $n = 135$ ).

## Respirometry and Behaviour

The typical behaviour observed in *Pterygoplichthys* during a progressive increase in water velocity is described below. At zero water velocity the fish remains on the bottom of the respirometer with the oral sucker applied to the substrate and the respiratory gap open. The pectoral fins are extended at all water velocities. When water velocity is increased slowly to approximately  $23 \text{ cm s}^{-1}$  the dorsal fin remains erect and there is movement to find secure attachment. At  $55 \text{ cm s}^{-1}$  the dorsal fin begins to flutter. At this moment the dorsal fin is folded and the oral sucker lips secure to the bottom with a noticeable reduction in the diameter of the respiratory gap and fissure. Repositioning movements increase at about  $81 \text{ cm s}^{-1}$ . During repositioning the dorsal fin becomes erect until the fish reattaches to the substrate. At  $94 \text{ cm s}^{-1}$  the tail and pelvic fin rays begin to flutter. At this water velocity there is a slight increase in the number of repositionings per minute, however, the fish does not slip. Slipping occurs at about  $105 \text{ cm s}^{-1}$  with a large increase in repositioning movement (Fig. 2.12). At  $120 \text{ cm s}^{-1}$  the tail and pelvic fin ray flutter increases, however, there is no change in posture. *Pterygoplichthys* starts to slide backwards into the electric grid at approximately  $153 \text{ cm s}^{-1}$ . When contact with the grid is made the fish burst swims to the front of the flow tank. However, sliding into the electric grid rarely occurred and is not necessary to initiate burst swimming. When the velocity is reduced to zero the fish extends the dorsal fin. The dorsal fin of larger specimens of *Pterygoplichthys* folds down at higher water velocities ( $50 \text{ cm s}^{-1}$ -  $64 \text{ cm s}^{-1}$ ) than smaller

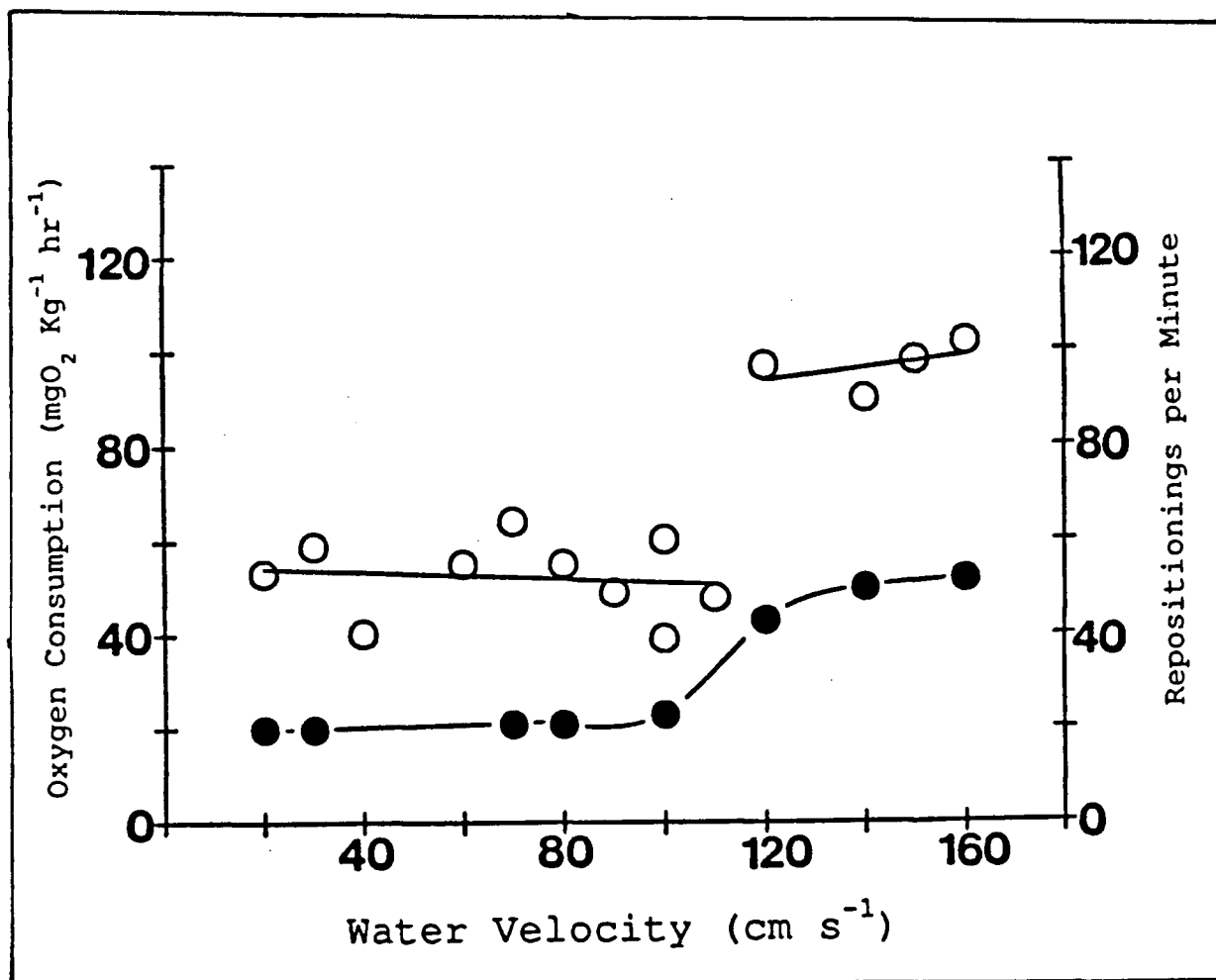


Fig. 2.12 Oxygen consumption (o) at 20-110 cm s<sup>-1</sup> and 120-160 cm s<sup>-1</sup> (mg O<sub>2</sub> kg<sup>-1</sup> hr<sup>-1</sup> =  $V(-0.04) + 55.0$ ,  $r^2 = 0.02$ ,  $n = 10$  and mg O<sub>2</sub> kg<sup>-1</sup> hr<sup>-1</sup> =  $V(0.13) + 77.7$ ,  $r^2 = 0.21$ ,  $n = 4$  respectively) and repositionings per minute (•) versus water velocity for *Pterygoplichthys*.

specimens ( $10 \text{ cm s}^{-1}$ - $20 \text{ cm s}^{-1}$ ).

Between water velocities  $20 \text{ cm s}^{-1}$  -  $110 \text{ cm s}^{-1}$  and  $120 \text{ cm s}^{-1}$  -  $160 \text{ cm s}^{-1}$  the oxygen consumption rate regression lines are  $\text{mg O}_2 \text{ kg}^{-1} \text{ hr}^{-1} = V (-0.04) + 55.0$ ,  $r^2 = 0.02$  and  $\text{mg O}_2 \text{ kg}^{-1} \text{ hr}^{-1} = V (0.13) + 77.7$ ,  $r^2 = 0.21$  respectively (Fig. 2.12). Correlation coefficients are not significantly different from zero (t-test, Accept  $H_0$ :  $\rho = 0$ ,  $p < 0.05$ ). Between water velocities  $110 \text{ cm s}^{-1}$  and  $120 \text{ cm s}^{-1}$  the mean oxygen consumption rate increases from  $52.2 (\pm \text{S.E.} = 2.59)$  to  $96.6 (\pm \text{S.E.} = 2.48) \text{ mg O}_2 \text{ kg}^{-1} \text{ hr}^{-1}$ . In addition, there is a gradual increase in the number of repositionings per minute between water velocities  $20 \text{ cm s}^{-1}$  and  $100 \text{ cm s}^{-1}$ . At  $120 \text{ cm s}^{-1}$  there is a large increase in the number of repositionings per minute from about 20 to 40. The large increase occurs at approximately the same time oxygen consumption rates increase.

The highest and lowest rheotactic suction pressures based on total ventral surface area are found in *Chaetostoma* ( $S_1 = 23.6 \text{ N m}^{-2}$ ) and *Farlowella* ( $S_1 = 2.04 \text{ N m}^{-2}$ ). *Hypostomus* ( $S_2 = 13.4 \text{ N m}^{-2}$ ) and *Chaetostoma* ( $S_2 = 173 \text{ N m}^{-2}$ ) have the lowest and highest rheotactic suction pressures based on sucker area ( $\pm \text{S.E.} = 0.1 - 5.2$ ; Table 2.3).

## DISCUSSION

### Sources of Error

Errors associated with calculating drag and lift coefficients include measurements of  $W_0$ ,  $A$ ,  $V$ ,  $V_2$ , and  $\mu$ . Errors in measuring  $W_0$ ,  $V$ ,  $V_2$  and  $\mu$  are unlikely. The weighing scale and current meter have reproducibilities of  $5 \times 10^{-4}$  g and  $0.50 \text{ cm s}^{-1}$  respectively. Furthermore, the standard error of  $\mu$  is less than 3 % of measured values (Table 2.1). Although drag coefficients of fish within genera vary, the drag velocity curves are consistent (Fig. 2.10). This suggests that the greatest error in calculating  $C_L$  and  $C_D$  arises from estimates of the total projected frontal area  $A$ .

Under estimates of  $A$  will result in increased calculated drag coefficients. Due to bony scutes along the head of *Pterygoplichthys* (occipital process, temporal and cleithrum), the  $A_b$  perimeter is not smooth. Although *Pterygoplichthys* has a rougher outline only a 6.8 % difference was found between two independent methods of estimation. The perimeter of  $A_b$  for *Otocinclus*, *Gyrinocheilus* and *Chaetostoma* is relatively smooth (Fig 1.1). Using geometry to estimate  $A_b$  in these fish would improve accuracy. In addition,  $A$  did not include the projected frontal area of the pectoral fin rays in the loricariids. The fin rays in these fish were not stable, but fluttered in water flow during drag measurements, producing unpredictable frontal areas. Rough estimates on the projected frontal area of the fin rays (using tracings and angle to flow) increases  $A_b$  by about 5 % for loricariids in a rheotactic posture.

This percent reduction in estimated area is compensated to a certain degree by an over estimate of  $A_f$  (assuming spine width does not change with length). In *Gyrinocheilus* fin ray projected frontal areas were substantially larger (40 % - 50 % of  $A$ ). For this reason their areas were estimated.

Furthermore, drag coefficients on dead specimens may be elevated if the body does not remain stiff or fin flutter occurs (Webb, 1975; Blake 1983). In this study live and dead specimens remained rigidly attached to the substrate eliminating body movement. Although pectoral fin ray flutter is minimal and not noticeably different in dead fish, it may contribute to increasing drag.

Arnold and Weihs (1978) found that the model used in this study may not be applicable for Reynold's numbers  $< 10^4$  without modification to the velocity exponent using a correction factor  $\sigma$  according to

$$C_L + \frac{C_D}{\mu} = \frac{2 W_o}{\rho_w A} V_2^{2-\sigma} \quad (2.14)$$

and

$$C_L = \frac{2 W_o}{\rho_w A} V_2^{2-\sigma} - \frac{2 D}{\mu \rho_w A} V_2^{2-\sigma} \quad (2.15)$$

*Otocinclus* is the only genera with Reynold's numbers consistently lower than  $10^4$  (Fig. 2.11). Following Arnold and Weihs (1978) a value of 0.2 for  $\sigma$  is applied to the velocity exponent of  $V_2$ . In addition,  $\sigma$  must be applied to the velocity ( $V$ ) exponent used to calculate  $\overline{C}_D$  (Equation 2.12). This produces a 30 % decrease in  $\overline{C}_D$  and 40 % increase in the ratio  $2W_o/\rho_w A V_2^2$  resulting in  $\overline{C}_L$ ,  $C_{L1}$ ,  $C_{L2}$  and  $\overline{C}_L/\overline{C}_D$  ratio equal to 0.83,

0.66, 1.01, and 2.41 respectively. The negative lift coefficient originally determined for *Otocinclus* using a maximum  $C_D$  value is eliminated by this correction. The minimum difference between lift coefficients calculated for *Otocinclus* at  $V_2$  with a velocity exponent equal to 1.8 and 2.0 is 50 %. The model is most sensitive to adjustments in the velocity exponent. However, from measurements it is apparent that the drag velocity curve is adequately described using a velocity exponent equal to 2 (Fig. 2.10 and Table 2.2). Although some measurements are below Reynold's numbers of  $10^4$  average values reduce their effect on calculated  $C_L$  and  $C_D$ .

Furthermore, boundary layer effects may reduce the water velocity experienced by smaller fish. *Otocinclus* generally had the smallest specimens (maximal body height = 0.5 cm - 0.7 cm). Measured boundary layer thickness at lower water velocities is similar to the height of *Otocinclus* (see Materials and Methods, Chapter II). However, drag measurements were taken at higher water velocities and specimens were placed at the front of the force plate. Both these methods would reduce boundary layer thickness resulting in a closer prediction (using free stream velocity) of the water velocity experienced by the fish.

### Density and Weight

The densities determined for *Otocinclus* and *Gyrinocheilus* (Fig. 2.9 and Table 2.1) are similar to those found in other benthic fish like the plaice (*Pleuronectes platessa*,  $\rho = 1.074 \text{ g cm}^{-3}$ ) and ray (*Raja clavata*,  $\rho = 1.066 \text{ g cm}^{-3}$ ; Arnold and Weihs, 1978; Webb, 1989; Table 2.1).

*Hypostomus*, *Chaetostoma* and *Farlowella* have particularly high body densities similar to several species of crab (*Callinectes sapidus*, *Cancer productus* and *Lopholithodes mandtii*,  $\rho = 1.13 \text{ g cm}^{-3} - 1.14 \text{ g cm}^{-3}$ ; Blake, 1985). Dense dermal plates in *Farlowella* and *Chaetostoma* contribute to high values (Alexander, 1965). *Pterygoplichthys* has a low  $\bar{\rho}$  relative to other genera. Although *Pterygoplichthys* was kept in a well oxygenated aquarium aerial respiration did occur in some specimens. Air trapped in accessory respiratory organs and swim bladders may account for the reduced density. Density measurements did not compensate for these gases (Gee, 1976). However, control of gases with these organs would allow *Pterygoplichthys* to increase density. Higher body density in all genera increases their effective submerged weight, resulting in higher frictional forces opposing drag. An increase in density with length, as seen in *Otocinclus* and *Gyrinocheilus*, may give older individuals increased station-holding ability (Fig. 2.9). According to Gee (1976) species of *Chaetostoma* (*C. fischeri*) are found in water velocities exceeding  $40 \text{ cm s}^{-1}$ . Fish in this type of environment have an advantage in preventing displacement if submerged weight is increased at a rapid rate as seen in this genus (Fig 2.8).

Frictional pads and odontodes in *Otocinclus* and other loricariids contribute to maximizing slipping speed on rough surfaces (Macdonnell and Blake, 1990). The frictional coefficients determined for the loricariids and *Gyrinocheilus* on a perspex surface are generally higher than those determined for other benthic fish (eg. *R. clavata* and *P. platessa*,  $\mu = 0.36$  and  $0.21$  respectively; Webb, 1989; Table 2.1). Besides acting as an effective method for protection the pectoral fin spines increase friction

(Schaefer, 1984). The odontodes of the loricariids are not particularly useful for increasing  $\mu$  on a smooth surface, however they would be on algal mats or rougher substrates. *Gyrinocheilus* and *Chaetostoma* have higher  $\bar{\mu}$  relative to the other genera. The smooth ventral surface of *Chaetostoma* and flexible pectoral fins and oral sucker of *Gyrinocheilus* provides intimate contact with the perspex increasing frictional coefficients. Both these characteristics would contribute to maximizing slipping velocity on smooth rock substrates.

### Morphology

Trade offs occur between lift and drag reflecting differences in body morphology. Lift and drag act to displace and remove the fish from the bottom in fast flow. Drag coefficients can be reduced by increasing fineness ratio ( $l/h \approx 10$ ), flattening ( $2b/h \approx 2$ ) and lengthening ( $x/l \approx 0.3$ ) the fore body (Hoerner, 1965). However, these changes in morphology increase lift (Hoerner and Borst, 1975). For fast stream fish morphological ratios  $2b/h$ ,  $l/h$  and  $x/l$  range between 0.9 - 2.0, 6.0 - 8.0, and 0.1 - 0.3 respectively (Chapter I).

In Fig. 2.10 fish number 1, 2, 2, and 2 of *Otocinclus*, *Hypostomus*, *Chaetostoma* and *Farlowella* respectively have their dorsal fins extended during drag measurements. Generally the mean drag coefficients calculated and drag measured for these fish is higher than those with the dorsal fin folded (Table 2.3). Lowering the dorsal fin and folding the tail in response to increased water velocity is a behaviour adapted to minimize drag. In contrast, at slipping speed *Otocinclus* extends its pectoral fins

(Macdonnell and Blake, 1990). This would increase drag; however, if the drag increase is low compared to the frictional forces gained (by negative lift and odontodes) the behaviour is advantageous to preventing displacement.

*Otocinclus* has low drag due to its small size (Fig. 2.10). However, over a similar Reynold's number range *Gyrinocheilus* has a lower  $C_D$  than *Otocinclus*, *Pterygoplichthys* and *Chaetostoma* (Table 2.3). This can be attributed to the lack of odontodes and smoother body surface found in *Gyrinocheilus*.

*Pterygoplichthys* and *Hypostomus* have similar body morphology. Most drag measurements are made on smaller specimens of *Pterygoplichthys* relative to *Hypostomus* (Table 2.2). However, for *Pterygoplichthys*, fish number 1 is considerably larger (Table 2.2), resulting in higher Reynold's numbers and in turn lower  $C_D$  similar to larger specimens of *Hypostomus* (Table 2.3). Relative to smooth bodies drag coefficients are elevated (Table 2.4). However, the relationship between Reynold's number and drag coefficient is typical for objects attached to surfaces (Fig. 2.11; eg. Hoerner, 1965 and Denny, 1988).

The highest  $C_L$  and  $C_L/C_D$  is found in *Farlowella* (Table 2.3). Its high fineness ratio and extended rostrum contribute to increasing lift. However, relative to flatter form fish lift coefficients are low (plaice  $C_L \approx 2.0$ ; Arnold and Weihs, 1978). *Gyrinocheilus* also has a high  $C_L/C_D$  ratio relative to the other loricariids. Flattening and elongation of the fore body is not present in *Gyrinocheilus* to the extent seen in the fast stream loricariids (Chapter I). However, *Gyrinocheilus*'s high fineness ratio contributes to increasing its lift coefficient. Relatively high

lift coefficients explain behavioural observations (tail instability for *Farlowella* and *Gyrinocheilus*; Chapter I). These observations are similar to those made by Stuart (1958) on body posture to increasing water velocity in the nymph *Rhithrogena semicolorata*.

*Farlowella* is found in slow moving waters, hiding in detritus and leaves on stream bottoms. If found in faster flow it is usually attached behind large logs or rocks, taking advantage of back eddies (Burgess, 1989). Low rheotactic suction pressures and high  $C_L/C_D$  in *Farlowella* are not characteristics that enhance station-holding ability. In contrast *Gyrinocheilus* can be found in open fast flowing water (Sterba, 1983). Unlike *Farlowella*, *Gyrinocheilus* is able to gain control of the tail at high water velocity.

The lift to drag ratios determined for *Otocinclus*, *Hypostomus*, *Pterygoplichthys* and *Chaetostoma* are similar to *Myoxocephalus scorpius* ( $C_L/C_D = 2.08$ ; Webb, 1989) and *Cancer productus* ( $C_L/C_D = 1.7-2.0$ ; Blake, 1985). All  $C_L/C_D$  ratios are relatively small compared to efficiently designed wings ( $C_L/C_D > 20$ ; Hoerner and Borst, 1975). Lower lift to drag ratios maximize slipping speed by allowing fish to utilize frictional devices for preventing displacement. In *Gyrinocheilus* higher lift to drag ratios can be compensated for by relatively high pressures produced by rheotaxis and suction (Table 2.3).

Another method of reducing lift is to have the pectoral fins act as wings, orientated at a negative angle to water flow. This occurs in all genera. Negative lift coefficients are calculated for *Pterygoplichthys* using maximum  $C_D$ . *Chaetostoma* has negative lift coefficients in all cases. These hill stream fish have their posterior pectoral fin rays at a

30° and 40° angle to the oncoming flow, the fin rays unfold easily and do not show movement drastically different from live fish during measurements. At the insertion point of the pectoral fin a small gap exists between the body, substrate and anterior pectoral fin spine. Water passing under the spine at high velocity maintains continuity of flow (Bernoulli's theorem) and could contribute to producing downward forces. Relatively large pectoral fin areas are correlated with benthic environments (Gatz, 1979). In addition, studies have observed behaviour suggesting that the pectoral fins act as negative lift hydrofoils. For example, Keast and Webb (1966), observed that the pectoral fins in the catfish, *Ictalurus nebulosus*, may produce forces that push the mouth against the substrate as it feeds. Lift by the pectoral fins may not be sufficient to give an overall negative  $C_L$  for the fish. However, they can act separately, producing forces sufficient to reduce lift.

Rheotactic suction pressure is produced by oral suction and rheotaxis opposing lateral displacement. *Gyrinocheilus*, *Pterygoplichthys* and *Chaetostoma* produce the largest pressures (Table 2.3). However, compared to pressures measured by Gibson (1969) in intertidal fish they are low (eg. *Liparis montagui*, 3 cm - 8 cm,  $S_2 = 8.2 \times 10^4 \text{ N m}^{-2}$  -  $1.5 \times 10^4 \text{ N m}^{-2}$  respectively). Although the pressures measured by Gibson (1969; perpendicular to the substrate) are not directly comparable to the rheotactic pressures determined for fish in this study, slipping velocities are comparable. The intertidal fish, *Liparis montagui*, *Liparis liparis*, and *Cyclopterus lumpus* are able to prevent slipping by water velocities equal to  $170 \text{ cm s}^{-1}$ . Powerful closed vacuum sucking discs in intertidal fish are derived from pelvic and pectoral fins specifically

adapted for adhesion. Although *Gyrinocheilus* has the ability to form a complete seal (closed sucker) other biological constraints (feeding) effect design which may limit pressures produced by the sucker (Benjamin, 1986).

Within the loricariids there are no gross differences in oral sucker morphology (Gradwell, 1971). However, there are large differences in suction pressure. *Otocinclus*, *Chaetostoma*, *Pterygoplichthys* and *Hypostomus* are found in fast flowing water (Burgess, 1989). *Otocinclus* and *Hypostomus* may rely on frictional devices to compensate for their lower suction pressures. Both these fish have dermal plates and odontodes on their ventral surface, high  $V_2$  and low  $V_1$ - $V_2$  (Chapter I). This is further supported by the reduction in rheotactic suction pressure for *Hypostomus*, relative to the other fish, when calculated using oral sucker area,  $S_2$  (Table 2.3). Morphology, oral sucker pressures, low  $V_2$  and high  $V_1$ - $V_2$  in *Pterygoplichthys* and *Chaetostoma* suggest that these fish place a greater reliance on suction for station-holding.

### Estimating Drag Coefficients

Technical bodies attached to surfaces have lower drag coefficients than bodies of similar fineness ratio and shape in the free stream (Hoerner, 1965). However, roughness (odontodes and eyes) and uneven transition to a substrate may increase drag coefficients by a factor of 2 (Arnold and Weihs, 1978; Webb 1989). In addition, appendages interfering with flow around a body can increase drag by 1.7 times (Hoerner, 1965). Interference drag is greatest when the appendage is inserted at the point

of maximal height. In the genera examined maximal height occurs at pectoral fin insertion. Taking these factors into consideration estimates of drag coefficients are compared to measured values.

In Table 2.4 drag coefficients measured from technical bodies  $C_{D_o}$  (smooth blisters attached to a surface; Hoerner, 1965), calculated laminar frictional coefficients  $C_{f(lam)}$  and estimates ( $C_{D_o}^1$  and  $C_{f(lam)}^1$ ) based on the above factors are listed. For streamlined bodies attached to surfaces the dominant force between Reynold's numbers of  $10^4$  and  $10^5$  is frictional drag. Frictional drag results from the tangential shear stresses developed between layers of fluid as it moves over the body. Values for the case of a frictional coefficient for turbulent flow give similar results to the laminar case at these Reynold's numbers and are not shown in Table 2.4. The frictional drag coefficient for a laminar boundary layer ( $C_{f(lam)}$ ) is obtained from the empirical equation

$$C_{f(lam)} = 1.33 (R_3^{-0.5}), \quad (2.16)$$

where  $R_3$  is the maximum and minimum Reynold's number for each genera taken from Table 2.3. From Hoerner (1965) drag coefficients for fineness ratios  $> 10$  (*Farlowella*) can be estimated using

$$C_{f(lam)}^1 = 0.5 C_{f(lam)}(l/h). \quad (2.17)$$

Using equation 2.16 measured drag coefficients are 2 to 30 times greater than  $C_{f(lam)}^1$  for Reynold's numbers ranging from  $10^4$  to  $10^5$  (Table 2.4). In general *Farlowella* has estimated drag coefficients closest to

	$C_{D_0}$	$C_{D_0}^1$	$C_{f(lam)}$	$C_{f(lam)}^1$	$\frac{\overline{C}_D}{C_{D_0}^1}$	$\frac{\overline{C}_D}{C_{f(lam)}^1}$
<i>Otocinclus</i>	0.042	0.14	0.012-0.017	0.04-0.06	3	8-11
<i>Gyrinocheilus</i>	0.035	0.12	0.009-0.017	0.03-0.06	4	7-14
<i>Hypostomus</i>	0.037	0.13	0.006-0.010	0.02-0.03	2	10-14
<i>Pterygoplichthys</i>	0.040	0.14	0.009-0.014	0.03-0.05	3	9-16
Fish 1	0.040	0.14	0.006-0.009	0.02-0.03	3	8-12
<i>Chaetostoma</i>	0.038	0.13	0.011-0.015	0.03-0.05	7	18-30
<i>Farlowella</i>	0.045	0.22	0.006-0.010	0.06-0.11 <sup>*</sup>	1	2-3

Table 2.4 Calculated laminar frictional drag coefficients  $C_{f(lam)}$ , drag coefficients measured from technical bodies  $C_{D_0}$  with fineness ratios equivalent to the fish and estimated values multiplied by a factor of 3.4,  $C_{f(lam)}^1$  and  $C_{D_0}^1$ . Multiple difference between measured and estimated drag coefficients,  $\overline{C}_D/C_{f(lam)}^1$  and  $\overline{C}_D/C_{D_0}^1$  for the Reynold's number range  $R_3$  in Table 2.3 ( $R_3 = 0.55 \times 10^4 - 4.76 \times 10^4$ ). Frictional drag coefficient determined from equation 2.17 (\*).

measured values (Table 2.4). The high fineness ratio, and small anterior pectoral fin spines contribute to a relatively smooth body and an accurate prediction of  $C_D$ . It would seem that estimating  $C_D$  is reliable for fineness ratios  $\geq 10$  using equations 2.16, 2.17 and technical body data. Estimated drag coefficients for lower fineness ratio forms ( $l/h < 10$ ) compares poorly with measured values. At fineness ratios less than 10 separation of the boundary layer over the fore body may produce varying degrees of pressure drag due to roughness that is difficult to predict.

In addition, it has already been pointed out that predicted values of drag and lift coefficients are unreliable for Reynold's numbers  $< 10^4$  where resistance is not a quadratic function of velocity. Force coefficients for fish of low fineness ratio at lower Reynold's number on a ground plane can not be accurately predicted and should be measured.

### Respirometry

Although fish are able to swim in a fast flowing environment (eg. *Salmo gairdneri*, 75.0 cm s<sup>-1</sup>- 90.0 cm s<sup>-1</sup>; Everest and Chapman, 1970), the ability to maintain position is dependant to a greater extent on the efficiency of their active propulsive mechanism rather than the passive methods seen in benthic fish. Even fish that tend to swim away from the bottom will utilize the substrate to prevent displacement (Keenleyside, 1962).

The resting O<sub>2</sub> consumption rate ( $\approx 50$  mg O<sub>2</sub> kg<sup>-1</sup> hr<sup>-1</sup>) in *Pterygoplichthys* is similar to other fish (eg. Beamish, 1964; Hughes et al. 1983). However, the O<sub>2</sub> consumption rate at higher water velocities is

lower than values determined for fish swimming in the free stream. For example, Steffensen et al. (1987) found Rainbow trout (*Salmo gairdneri*, 285-700 g) had  $O_2$  consumption rates of approximately  $300 \text{ mg } O_2 \text{ kg}^{-1} \text{ hr}^{-1}$  at a water velocity of  $85 \text{ cm s}^{-1}$  for a 20 to 40 min swim time. In contrast the  $O_2$  consumption rates at even higher water velocities in *Pterygoplichthys* are lower ( $97 \text{ mg } O_2 \text{ kg}^{-1} \text{ hr}^{-1}$ ,  $120 - 160 \text{ cm s}^{-1}$ , 20 min swim time). Utilizing the substrate to prevent displacement using body morphology (odontodes and spines) and rheotactic behaviour is advantageous for reducing the effort required to maintain position. From the respirometry results (Fig. 2.12) an increase in oxygen consumption and repositioning occurs at approximately the same water velocity ( $110 \text{ cm s}^{-1}$ ). This indicates that at critical speeds (slipping speed) the fish exerts greater effort to maintain position. This is accomplished by increasing rheotactic suction pressure and burst swimming. Unlike littoral zone fish, that use a ventral sucking disc made from modified fins (Gibson, 1969), the loricariids must form suction with their mouths. At faster water velocities, where suction is an asset, the effort required to maintain position increases. However, the respiratory fissure becomes smaller and flaring of the gap more pronounced which may restrict water flow. To compensate for reduced flow the breathing rate may be increased (Burgess, 1989) or alternate methods of respiration utilized (Sawaya and Petrini, 1960). This particular diphasic oxygen consumption rate is probably applicable to the loricariids. However, *Gyrinocheilus* uses a different mechanism of suction that may result in a different oxygen consumption curve.

In a natural habitat fish have a number of options not presented to

them in this study. These include positioning in back eddies behind rocks and boulders, moving into reduced water flow along the sides of rivers, borrowing and selection of substrate (Probst et al. 1984 and Daniels, 1989). Furthermore, other ecological factors like predation and food resources effect their distribution (Zaret, 1970; Colgan and Cross, 1982). Power (1984) found size-specific depth distributions occur for four species of loricariids (*Ancistrus*, *Hypostomus*, *Chaetostoma*, and *Rineloricaria*). During the day fish opt for deeper waters where they can avoid predation from birds, moving into shallow algal rich areas during the night to feed. However, hill stream fish are generally restricted to fast flow. Species of *Hypostomus* must remain in cataracts where oxygen content is high (Boseman, 1968).

Behavioural and morphological adaptations found in fast stream fish (*Otocinclus*, *Gyrinocheilus*, *Hypostomus*, *Pterygoplichthys*, and *Chaetostoma*) do maximize slipping speed and, likely, reduce the energy required for maintaining position. Frictional devices (spines, odontodes, and frictional pad), high rheotactic suction pressures, tissue densities and hydrodynamic characteristics increase forces opposing drag and lift. In contrast, *Farlowella* exhibits hydrodynamic characteristics (high  $C_L$  and  $C_L/C_D$ ), low rheotactic suction pressure, and behaviour (passive rheotactic behaviour) indicating that relative to station-holding other factors are of greater priority in determining habitat adaptation.

## Concluding Comments

Results from Chapter I suggest that behavioural and morphological adaptations in fast stream fish contribute to increasing station-holding ability. Although drag coefficients for fast stream fish are relatively high, geometry conforms to low drag shapes. The presence of dorso-ventral flattening and frictional devices in the loricariids are characteristics similar to the fast stream fish studied by Hora (1921 - 1930). Furthermore, variation in body geometry and density with size may be a contributing factor in determining the micro-habitats fish are able to exploit within species. The physical parameters placed on fast stream fish may be a significant component in determining adaptation.

In addition, the contribution of pectoral fin extension to station-holding may provide insight into the reasons for this behaviour in *Otocinclus*. This study supports previous observations suggesting that the pectoral fins act to produce negative lift. By adapting current methods it may be possible to measure the lift and drag acting on benthic fish with and without fins, therefore, ascertaining their contribution to station-holding.

Results from Chapters I and II indicate that a significant proportion of their station-holding ability is dependant on suction. Direct measurement of the actual suction pressure produced by these fish from a variety of directions would be a useful exercise. Trade offs between suction pressure and morphology adapted to maximize friction may occur depending on the substrate.

It would seem that, besides biological factors, the extreme environmental conditions that these fish face have a significant effect on hydrodynamic adaptation. Detailed investigation into the physical constraints (eg. water velocity, substrate type and natural shelter) placed on these fish may reveal evidence supporting the explanations based on the behavioural, morphological and hydrodynamic data obtained in this study.

## LITERATURE CITED

Alexander, R. McN. (1965). Structure and Function in the Catfish. J. Zool. 148, 88-152.

Annandale, N. and Hora, S.L. (1920). The Fish of Seistan. Rec. Indian Mus. 18, 191.

Annandale, N. and Hora, S.L. (1922). Parallel evolution in the fish and tadpoles of mountain torrents. Rec. Indian Mus. 24, 505-509.

Annandale, N., and Hora, S.L. (1925). The Fresh Water Fish from the Andaman Islands. Rec. Indian Mus. 27, 33-43.

Arnold, G.P. (1969). A flume for behaviour studies of marine fish, J. Exp. Biol. 51, 671-679.

Arnold, G.P. and Weihs, D. (1978). The hydrodynamics of rheotaxis in the plaice (*Pleuronectes platessa* L.). J. Exp. Biol. 75, 147-169.

Beamish, F.W.H. (1964). Influence of starvation on standard and routine oxygen consumption. Trans. Am. Fish. Soc. 93: 103-107.

Benjamin, M. (1986). The oral sucker in *Gyrinocheilus aymonieri* (Teleostei: Cypriniformes). J. Zool. B 1, 211-254.

Blake, R.W. (1983). Fish Locomotion. Cambridge University Press, Great Britain.

Blake, R.W. (1985). Crab Carapace Hydrodynamics. J. Zool. A 207, 407-423.

Boseman, M. (1968). The Genus *Hypostomus* Lacépède, 1803, and its Surinam representatives (Siluriformes, Loricariidae). Zool. Verh. 99, 1-89.

Burgess, W.E. (1989). An Atlas of Freshwater and Marine Catfishes (A preliminary survey of the Siluriformes). T. F. H. Publications Inc.

Colgan, W.P. and Cross, J.A. (1982). Laboratory food exploitation in the algae-eater (*Gyrinocheilus aymonieri*) (Tirant 1883) Pisces: Cypriniformes. Biol. Behav. 7, 109-117.

Cope, E.D. (1871). [Prof. Cope demonstrated some anatomical points of importance in the classification of some of the siluroids of the Amazon, etc.]. Proc. Acad. Nat. Sci. Phila. 23, 112.

Daniels, R.A. (1989). Significance of Burying in *Ammocrypta pellucida*. Copeia. 29-34.

Denny, M. (1988). A limpet shell shape that reduces drag: laboratory demonstration of a hydrodynamic mechanism and an exploration of its effectiveness in nature. Can. J. Zool. 67, 2098-2106.

Eaton, T.H. (1935). The teeth of *Plecostomus*, an armoured catfish. Copeia. 161-163.

Eigenmann, C.H. and Eigenmann, R.S. (1889). Preliminary notes of the south American nematognathi. Proc. Calif. Acad. Sci. (2) 2, 28-56.

Everst, F.H. and Chapman, D.W. (1972). Habitat selection and spatial interaction by juvenile chinook salmon and steelhead trout in two Idaho streams. J. Fish. Res. Board Can. 29, 91-100.

Fowler, H.W. (1937). Zoological results of the third De Schauensee Siamese Expedition. Part 8. Fishes obtained in 1936. Proc. Acad. Nat. Sci. Phila. 89, 125-264.

Gatz, A.J. (1979). Ecological morphology of fresh water streamfishes. Tulane Stud. Zool. Biol. (21) 2, 91-124.

Gee, J.H. (1976). Buoyancy and aerial respiration: factors influencing the evolution of reduced swim-bladder volume of some Central American catfishes (Trichomycteridae, Callichthyidae, Loricariidae, Astroblepidae). Can. J. Zool. 54, 1030-1037.

Gehrke, P.C., Fidler, L.E., Mense, D.C., and Randall, D.J. (1990). A respirometer with controlled water quality and computerized data acquisition for experiments with swimming fish. *Fish Physiol. Bioch.* (8) 1, 61-67.

Gibson, R.N. (1969). Powers of adhesion in *Liparis Montagu* (Donovan) and other shore fish, *J. Exp. Mar. Biol. Ecol.* 3, 179-190.

Gill, T. (1858). Synopsis of the fresh water fishes of the western portion of the island of Trinidad, W.I. *Ann. Lyceum Nat. Sci. Hist.* (New York). 6, (38), 363-339.

Gradwell, N. (1971). A Muscular Oral Valve Unique in Fishes. *Can. J. Zool.* 49, 837-839.

Hoerner, S.F. (1965). *Fluid-Dynamic Drag*. Brick Town, NJ: Hoerner Fluid Dynamics.

Hoerner, S.F. (1975). *Fluid-Dynamic Lift*. Brick Town, NJ: Hoerner Fluid Dynamics. Ed. H.V. Borst.

Hora, S.L. (1921). Indian Cyprinoid fishes belonging to the Genus *Garra*, with Notes on Related Species from other Countries. *Rec. Indian Mus.* 29, 633-683.

Hora, S.L. (1922). Structural modifications in the fish of mountain torrents. *Rec. Indian Mus.* 24, 31-61.

Hora, S.L. (1923a). The adhesive apparatus of the sucking fish. *Nature* 111, 668.

Hora, S.L. (1923b). On a collection of fish from Siam. *J. Nat. His. Soc. Siam.* 6, 143-184.

Hora, S.L. (1925a). The adhesive apparatus of the sucking fish. *Nature* 115, 48.

Hora, S.L. (1925b). Notes on fishes in the Indian museum. *Rec. Indian Mus.* 25, 1-44.

Hora, S.L. (1925c). Observations on the fauna of certain torrential streams in the Khasi hills. *Rec. Indian Mus.* 25, 579-605.

Hora, S.L. (1927). Animal Life in Torrential Streams. *J. Bombay Nat. Hist. Soc.* 32, 111-126.

Hora, S.L. (1930). Ecology, bionomics and evolution of the torrential fauna, with special reference to the organs of attachment. *Philos. Trans. R. Soc. Lond. B* 218, 171-282.

Hughes, G.M., Albers, C., Muster, D., and Götz, K.H. (1983). Respiration of the carp, *Cyprinus carpio* L., at 10° and 20° C and the effects of hypoxia. J. Fish Biol. 22, 613-628.

Isbrüker, I.J.H. (1980). Classification and catalogue of the mailed catfish (Pisces, Siluriformes). Verslagen Tech. Gegevens. 22, 1-181.

Jones, W.E. (1968). Exposure to wave action: Measurements of an important ecological parameter on rocky shores on Anglesey, J. Exp. Mar. Biol. Ecol. 2, 46-63.

Keast, A., and Webb, D. (1966). Mouth and body form relative to feeding ecology in the fish fauna of a small lake, lake Opinicon, Ontario. J. Fish. Res. Board Can. 23 (12), 1845-1874.

Keenleyside, M.H.A. (1962). Skin-diving observations of Atlantic salmon and brook trout in the Miramichi River, New Brunswick. J. Fish. Res. Board Can. 19, 625-634.

Lundberg, J.C. and Marsh, E. (1976). Evolution and functional anatomy of the pectoral fin rays in the cyprinoid fishes, with emphasis on the suckers (family Catostomidae). Am. Midl. Nat. 96, 332-349.

Lacépède, B.G.E. (1803). Histoire naturelle des poissons, dédiée à Anne-Caroline La Cepè, par le Citoyen La Cepè (P. Plassen, Paris), 5 (1), 1-803.

- Macdonnell, A.J. and Blake R.W. (1990). Rheotaxis in *Otocinclus* sp. (Teleostei: Loricariidae). Can. J. Zool. In Press.
- Matthews, W.J. (1985). Critical current speeds and microhabitats of the benthic fishes *Percina roanoka* and *Etheostoma flabellare*. Envir. Biol. Fishes. 12, 303-308.
- Maude, S. H. and Williams, D.D. (1983). Behavior of the crayfish in water currents: hydrodynamics of eight species with reference to their distribution patterns in Southern Ontario. Can. J. Fish. Aquat. Sci. 40, 68-77.
- Mittal, A. K. and Whitear, M. (1979). Keratinization of fish skin with special reference to the Catfish *Bagarius bagarius*. Cell Tissue Res. 202, 213-230.
- Nachtigall, W. (1974). Biological mechanisms of attachment (transl. by M.A. Biederman-Thorson). Springer-Verlag, Berlin.
- Ørvig, T. (1977). A survey of odontodes ("Dermal teeth") from a developmental, structural, functional and phyletic point of view. Linn. Soc. Sym. Ser. No. 4. Problems in vertebrate evolution. Academic Press, London.

- Power, M.E. (1984). Depth distribution of armoured catfish: Predator induced resource avoidance? Ecology 65 (2), 523-528.
- Probst, W.E., C.F., Rabeni, W.G., Covington and R.E., Marteney. (1984). Resource use by stream dwelling rock bass and small mouth bass. Am. Fish. Soc. 113, 283-294.
- Roberts, T.R. (1982). Unclui (horny projections arising from single cells), an adaptive feature of the epidermis of ostariophysin fishes. Zool. Scr. 11, 55-76.
- Sawaya, P. and Petrini, L. M. de (1960). Sobre a presença de cloaca e respiração intestinal no Cascudo (Loricariidae: *Plecostomus plecostomus* (Linn.)). Bolm Fac. Filos. Cienc. Univ. S. Paulo 23, 5-23.
- Schaefer, S.A. (1984). Mechanical strength of the pectoral spine/girdle complex in *Pterygoplichthys* (Loricariidae: Siluroidei). Copeia. 1005-1008.
- Smith, H.M. (1945). The fresh-water fishes of Siam, or Thailand. U. S. Nat. Mus. Bull. 188, 1-622.
- Statzner, B. and Holme, T.F. (1989). Morphological adaptations of Shape to Flow: Microcurrents around Lotic Macroinvertebrates with known Reynolds numbers at quasi-natural flow conditions. Oecologia 79, 145-157.

- Steffensen, J.F., Tufts, B.L. and Randall, D.J. (1987). Effect of burst swimming and adrenaline infusion on  $O_2$  consumption and  $CO_2$  excretion in Rainbow trout, *Salmo gairdneri*. J. Exp. Biol. 131, 427-434.
- Sterba, G. (1983). Aquarium Encyclopedia. (transl. Susan Simpson). M.I.T. Press. Cambridge, Massachusetts.
- Streeter, V.L. and Wylie, E.B. (1979). Fluid Mechanics. McGraw-Hill, Inc.
- Stuart A.M. (1958). The efficiency of adaptive structures in the nymph of *Rhithrogena semicolorata* (Curtis) (Ephemeroptera). J. Exp. Biol. 35, 27-38.
- Taylor, E. B. (1988). Adaptive Variation and Agonistic Behavior in Newly Emerged Fry of Chinook Salmon, *Oncorhynchus tshawytscha*, from Ocean - and Stream - Type Populations. Can. J. Fish. Aquat. Sci., Vol. 45, 237-243.
- Tirant, G. (1883). Note sur quelques espèces de poissons des montagnes de Samrong-Tong (Cambodge). Bull. Soc. Etudes Indochinoises Saigon. (Reprint in 1929 as one of the series of papers under the title: Oeuvre ichthyologique de G. Tirant. Réimpression. Note Service Océan. Pêches Indochine Saigon. 6, 1-175.
- Tschudi, J.J. von. (1845). Untersuchungen über die Fauna peruana. Ichthyologie (Scheitlin and Zollikofer, St. Gallen). 1-35

Vandewalle, P., Brunin P., and Chardon M. (1986). Functional approach to the morphology of the buccal region of *Cteniloricaria platystoma* (Gunther) (Pisces, Ostariophysi, Loricariidae) with respect to a peculiar respiration, Zool. Anz. 217, 363-373.

Vogel, S. (1981). Life in Moving Fluids. Princeton: Princeton Univ. Press.

Webb, P.W. (1975). Hydrodynamics and Energetics of Fish Propulsion. Bull. Fish. Res. Can. 190, 1-158.

Webb, P. W. (1989). Station-holding by three species of benthic fish. J. Exp. Biol. 145, 303-320.

Wheeler, A. (1975). Fishes of the World. MacMillan Publishing Co. Inc., New York.

Zaret, T.M., and A.S. Rand. (1971). Competition in tropical stream fishes: support for the competitive exclusion principle. Ecology 52, 336-342.